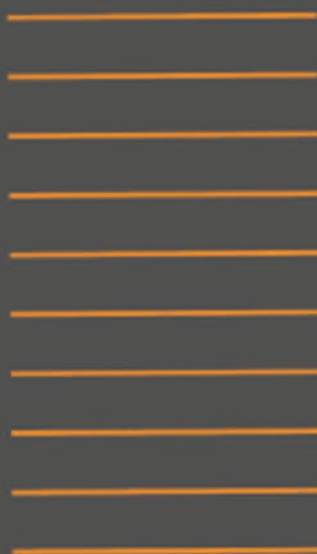




Application of Stress-Wave Theory to Piles

**Quality Assurance on
Land and Offshore Piling**

S. Niyama
J. Beim
Editors



APPLICATION OF STRESS-WAVE THEORY TO PILES



Taylor & Francis

Taylor & Francis Group

<http://taylorandfrancis.com>

PROCEEDINGS OF THE SIXTH INTERNATIONAL CONFERENCE ON THE APPLICATION
OF STRESS-WAVE THEORY TO PILES/SÃO PAULO/BRAZIL/11 – 13 SEPTEMBER 2000

Application of Stress-Wave Theory to Piles

Quality Assurance on Land and Offshore Piling

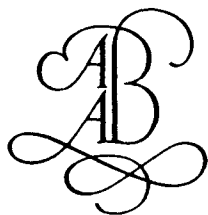
Edited by

Sussumu Niyama

Institute for Technological Research – IPT, São Paulo, Brazil

Jorge Beim

PDI Engenharia, Rio de Janeiro, Brazil



A.A. BALKEMA/ROTTERDAM/BROOKFIELD/2000

This conference was organized by the Brazilian Society for Soil Mechanics and Geotechnical Engineering

The texts of the various papers in this volume were set individually by typists under the supervision of each of the authors concerned.

Authorization to photocopy items for internal or personal use, or the internal or personal use of specific clients, is granted by A.A. Balkema, Rotterdam, provided that the base fee of US\$ 1.50 per copy, plus US\$ 0.10 per page is paid directly to Copyright Clearance Center, 222 Rosewood Drive, Danvers, MA 01923, USA. For those organizations that have been granted a photocopy license by CCC, a separate system of payment has been arranged. The fee code for users of the Transactional Reporting Service is: 90 5809 150 3/00 US\$ 1.50 + US\$ 0.10.

Published by

A.A. Balkema, P.O. Box 1675, 3000 BR Rotterdam, Netherlands

Fax: +31.10.413.5947; E-mail: balkema@balkema.nl; Internet site: www.balkema.nl

A.A. Balkema Publishers, Old Post Road, Brookfield, VT 05036-9704, USA

Fax: 802.276.3837; E-mail: info@ashgate.com

ISBN 90 5809 150 3

© 2000 A.A. Balkema, Rotterdam

Printed in the Netherlands

Table of contents

Preface	XIII
Organization	XV
Acknowledgements	XVII
1 Wave mechanics and its application to pile analysis	
Keynote lecture: Some wave mechanics applications <i>G.G.Goble</i>	3
Analysis of bearing capacity of rock-socketed piles based on wave equation theory <i>L.B. Cai</i>	11
Pile acceptance based on combined CAPWAP analyses <i>R.F.Stevens</i>	17
Theoretical study on effect of pile shaft resistance on rebound during pile driving <i>R.P.Chen & Y.M.Chen</i>	29
Time effect in determining pile capacity by dynamic methods <i>M.R.Svinkin</i>	35
Set-up considerations in wave equation analysis of pile driving <i>C.W.Cho, M.W.Lee & M.F.Randolph</i>	41
Drivability and performance of model piles driven into cemented calcareous sand <i>D.Bruno, M.F.Randolph, C.W.Cho & H.A.Joer</i>	47
Automatic signal matching with CAPWAP <i>F.Rausche, L.Liang & B.Robinson</i>	53
Combining static pile design and dynamic installation analysis in GRLWEAP <i>F.Rausche, B.Robinson & J.Seidel</i>	59
Rules of thumb for field and construction engineer in relation to impact pile driving <i>W.J.Lucieer</i>	65

2 *Driving equipment and recent developments – New technologies for quality assurance of piles*

Keynote lecture: Pile driving equipment: Capabilities and properties <i>F.Rausche</i>	75
Hammer system design using wave equation analysis for testing cast-in-situ concrete piles <i>M.A.Mukaddam, W.M.Iskandarani & M.Hussein</i>	91
Analysis of pile load transfer using optical fiber sensor <i>J.-H.Oh, W.-J.Lee, S.-B.Lee & W.-J.Lee</i>	99
Set-up effect of cohesive soils in pile capacity <i>M.R.Svinkin & R.Skov</i>	107
Modulus of elasticity and stiffness of composite hammer cushions <i>M.R.Svinkin</i>	113
A new technique to drive piles: Down-the-hole piling <i>A.Benamar</i>	117
Simplified neural network models for estimating soil resistance using dynamic pile test <i>R.Liang & N.O.Nawari</i>	121
Pile capacity prediction using neural networks technique <i>A.S.Dyminsky, E.Parente-Ribeiro, C.Romanel & J.W.Beim</i>	127
Hammer and pile cushion optimisation <i>G.Jonker & R.J.van Foeken</i>	135

3 *Pile integrity and low strain dynamic testing*

Keynote lecture: Øresundlink, grouting work under West Pylon: Integrity test of a giant pile <i>J.Romell</i>	145
A study for the shape of pile with reflect-wave method <i>Yang Wu</i>	153
Evaluation of the performance of an existing foundation via PIT tests <i>S.B.Foá, J.H.F.Pereira, R.P.Cunha & J.Camapum de Carvalho</i>	157
Sonic integrity test of piles-integrity effected by basement excavation in Bangkok soft clay <i>N.Thasnanipan, A.W.Maung, P.Tanseng & Z.Z.Aye</i>	163
Non-destructive integrity testing on piles founded in Bangkok subsoil <i>N.Thasnanipan, A.W.Maung, T.Navaneethan & Z.Z.Aye</i>	171
Estimation of pile head stiffness using sonic integrity testing <i>K.Imada, T.Matsumoto & Y.Nakata</i>	179
Integrity testing of cast-in-situ concrete piles associated with the construction of New Haccho Bridge <i>Y.Michi, T.Matsumoto & Y.Matsuda</i>	187
Presentation of low strain integrity testing in the time-frequency domain <i>J.P.Seidel</i>	193

First experiences in the application of the stress wave theory to foundations in Uruguay <i>A.Gutiérrez, L.Abreu, Ch.Hoffmann & D.Hasard</i>	201
Detection and prevention of anomalies for augercast piling <i>G.Likins, G.Piscsalko, F.Rausche & C.M.Morgano</i>	205
Recent advances and proper use of PDI low strain pile integrity testing <i>G.Likins & F.Rausche</i>	211
Stress wave propagation velocity at early ages <i>C.Restrepo</i>	219
Examination of a new cross-hole sonic logging system for integrity testing of drilled shafts <i>S.G.Paikowsky, L.R.Chernauskas, L.J.Hart, C.D.Ealy & A.F.DiMillio</i>	223
 4 Pile-soil interaction	
Keynote lecture: Identification of soil-pile model interaction parameters from recorded time-displacement signals <i>A.I.Husein Malkawi & I.M.Ayasrah</i>	233
Load transfer analysis from increasing energy dynamic load tests in concrete piles driven in very soft clay formation <i>J.Balech & N.Aoki</i>	241
Dynamic pile testing and finite element calculations for the bearing capacity of a quay wall foundation – Container terminal Altenwerder, Port of Hamburg <i>F.Kirsch, B.Plaßmann, T.Huch & W.Rodatz</i>	249
The shaft dynamic response of a pile in clay: Induced pore pressure <i>A.Benamar</i>	255
An investigation of pile diameter influence in the bearing capacity on Dynamic Load Test (DLT) <i>G.P.Bernardes, C.S.Andreo & C.Gonçalves</i>	261
Pile set-up in sands <i>J.P.Seidel & M.Kalinowski</i>	267
Modeling pore pressure generation during dynamic testing of deep foundations <i>P.L.Pinto</i>	275
 5 Codes	
Keynote lecture: The performance of the dynamic methods, their controlling parameters and deep foundation specifications <i>S.G.Paikowsky & K.L.Stenersen</i>	281
LRFD design codes for pile foundations – A review <i>G.G.Goble</i>	305
Pile testing competitions – A critical review <i>J.M.Amir & B.H.Fellenius</i>	313

The need for quality assurance in the dynamic pile testing industry <i>J.P.Seidel</i>	319
High strain dynamic pile testing, equipment and practice <i>G.Likins, F.Rausche & G.G.Goble</i>	327
Dynamic load testing and Statnamic load testing for acceptance and design of driven piles in Japan <i>T.Matsumoto, K.Fujita, O.Kusakabe, M.Okahara, N.Kawabata & S.Nishimura</i>	335
Ethics and money. Are they compatible? <i>H.Goldemberg & J.J.Goldemberg</i>	345
6 High strain dynamic testing of driven and cast in situ piles – Dynamic testing of large piles	
Keynote lecture: Pile acceptance criteria for large diameter and cast in situ piles <i>R.F.Stevens</i>	351
Analyzing the bearing capacity mechanism of large diameter diving casing cast-in-situ concrete piles by using high strain dynamic testing <i>Xi Liang</i>	369
Analysis of dynamic load tests on steel rails piles <i>F.M.A.Lima, J.C.A.Cintra & N.Aoki</i>	375
A discussion of penetration matching on high strain dynamic pile testing <i>D.Xu, S.Wu & L.Xiao</i>	383
Experience gained and difficulties in performing dynamic load test in composite piles made with steel rails <i>G.P.Bernardes, C.S.Andreo & C.Gonçalves</i>	389
The application of high strain dynamic pile testing to screwed steel piles <i>J.G.Cannon</i>	393
Case study on the application of high strain dynamic pile testing to non-uniform bored piles <i>J.G.Cannon</i>	399
High capacity dynamic load tests for bored piles in Sydney shale <i>D.J.Klingberg & P.Mackenzie</i>	403
Predicting uplift deflection from dynamic pile testing <i>W.G.Chambers & D.J.Klingberg</i>	407
Applicability of dynamic load test on a toe improved pile <i>J.Sakimoto, N.Kita, S.Nishimura & T.Takeda</i>	411
Dynamic pile testing practice in Finland <i>H.Jokiniemi, J.Hartikainen & P.Korkeakoski</i>	415
Driving behavior of large diameter steel pipe piles <i>Y.-N.Lee & J.-S.Lee</i>	421

Dynamic load test of cast in place pile using a free fall hammer <i>S.Niyama, G.C.de Campos, S.Navajas, S.C.Paraíso, C.M.C.Costa & G.E.Barbosa</i>	429
Dynamic testing of large auger pile using free fall loading system in a harbour work <i>S.Niyama, S.Navajas & G.C.de Campos</i>	435
Dynamic load test on high capacity pile socketed in basaltic rock <i>S.C.Paraíso, C.M.C.Costa & E.Pinto Soares</i>	441
 <i>7 SPT measurements and special field monitoring test</i>	
Keynote lecture: Frequency characteristics of stress wave and penetration during SPT <i>K.Fujita</i>	451
The application of energy conservation Hamilton's principle to the determination of energy efficiency in SPT tests <i>N.Aoki & J.C.A.Cintra</i>	457
Correlative study of Smith damping coefficient and SPT blow count <i>R.Y.Liang</i>	461
Stress wave theory application to standard penetration test in Japan <i>K.Fujita & M.Ohno</i>	469
 <i>8 Vibratory pile driving – Vibration in pile driving</i>	
Keynote lecture: Vibratory driving analysis <i>A.E.Holeyman</i>	479
Computation of ground waves due to piling <i>C.L.Ramshaw, A.R.Selby & P.Bettess</i>	495
The effect of pile impedance on energy transfer to pile and ground vibrations <i>M.R.Svinkin, B.C.Roth & W.R.Hannen</i>	503
Determination of modulus of subgrade reaction in a pile with a vibrating apparatus <i>M.Hilmi Acar</i>	511
Analysis of crosswise vibration of pile driving <i>R.P.Chen, B.Zhu & Y.M.Chen</i>	517
Monitoring and control of dynamic effects of pile installation prior to pile driving <i>M.R.Svinkin</i>	525
Full-scale field-test study of dynamic soil resistance of vibratory driven sheet piles <i>K.Viking</i>	533
Accelerations of a driven pile and the surrounding soil <i>E.L.Hajduk, S.G.Paikowsky, P.Hölscher & F.B.J.Barends</i>	541
 <i>9 Statnamic and other similar techniques</i>	
Keynote lecture: Statnamic, the engineering of art <i>P.Middendorp</i>	551

Keynote lecture: Three-dimensional finite element analysis of statnamic load test <i>T.Boonyatee, M.Kimura & F.Zhang</i>	563
Lateral statnamic load testing of model piles <i>M.Kimura & T.Boonyatee</i>	569
Application of the Stress Wave method to automatic signal matching and to statnamic predictions <i>G.Esposito, W.M.G.Courage & R.J.van Foeken</i>	575
A comparative study of static, dynamic and statnamic load tests of steel pipe piles driven in sand <i>A.Shibata, N.Kawabata, Y.Wakiya, Y.Yoshizawa, M.Hayashi & T.Matsumoto</i>	583
Case studies of statnamic load testing in Japan <i>S.Nishimura, T.Matsumoto, O.Kusakabe, K.Nishiumi & Y.Yoshizawa</i>	591
Statnamic and dynamic load tests for large diameter steel pipe piles supported by a thin bearing layer at Nagoya port in Japan <i>Y.Kikuchi, S.Nishimura & M.Tatsuta</i>	599
Statnamic load testing using water as reaction mass <i>M.D.Justason, M.C.Janes, P.Middendorp & A.G.Mullins</i>	609
Introducing statnamic load testing in Europe: Case studies in the Netherlands <i>G.J.J.van Ginneken & P.Middendorp</i>	617
The advantages and disadvantages of dynamic load testing and statnamic load testing <i>P.Middendorp, G.J.J.van Ginneken & R.J.van Foeken</i>	625
10 Case histories, pile set-up and correlations between test methods	
<i>– Prediction reliability</i>	
Keynote lecture: Improving the reliability of pile bearing capacity prediction by the dynamic increasing energy test (DIET) <i>N.Aoki</i>	635
Correlation analyses of dynamic and static loading tests for nine piles <i>Y.M.Zheng, J.M.Zheng & B.Chen</i>	651
Back-analyses of steel pile driving records for quality assurance <i>B.R.Danziger & J.S.Ferreira</i>	657
Evaluation of pile set-up from penetration per blow <i>G.Axelsson & S.Hintze</i>	665
Comparative analysis of dynamic and static test of foundation pile <i>G.Zhou & J.Wu</i>	673
Dynamic load test and elastic rebound analysis for estimation of the bearing capacity of piles in residual soil <i>P.J.R.de Albuquerque & D.de Carvalho</i>	677
Strain dynamic testing on pressure-grouted piles <i>Liu Xi-An & Zhang Yao-Nian</i>	683

Assessment of the interface between dynamic and rapid loading tests <i>M.B. Karkee, Y. Sugimura & T. Horiguchi</i>	689
Dynamic load testing on 102 steel pipe piles for bridge foundations on mudstone <i>M. Hayashi, T. Matsumoto & M. Suzuki</i>	697
Behavior of short CFA piles in an overconsolidated clay based on static and dynamic load tests <i>A.C.M. Kormann, P.R. Chamecki, L. Russo Neto, L. Antoniutti Neto & G.P. Bernardes</i>	707
Static and dynamic testing of the ‘Campile’ – A displacement, cast-in-situ pile <i>D.J. Klingberg & P. Mackenzie</i>	715
Is DLT the final word? Correlation between DLT and SLT <i>H. Goldemberg & J.J. Goldemberg</i>	719
Results of an international pile dynamic testing prediction event <i>A. Holeyman, J. Maertens, N. Huybrechts & C. Legrand</i>	725
Preparation of an international pile dynamic testing prediction event <i>A. Holeyman, J. Maertens, N. Huybrechts & C. Legrand</i>	733
Case studies of dynamic load testing in Japan <i>Y. Wakiya, K. Nishiumi, M. Hayashi, A. Shibata, S. Nishimura & T. Matsumoto</i>	741
Case studies of high capacity CFA pile testing in Australia <i>S. Baycan</i>	751
 11 Supplement	
Keynote lecture: Retrospective of Sonic Integrity Tests – Its application to the control quality on piles <i>J.J. Goldemberg</i>	757
 Author index	 771



Taylor & Francis

Taylor & Francis Group

<http://taylorandfrancis.com>

Preface

The application of dynamic testing based on the wave equation theory was first introduced in Brazil in 1981. Differently from other countries, its first application was on offshore piling. At that time, a great number of jacket type platforms began to be installed in the country by the Brazilian Oil Company, in waters with depths varying from 50 to 250 meters. The use of this technique also on land job sites experimented a continuous growth since then. In 1989, low strain integrity testing was introduced. In 1994, a code on the dynamic load testing of piles was issued by the Brazilian Technical Standards Association – ABNT. A couple of years later, in 1996, the same ABNT edited a revision of the Standard for Design and Execution of Foundations, which now accepts the use of dynamic load testing as one of the alternatives for bearing capacity evaluation. In the case of driven piles, it also allows for a reduction of the safety factor, from the usual value of 2 down to 1.6, provided that dynamic testing is performed on at least 3% of the piles on the job site, and that it is applied since the beginning of the piling.

The present event in the Southern Hemisphere, and particularly in South America, certainly will contribute to increase the utilization of this technique, thus helping improve the quality of pile installation in this region.

The support of the Brazilian Society for Soil Mechanics and Geotechnical Engineering – ABMS in hosting this conference had the purpose of trying to make the geotechnical and foundation engineering communities and the wave equation theory users work more closely together. The conference structure was modified, eliminating the traditional presentation of the papers, thus allowing more time for discussions. After five conferences, the first one organized by Dr H. Bredenberg of the Swedish Geotechnical Institute in 1984, we hope that discussions based on the papers and lectures presented in this proceedings might have contributed to improve the understanding and better interpretation of dynamic tests, not only for the executioners but specially for the users of the the tests.

Sussumu Niyama
Jorge Beim
Editors

SPONSORSHIP

Brazilian Society for Soil Mechanics and Geotechnical Engineering

SUPPORT

FINEP

Organization

ORGANIZING COMMITTEE

Niyama, Sussumu *Chairman*
Beim, Jorge *Secretary*

Andreo, Cristiana	Gonçalves, Cláudio
Aoki, Nelson	Mello, Jayme Ricardo de
Bernardes, George	Kormann, Alessander Morales
Campos, Gisleine Coelho	Merighi, Valmir
Cintra, José Carlos	Navajas, Sérgio
Danziger, Bernadete	Paraiso, Sérgio C.
Falconi, Frederico F.	Valverde, Sérgio

CONFERENCE ADVISORY COMMITTEE

Lopes, Francisco Rezende
Velloso, Dirceu de A.
Décourt, Luciano
Golombek, Sigmundo
Mello, Victor F.B. de

INTERNATIONAL ADVISORY COMMITTEE

Altaee, Ameir – Canada	Likins, Garland – USA
Amir, Joram M. – Israel	Matsumoto, Tatsunori – Japan
Burbano, Germán J. – Spain	Mendiguren, Eugenio – Argentina
Fellenius, Bengt H. – Canada	Middendorp, Peter – Netherlands
Fujita, Keiichi – Japan	Paikowsky, Samuel G. – USA
Goble, George G. – USA	Pinto, Paulo – Portugal
Goldemberg, Juan J. – Argentina	Randolph, Mark – Australia
Grävare, Carl-John – Sweden	Rausche, Frank – USA
Gutiérrez, Alvaro – Uruguay	Sakai, Tomoaki – Japan
Holeyman, Alain E. – USA	Seidel, Julian P. – Australia
Holloway, D. Michael – USA	Towsend, Frank C. – USA
Hussein, Mohamad H. – USA	Van Impe, William – Belgium
Kusakabe, Osamu – Japan	Van Weele, A.F. – Netherlands
Liang, Xu Ding – China	Veiga, Jose – Chile



Taylor & Francis

Taylor & Francis Group

<http://taylorandfrancis.com>

Acknowledgements

The editors are grateful to the following persons who helped to review the manuscripts and thus greatly assisted in improving the overall technical standard and presentation of the papers in these proceedings:

Kormann, Alessander Morales
Danziger, Bernadete
Grävare, Carl-John
Velloso, Dirceu de A.
Lopes, Francisco Rezende
Goldemberg, Hermán
Amir, Joram M.
Seidel, Julian P.
Svinkin, Mark R.
Randolph, Mark
Kusakabe, Osamu
Middendorp, Peter
Goble, George G.
Holeyman, Alain E.
Paikowsky, Samuel G.
Paraiso, Sérgio C.
Matsumoto, Tatsunori
Likins, Garland



Taylor & Francis

Taylor & Francis Group

<http://taylorandfrancis.com>

1 Wave mechanics and its application to pile analysis



Taylor & Francis

Taylor & Francis Group

<http://taylorandfrancis.com>

Keynote lecture: Some wave mechanics applications

George G.Goble

George G.Goble Consulting Engineer, University of Colorado, Boulder, Colo., USA

ABSTRACT: The solution to the one dimensional wave equation is used to determine the maximum impact force at the top of a concrete pile for a given ram weight, cushion stiffness, and pile impedance. The result is used to generate a set of curves that can be used to assist in the selection of a pile cushion as limited by maximum compression stress. A second problem, the wave equation modeling of the Statnamic load testing system, was also studied. The testing process was modeled using a wave equation computer program. A comparison of the commonly used damping model, Smith damping, with the Rausche model can be used to evaluate the appropriateness of the two models. This study indicates the desirability of the Rausche model and the necessity for further study to recommend appropriate values for the Rausche damping constant.

1 INTRODUCTION

The interest in one dimensional wave propagation theory for understanding pile driving is more than a century old. Perhaps, the pile driving problem was a major motivation in deriving and solving the one dimensional wave equation since those people that were active in that effort were mostly Civil Engineers. The important work done in this area that relates directly to current applications to pile driving started shortly after the Second World War and continued to the present.

Today it can be said, with confidence, that the use of one dimensional wave propagation theory is generally accepted and widely used in the pile driving industry. The hallmark of these applications is that they have centered on useful applications of the theory. In this paper, two topics will be discussed, one dealing with the closed form solution of the wave equation and the other, the discrete solution. Useful results will be presented in each case.

The one dimensional wave equation was derived and solved in the nineteenth century. Probably the most important contributions to the use of the closed form solution were made by Professor Fischer of Upsala University beginning in the early 1950's. He developed many useful applications of the solution including several graphical approaches. A summary of this work was presented at the Second Conference on the Application of Stress Wave Theory to Piles (Fischer 1984). This work laid the basis for the dis-

plays now generally used for presenting dynamic measurements, for many of the useful concepts for visually evaluating those measurements, and for current approaches to integrity testing of deep foundations. Since the basic work is complete and many direct applications of the theory well established it is unlikely that further fundamental developments will occur. It is appropriate to note that, while the use of the closed form solution has been very important in developing conceptual understanding of the mechanics of pile driving, it has been less useful for obtaining quantitative results.

Probably the most remarkable work in developing quantitative solutions was done by E. A. L. Smith, then Chief Engineer of the Raymond Company, at that time, the largest pile driving company in the world. Before 1950, he published notes on the development of a numerical solution to the wave propagation problem applied to pile driving (Smith, 1950). Shortly after, a proprietary program was operating on an electronic digital computer. Smith called this program the "Wave Equation" and it was widely publicized (for example, Smith, 1957; Smith, 1960). This program may have been the first application of electronic digital computers to a civilian engineering problem.

The implementation of wave equation analysis has been painstakingly slow. A public domain program was developed in the early 1960's at Texas A&M University and it was widely used in the offshore industry (Samson, et al 1963). Today, the

GRLWEAP™ program (Goble & Rausche 1976, GRLWEAP™, 1998) is widely used in the United States and that usage is increasing rapidly. It is becoming standard practice to perform driveability analyses both during the foundation design stage and at the beginning of construction. However, outside the United States usage is much less common.

2 PILE CUSHION SELECTION

A direct application of a closed form solution to the problem of selection of a pile cushion for driving a concrete pile will be presented. This solution can be used with the aid of graphs and it may be found to be useful in practice. Clough and Penzien (1975) solved the problem shown in Figure 1. The pile driving system is modeled by three elements, a rigid ram, a linear spring (cushion) and an elastic pile. The solution provides the maximum delivered impact velocity induced at the pile top during the first wave passage (among other things). This solution is used to generate curves for selection of the cushion stiffness required to limit the induced compression stress to some selected value.

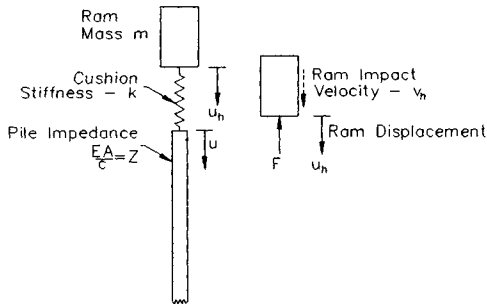


Figure 1. Pile Driving System Model

The equation of motion for the ram in contact with the cushion can be written

$$F = mg - m\ddot{u}_h \quad (1)$$

where the variables are defined in Fig. 1. Continuity of displacements requires that the ram motion equal the pile top motion plus the spring deformation.

$$F = u + \frac{F}{k} \quad (2)$$

This expression is differentiated twice and substituted into Equation (1). The resulting expression is solved for F and then expressed in terms of the stress in the pile as given by one dimensional wave mechanics.

$$F = \sigma A = AE\epsilon = AE \frac{\partial u}{\partial X} = \frac{AE}{c} \frac{\partial u}{\partial t} \quad (3)$$

where A is the cross sectional area of the pile, E is its elastic modulus, c is the velocity of wave propagation, σ is the stress at the top of the pile, ϵ is the strain at the top of the pile, x defines the distance from the top of the pile to some point on the pile, and t is time. This expression is substituted into the expression for the driving force, F, in Equation (1). It is then written in terms of the displacement of the pile top and the resulting expression is rearranged and expressed in terms of the pile top velocity, v.

$$\ddot{v} + \frac{k}{Z} \dot{v} + \frac{k}{m} v = 0 \quad (4)$$

In Equation (4), the weight of the ram has been neglected and Z is the pile impedance, EA/c. This familiar equation form has the solution

$$v = e^{-\xi\omega t} (A \sin \omega_D t + B \cos \omega_D t) \quad (5)$$

The variables k/m and k/Z in Equation (4) have been replaced by ω^2 and $2\omega\xi$, respectively, and

$$\omega_D = \omega \sqrt{1 - \xi^2} \quad (6)$$

If the initial conditions of the pile top velocity, v, and the ram impact velocity, v_h , are imposed, the expression for the velocity at the top of the pile becomes

$$\frac{v}{v_h} = \frac{2\xi\omega}{\omega_D} e^{\xi\omega t} \sin \omega_D t \quad (7)$$

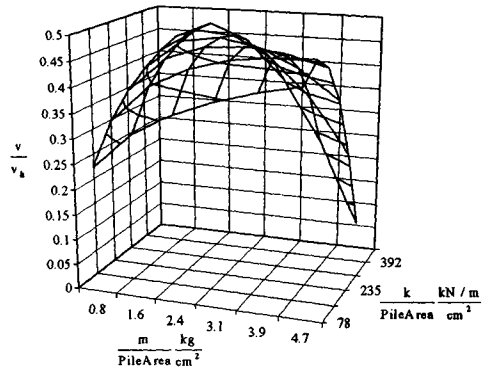


Figure 2. Values v/v_h for pile stiffness, ram mass, with given impedance

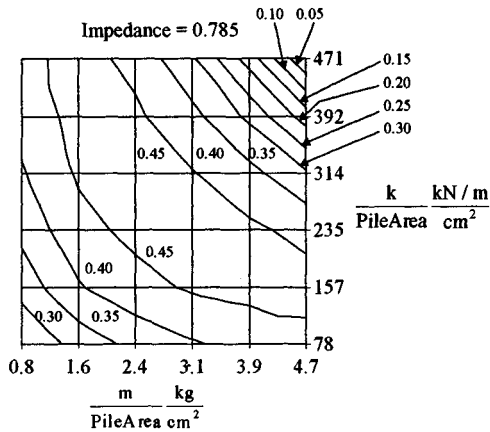


Figure 3. Values v/v_h for pile stiffness, ram mass, and impedance all divided by pile area

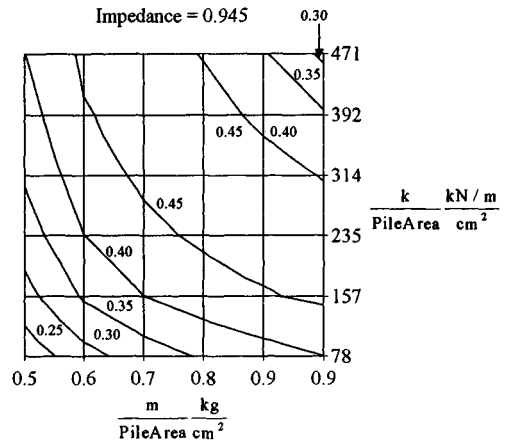


Figure 5. Values v/v_h for pile stiffness, ram mass, and impedance all divided by pile area

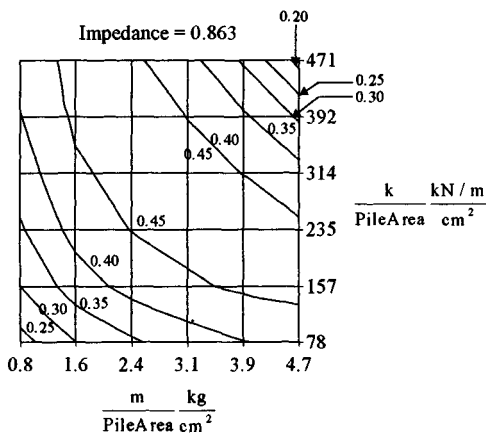


Figure 4. Values v/v_h for pile stiffness, ram mass, and impedance all divided by pile area

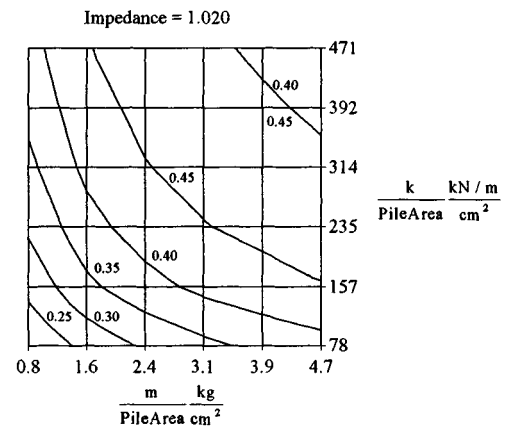


Figure 6. Values v/v_h for pile stiffness, ram mass, and impedance all divided by pile area

Maximum values of v/v_h were determined for a range of values of ram mass, cushion stiffness, and pile impedance.

A parameter study was made for a 300 mm square pile with a full range of practical values of ram mass, cushion thickness, and concrete modulus. Values of the ratio of the pile top velocity to the ram impact velocity, v/v_h , were determined for a range of values of ram mass and cushion stiffness, and four values of pile impedance. An example of the results is shown in Figure 2 where the surface of v/v_h is given for a range of values of k and m with a specific value of pile impedance, Z . Such a representation cannot be

used quantitatively so contours for four values of Z are given in Figures 3 through 6.

In order to use the curves, trial cushion stiffness and ram mass is selected, and they are divided by the pile area. Likewise, the pile impedance divided by the pile area is also determined. Using the appropriate figure, the pile velocity–ram velocity ratio is determined from the curve. This quantity is multiplied by the anticipated ram impact velocity to obtain the maximum particle velocity transmitted to the pile top. The particle velocity times the pile impedance gives the maximum impact force transmitted to the pile.

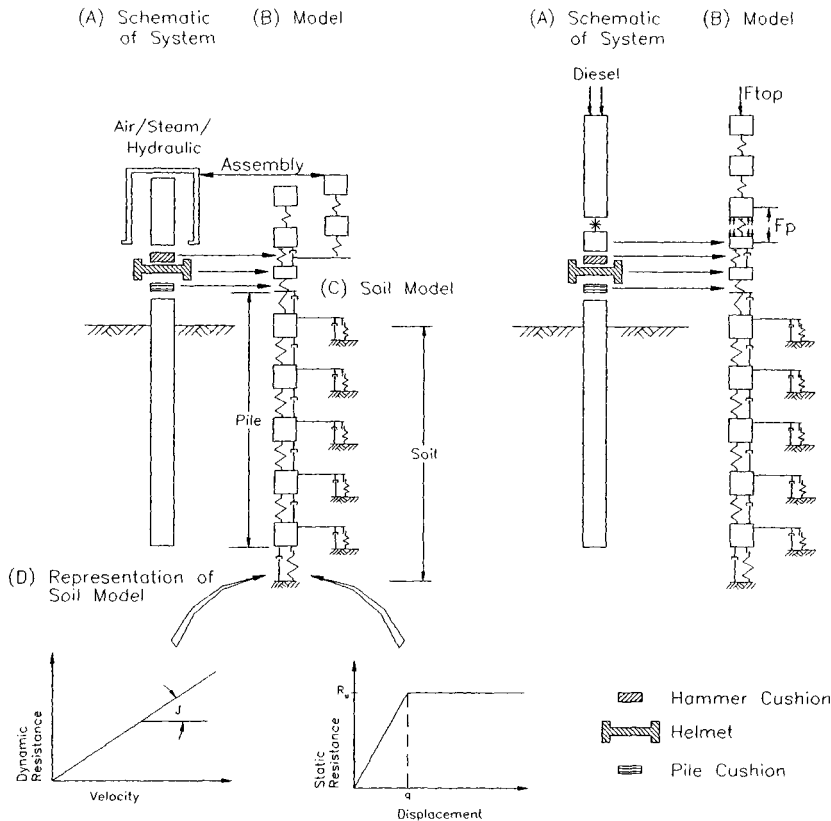


Figure 7. Wave equation model

It should be noted that the model does not include the hammer cushion or the helmet mass. Furthermore, the result has not been tested against field experience and such testing must be done to assure the usefulness of the results.

3 WAVE EQUATION DAMPING MODEL

Wave equation analysis is now used routinely in land pile driving practice in the United States and also in controlling the installation of piles for offshore petroleum recovery platforms. The model used for wave equation analysis is shown in Figure 7. The three principal problems that limit the accuracy of wave equation analysis are a lack of knowledge of the driving efficiency for a particular pile driving hammer, an occasional, surprisingly large quake value, q , and a lack of accuracy in the soil damping constant, j .

There can be little hope of ever accurately knowing the actual hammer efficiency prior to going to the field. Even after beginning driving the hammer efficiency will only be known when measurements are available.

The actual quake that exists during pile installation is dependent on the size of the pile cross section and on soil properties. Quake values can be assigned based on the pile cross section but when a large quake is due to soil properties it cannot be predicted in the current state-of-the-art. Fortunately, this characteristic occurs infrequently. Experience with dynamic measurements and signal matching analysis indicates that this problem usually occurs during extended driving and is probably pore pressure dependent. It disappears in re-strike testing. A solution to this problem will depend on a better understanding of soil behavior.

Damping constants have been selected based on tradition using the original recommendations of Smith (1960). They are selected based on soil type and they show a wide range of accuracy based on signal matching analyses (Rausche et al 1994). This variability can strongly affect the results of wave equation analysis. Rausche et al (1994) suggested a different model that is based on the work of Coyle and Gibson (1970). Coyle's research, further proven by Herema (1979), indicates that the dynamic resistance has a strongly nonlinear relationship to the velocity of pile motion. The study by Rausche et al indicated that the direct application of the Coyle research caused numerical problems. A suggestion by Rausche avoided those problems.

The traditionally used Smith model states

$$R_t = R_s(1 + j_s v) \quad (8)$$

where R_t is the total soil resistance, R_s is the current value of the static resistance, and j_s is the Smith damping constant. This model becomes viscous when the static resistance is equal the ultimate resistance. Based on laboratory testing Coyle showed that a more appropriate law would be

$$R_t = R_s(1 + j_g v^N) \quad (9)$$

where j_g is the Gibson damping constant and N is an exponent, typically less than 1.0. The difficulty with this representation is that numerical problems arise when the velocity changes sign. Rausche suggested that damping be represented by

$$R_t = R_s \left[1 + j_R v_x^N \frac{v}{v_x} \frac{R_s}{R_s} \right] \quad (10)$$

where j_R is the Rausche damping constant, v_x is the maximum velocity achieved up to a particular time during the blow, and R_s is the maximum static resistance actuated prior to the time under consideration. Both the Smith and the Rausche model are available in GRLWEAP™.

The Statnamic method (Janes et al 1994) uses a charge of slow burning explosive to generate a force between a large mass and the pile top. As the mass is accelerated upward a downward acting force is induced against the pile top. This force has a slower rate of increase than the typical ram impact used in dynamic testing. Force pulses of the length of 80-100 ms are common. The resulting test must still be

evaluated as dynamic but it is slower than the traditional dynamic test.

The Statnamic test was modeled using a mass of the typically used size as a "ram" in GRLWEAP™. It was dropped on the top of the pile with a cushion having a very soft spring. The spring constant was selected by trial-and-error so that a force pulse of about 100 ms was generated. The magnitude of the peak force was controlled by the ram drop height. The test pile used in the study was a closed-end steel pipe with a length of 24 meters and an ultimate capacity of 4000 kN. An example of the force-time and velocity-time record for one of the tests is shown in Figure 8.

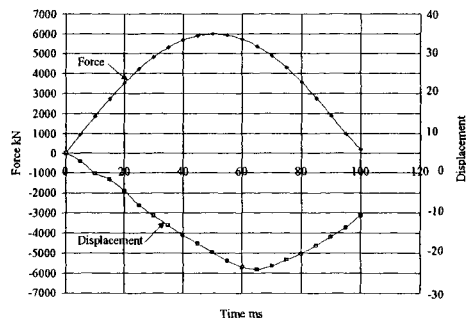


Figure 8. Statnamic Test – Force and Displacement vs. Time

Four cases were studied, each with a range of applied forces. They are (a) Smith damping for sand, (b) Rausche damping for sand, (c) Smith damping for clay, and (d) Rausche damping for clay. The results are given in Figures 9 through 12.

In Figure 9 the force-displacement results for the case of the pipe pile in sand is shown. The wave equation results include the top force in the pile as a function of time together with the pile top displacement. The maximum applied force was 5200 kN. In this case a maximum displacement of 55 mm was achieved. The method that has been recommended for use in determining the static capacity was to use the force at the time of zero velocity and adjust this force by the mass of the pile times the acceleration at that same time. This method was first suggested by Nara (1970) and was used by the Case Research project (Goble & Rausche, 1970). It can be seen in Figure 9 that this method gives quite good results when compared with the specified static capacity of 4000 Kn. The applied forces were 5200 kN, 4840

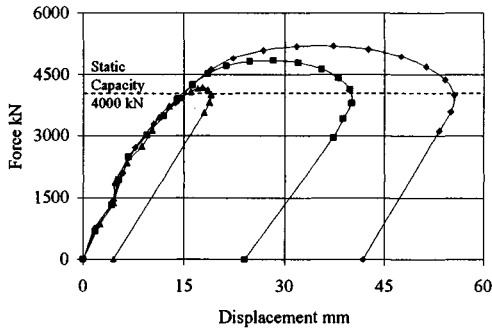


Figure 9. Force-displacement curves for three tests modeled by GRLWEAP using Smith damping for sand.

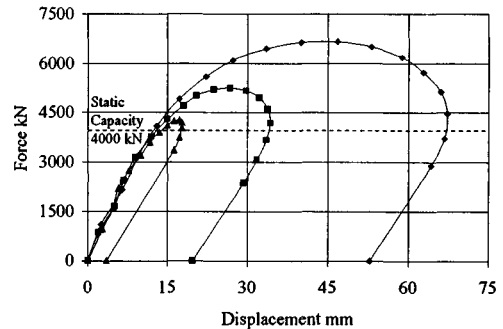


Figure 11. Force-displacement curves for three statnamic tests modeled by GRLWEAP using Smith damping clay.

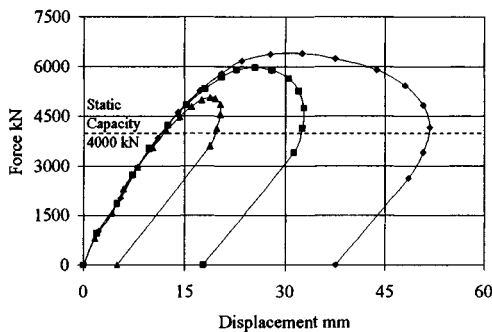


Figure 10. Force-displacement curves for three tests modeled by GRLWEAP Rausche damping for sand

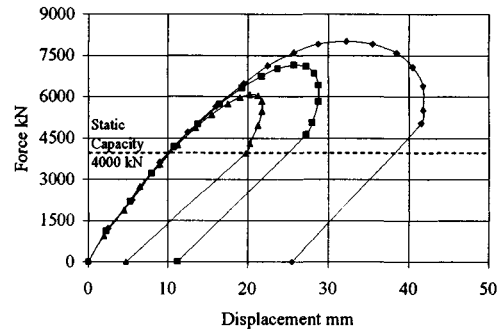


Figure 12. Force-displacement curves for three tests modeled by GRLWEAP using Rausche damping Clay.

kn, and 4180 kN. In all three cases the capacity at maximum displacement was about 4000 kN. The adjustment for the acceleration at zero velocity (inertia force) would be small due to the low mass of the pile.

Rausche damping was applied to the same sand example and the results are shown in Figure 10. Forces of 6400 kN, 5960 kN, and 5060 kN were applied. The results for the two larger forces, given by the capacity at zero velocity, are reasonably close to the static capacity. However, the case of the smallest applied force gives a predicted static capacity of about 4800 kN, about 20 percent larger than the given capacity.

Examples of the modeling of Statnamic tests in clay for the same pile that was analyzed above are given in Figures 11 and 12. Figure 11 shows the results for three Statnamic tests of different applied force levels

in a clay soil. The usual Smith damping constant result is given in Figure 11. The predicted static capacity for all three Statnamic load levels are all quite close to the known static capacity.

Figure 12 shows the result for Rausche damping in clay for applied forces of 8000 kN, 7150 kN, 6070 kN, and 5450 kN. The associated predicted static capacities are 6400 kN, 6400 kN, 5830 kN, and 5240 kN, respectively. All of these values are quite high with the largest 60 percent too large.

This study showed that it was possible to induce Statnamic-like forces using a wave equation analysis by GRLWEAP™ without modification for this particular application. The force time record is of the appropriate length and a similar shape. The force-displacement curve has the appropriate shape and appearance.

It is well-known that the Smith damping representation does not produce results that agree with experience. (Rausche et al 1994) has shown that the Smith damping constant does not agree with measurements for the assumptions used. Some results reported for Statnamic (James et al 1994) show a character of result that agree with the wave equation analysis. In particular, the case presented with Rausche damping for sand has the observed result. As the applied Statnamic force is increased the agreement between the evaluation method used and the actual capacity is improved. The conclusion has been reached that a substantial permanent set should be achieved.

The results presented here support the idea that the Rausche damping constant should be studied further and that recommendations should be developed for the required damping constants.

CONCLUSIONS

Curves are presented to assist in obtaining cushion stiffness requirements for concrete piles to limit the induced compression stress at the top of the pile. Impact stresses can be determined for a selected set of ram mass, cushion stiffness, and pile impedance. These values have been found for reasonable ranges of the variables using a closed form solution of the one dimensional wave equation. They have not been checked against field measurements and such checks should be performed. It should also be noted that the analysis does not include the pile cushion and the helmet.

A wave equation study is reported on the modeling of the Statnamic test. The model matches the variation of the induced force at the pile top quite well. Smith and Rausche damping representations have been studied. The Rausche damping representation seems to match the field observed results. In view of the observed poor comparison between the Smith representation and field observations it would be desirable to determine appropriate Rausche damping constants by additional studies.

REFERENCES

- Clough & Penzien 1975. *Dynamics of Structures*. McGraw-Hill, Inc., New York.
- Coyle, H. M. & G. C. Gibson 1970. Empirical damping constants for sands and clays. *Journal of Soil Mechanics and Foundations Division*, ASCE.
- Fischer, H. C. 1984. Stress wave theory for pile driving application. lecture at the *Second International Conference on the Application of Stress Wave Theory on Piles*, Stockholm, Sweden.
- Goble, G. & F. Rausche 1970. Pile load test by impact driving. *Highway Research Record*, No. 333.
- Goble, G. G. & F. Rausche, 1976 Wave equation analysis of pile driving - WEAP program. Volumes 1 through 4, FHWA #IP-76-14.1 Through #IP-76-14.4.
- GRLWEAP™ - Wave equation analysis of pile driving 1998. Goble Rausche Likins and Associates, Inc., Cleveland, Ohio.
- James, M., A. Sy, & R. Campanella 1994. A comparison of statnamic and static load tests on steel pipe piles in the Fraser Delta. *Proceeding of the 8th Annual Symposium on Deep Foundations*, Vancouver Geotechnical Society, Vancouver, B.C., Canada.
- Heerema, E. P. 1979. Relationships between wall friction displacement velocity and horizontal stress in clay and in sand for piled driveability analysis. *Ground Engineering*.
- Rausche, F., G. Likins, and G. Goble 1994. A rational and usable wave equation soil model based on field test correlation. *Proceeding International Conference on Design and Construction of Deep Foundations*, Orlando, Florida, December.
- Rausche, F., G. Thendean, H. Abou-matar, and G. Goble 1994. Investigation of dynamic and static pile behavior from modified standard penetration tests, *Federal Highway Administration Report*.
- Samson, C. H., T. J. Hirsch, jr., & L. L. Lowery, 1963. Computer study for dynamic behavior of piling. *Journal of the Structural Division*, ASCE, Volume 89, No. ST4.
- Smith, E. A. L. 1950. Fundamentals of electronic calculation - pile driving impact. International Business Machines.
- Smith E. A. L. 1957. What happens when hammer hits pile. *Engineering News-Record* 159, September, 5.
- Smith, E. A. L. 1960. Pile driving analysis with the wave equation. *Journal of the Soil Mechanics and Foundation Engineering Division*, ASCE, No. 86, August.



Taylor & Francis

Taylor & Francis Group

<http://taylorandfrancis.com>

Analysis of bearing capacity of rock-socketed piles based on wave equation theory

Lai-bing Cai

Fujian Academy of Building Research, Fuzhou, People's Republic of China

ABSTRACT: Based on wave equation theory, a dynamic loading model is used to analyze the behaviors of rock-socketed piles in this paper. The results of dynamic loading tests are analyzed by CAPWAP. From the analyzed results of twelve dynamic loading tests on rock-socketed piles, the behaviors of shaft resistance of the socket and toe resistance are discussed, a relationship of shaft resistance of socket to the length of socket and the rock strength and the construction of piles is presented. And the parameters of dynamic loading tests are estimated. Some suggestions for dynamic loading tests of rock-socketed are made to analyze the bearing capacity.

1 INTRODUCTION

Smith (1960) initially made numerical analysis on one-dimensional wave equation of pile foundation with the finite difference scheme. From then on, many scholars put up with their numerical models and gave the calculating formulations all over the world, so wave equation analyzing method was widely applied to engineering practice. Basing on the previous research results, Goble et al. (1980) modified the model with better formulation, and put out the program of CAPWAP, which can better simulate the fact of pile-soil interaction. Thereby, it was virtual stage for wave equation taken into engineering practice. At present, wave equation analyses are used to simulate the process of driving pile, judge the feasibility of driving pile and the damage of pile, and determine the bearing capacity of pile.

Rock-socketed pile foundations can provide an effective and economical means of transmitting large concentrated structural loads through overburden soils to underlying rock, especially under the condition of overburden soil being soft and rock embedding shallowly. The bearing behaviors of rock-socketed pile change with rock geological condition, construction technology, sediments of pile bottom, rock-socketed depth and so on. It would be taken much manpower and many financial or material resources to determine bearing capacity of rock-socketed pile by static loading tests.

Based on the theory of wave equation, a dynamic loading model of rock-socketed pile is ad-

vanced in this paper. Through analyzed the results of CAPWAP, the bearing behaviors of rock-socketed pile are discussed and a method is given to determine the bearing capacity.

2 DYNAMIC LOADING MODEL

During wave equation analyzing, the total driving resistance R can be broken up into two distinct portions: the static resistance R_s and dynamic resistance R_d ,

$$R = R_s + R_d \quad (2.1)$$

The static resistance and the dynamic resistance are represented by

$$R_s = \begin{cases} k_s \cdot u, & u < q \\ R_u, & u \geq q \end{cases} \quad (2.2)$$

$$R_d = J_v \cdot v = J \cdot R_s \cdot v \quad (2.3)$$

In above equations (2.2) and (2.3), k_s is soil stiffness, R_u is ultimate static resistance, q is loading quake, J_v is viscous damping factor, J is Smith damping factor.

When the pile exerts a force on the soil, it causes the soil surrounding the pile to move. By analyzing energy formula, as the pile motions are small such that a shear failure of soil around pile does not occur, a wave is generated in the soil

$$E_{pile} = R \cdot u + E_{wav} \quad (2.4)$$

Where E_{pile} is energy in pile, E_{wav} is energy of wave generating in soil.

A radiation damping dynamic model is built to resolve the energy dissipating in pile-soil interfaces, where the energy is radiated rather than consumed for soil shearing, shown as Figure 1.

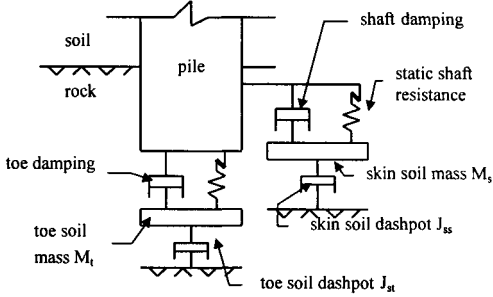


Figure 1. Radiation damping dynamic model for rock-socketed pile

For the above model, the soil support dashpots work only during dynamic event, not during static event. The governing equation (2.2) and (2.3) are changed in that the pile motion variables u , v are replaced by the relative variables u_r , v_r .

The motion variables u_s , v_s of the soil support mass are calculated simply by

$$\begin{aligned} u_{s,j} &= u_{s,j-1} + v_{s,j-1} \cdot \Delta t \\ v_{s,j} &= v_{s,j-1} + (R_s \pm v_{s,j-1} \cdot J_r) / (J_r + M_r / \Delta t) \end{aligned} \quad (2.5)$$

Where Δt : time increment, J_r : shaft soil radiation dashpot or toe soil radiation dashpot, M_r : shaft soil support mass or toe soil support mass.

The relative variables u_r , v_r can be written as

$$\begin{aligned} u_{r,i} &= u_i - u_{s,i} \\ v_{r,i} &= v_i - v_{s,i} \end{aligned} \quad (2.6)$$

3 BEARING BEHAVIORS OF ROCK-SOCKETED PILE

The bearing capacity of rock-socketed pile can be divided into three components: shaft resistance of overburden soils Q_{sk} , shaft resistance and toe resistance of the socket, shown as

$$Q_{uk} = Q_{sk} + c\zeta_s f_w l_r + \zeta_t f_w A_t \quad (3.1)$$

Where c : circumference of pile, ζ_s , ζ_t : are respectively shaft resistance coefficient and toe resistance coefficient.

The behaviors of shaft resistance and toe resistance of socket are expounded as following.

3.1 Shaft resistance

The behaviors of shaft resistance of socket can be influenced by the roughness of the socket wall.

However, the construction of pile influences the roughness. Two cases are taken into account: case (I), for hand-dug belled pile, explosion is used to mine the rock, which results in the very roughness of socket wall and relatively fractured rock under pile bottom. The same outcomes arise for percussion-drilled pile. Case (II), for bored pile, the socket wall is relatively smooth and the rock under pile bottom is relatively less shattered. Compared to case (II), the shaft resistance raises and the toe resistance falls somewhat in case (I).

According to the results of the static load tests^{[6],[7]}, the relations between the shaft resistance and the relative displacement for the above two cases are shown as Figure 2.

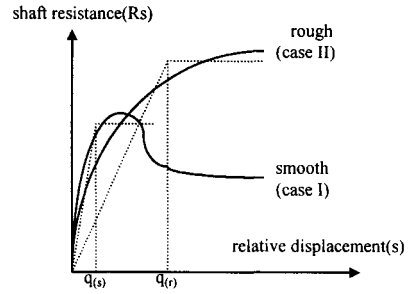


Figure 2. Relation between shaft resistance and relative displacement

In case (I), the shaft resistance R_s increases with the relative displacement, and it shows a harden trend. For dynamic analyses of rock-socketed pile, the trend can be regarded as an elastic-plastic relation, and the elastic quake may value between 4mm and 6mm, and the ultimate static resistance ranges $(0.15 \sim 0.20) \sqrt{f_w}$ (f_w is unconfined compressive strength of rock)^{[6],[7]}.

In case (II), the trend differs by the shaft resistance decreasing after the mobilized displacement. And the quake q_s takes value between 2mm and 4mm, the value of ultimate static resistance is about $(0.15 \sim 0.20) \sqrt{f_w}$ ^{[6],[7]}.

3.2 Toe resistance

Toe resistance raises slowly with the displacement unless the concrete of pile comes to failure. It needs a large displacement for toe rock to reach plastic failure. The fractured rock makes the difference of toe resistance: a more fractured rock produced more reduction of toe resistance. Therefore, a high value of toe resistance happens in case (I) against case (II). The shaft resistance and the toe resistance should be adjusted according to the construction of rock-socketed pile.

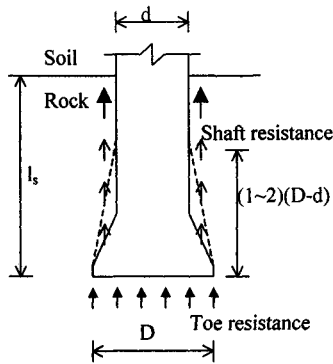


Figure 3. Behaviors of hand-dug belled pile

4 DYNAMIC ANALYSES OF ROCK-SOCKETED PILE

Based on the above model, the results of twelve dynamic load tests on rock-socketed piles are discussed. The parameters of piles and the results of CAPWAP are given in Tab. 1 and the CAPWAP results of TP1 are shown in Figure 4.

4.1 Analyses of bearing behaviors

Piles TP1 to TP4 were hand-dug belled piles, and the toe rock was medium weathered marl breccia, which belonged to soft rock. Note that the ratio $t_s (=R_s/R_t)$ of shaft resistance over toe resistance has a value of 1/16~1/13. The results of CAPWAP for pile TP1 shows that the shaft resistance of 1.8 time $(D-d)$ (d, D are respectively shaft diameter and belled bottom diameter) length over belled bottom is lower than other portions of socket,

shown as Figure 3. It comes to conclusion that the belled bottom reduces the shaft resistance above it. This result reasonably conforms to the results of static loading tests^[6]. Medium weathered granites were observed as the bearing strata of pile TP5 to pile TP11. The ratio t_s achieves values of 1/24 to 1/20 for TP5~TP7 and 1/36~1/30 for TP8~TP11 (see Table 2).

Pile TP12, 72.0m length, was socketed into medium weathered granite about 2.0m. Length of strongly weathered granite was up to 45.0m and the corresponding mobilized shaft resistance was 94kPa, which shared about 80% total load. The socket only bore 20% total load.

As stated, the bearing behaviors of rock-socketed pile depend on the length of pile, the construction, the rock type, and the roughness of socket wall. A long pile ($l/d > 40$) lowers the mobilization of the socket to a degree. The socket wall of hand-dug belled pile or percussion-drilled pile is rougher than that of bored pile, which causes high shaft resistance. And the shaft resistance differs with the rock type. The behaviors of rock-socketed piles with long length are coincident to the results of static loading tests^[11,13].

4.2 Analyses of dynamic parameters

Tab. 2 presents the results of dynamic parameters of radiation damping dynamic model for the twelve tests. Final values of dynamic parameters are observed as following: $(0.4\sim 1.5)EA/c$ for shaft soil dashpot J_{ss} ; $(1\sim 20)EA/c$ for toe soil dashpot J_{st} ; the weight of the soil in a cylinder with same length and diameter equal to 3 time pile diameter for shaft soil support mass M_s ; the weight of the soil in a cylinder with same toe plate and depth extending to 5 time socket diameter for toe soil support mass M_t .

Table 1. Parameters of piles and dynamic analyzing results

Pile No.	Diameter d (mm)	Length l (m)	Length of socket (m)	Toe bearing Q_t (kN)	Load of pile Q (kN)	Ratio $t_q (Q_t/Q)$	Rock type of socket
TP1 ⁽¹⁾	1400	11.33	4.50	24700	34200	0.722	Marl breccia
TP2 ⁽¹⁾	900	10.12	0.80	9900	12600	0.786	Marl breccia
TP3 ⁽¹⁾	1400	10.10	1.30	27000	34600	0.780	Marl breccia
TP4 ⁽¹⁾	1400	10.83	1.00	25000	31000	0.806	Marl breccia
TP5 ⁽²⁾	1200	17.30	1.50	15200	25000	0.608	Granite
TP6 ⁽²⁾	1200	6.42	0.80	18800	26400	0.712	Granite
TP7 ⁽²⁾	800	7.48	0.60	5100	7550	0.675	Granite
TP8 ⁽³⁾	1200	8.08	1.00	19900	25500	0.780	Granite
TP9 ⁽³⁾	1200	7.14	1.00	16000	22000	0.727	Granite
TP10 ⁽³⁾	1000	7.93	1.00	15600	21900	0.712	Granite
TP11 ⁽³⁾	1000	8.35	1.00	13200	19500	0.677	Granite
TP12 ⁽⁶⁾	1300	72.17	2.00	3000	24500	0.112	Granite

- (1) The piles were hand-dug belled piles, and the belled bottom diameters of TP1, TP2, TP3, and TP4 were respectively 2600 mm, 1900 mm, 3000 mm, and 2600 mm;
- (2) The piles were percussion-drilled piles;
- (3) The piles were bored piles;

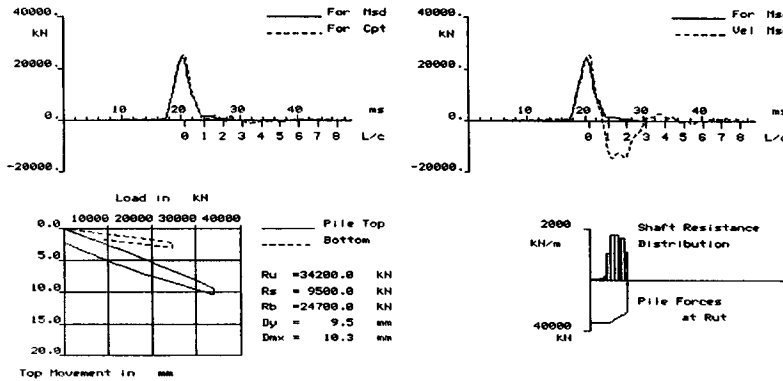


Figure 4. The results of CAPWAP for TP1

Table 2. Shaft resistance of socket, toe resistance and dynamic parameters

Pile No.	Shaft resistance (kPa)	Toe resistance (kPa)	Unconfined compression f_w (MPa)	Shaft damping dashpot J_{ss} (EA/c)	Toe damping dashpot J_{st} (EA/c)	Shaft soil support mass M_s (kN)	Toe soil support mass M_t (kN)
TP1	340	4600		0.50	4.00	150	300
TP2	290	3500		0.60	19.80	60	200
TP3	250	3800	2.0~8.0	0.45	19.00	150	300
TP4	300	4700		0.45	9.30	50	150
TP5	630	13400		0.60	6.50	50	120
TP6	710	16500	10.0~40.0	0.80	12.00	80	150
TP7	550	11500		1.00	17.00	50	80
TP8	490	17500		0.60	14.00	100	150
TP9	460	14100		1.20	11.60	150	200
TP10	560	19800	10.0~40.0	1.50	5.50	100	200
TP11	480	16800		1.00	16.00	100	200
TP12	120	2260					

5 CONCLUSIONS

Utilizing wave equation, a radiation damping dynamic model is suggested herein for rock-socketed pile. By analyzing the results of twelve dynamic loading tests, the following conclusions are made.

1. Radiation damping dynamic model resolves the energy dissipating in pile-rock interfaces for rock-socketed pile.
2. Bearing behaviors of rock-socketed pile depend on the length of pile. A long pile ($l/d > 40$) has less mobilizing action of the socket, but for a short pile ($l < 20\text{m}$ and $d \geq 800\text{mm}$) the socket will undertake 70%~95% total load.
3. The ratio t_s of shaft resistance to toe resistance depend on the rock type and the construction of pile. For soft rock, the ratio t_s achieve values of 1/20 to 1/10, but for granite, it ranges between 1/40 and 1/20.
4. For hand-dug belled pile, belled bottom reduces the shaft resistance of socket and the influent length over bottom ranges about $(1\sim 2)(D-d)$.
5. The bearing capacity of rock-socketed pile can be determined by dynamic loading test with rational dynamic parameters.

REFERENCES

- [1] Shi Pei-dong. Vertical Bearing Capacity of Rock-Socketed Pile. *Chinese Journal of Geotechnical Engineering*, Vol.16, No.4, 1994.
- [2] Robert G.Horvath & T. Cameron Kenney. Shaft Resistance of Rock-Socketed Drilled Piers. *Deep foundation*, 182-211.
- [3] *Code for Design and Investigation of Building Soil and Foundation*, DBJ13-07-91, Fujian province in China.
- [4] *Technical Code for Building Pile Foundation*, JGJ94-94, China
- [5] *CAPWAP Manual*. Goble Rausche Likins and Associates, Inc. 1993
- [6] Feng Shi, Chun Liu & Lai-bing Cai. *Experimental Research on Bearing Capacity of Belled Piles*, Fujian Academy of Building Research, 1997
- [7] Zhang Yiao-nian & Gong Yi-ming. *Research on Bearing Capacity of Large-Diameter Pile in Fuzhou*, Fujian Academy of Building Research, 1995



Taylor & Francis

Taylor & Francis Group

<http://taylorandfrancis.com>

Pile acceptance based on combined CAPWAP analyses

Robert F. Stevens

Fugro-McClelland Marine Geosciences Incorporated, Houston, Tex., USA

ABSTRACT: The pile driving hammer selected for a particular installation may be large enough to drive the piles to design penetration, but not large enough to overcome the long-term static capacity. In clay, the skin friction during driving is generally much smaller than that mobilized under static loading because large excess pore pressures are generated during continuous driving. CAPWAP analyses are used to estimate the distribution of the soil resistance to driving along the length and at the toe of a pile during continuous driving and after a set-up period. It is shown that by combining these results, it is possible to proof test a pile without the expense of mobilizing a larger hammer to the site. Examples are provided to illustrate the use of combined CAPWAP analyses to interpret the results of redrive tests in clay and to estimate the static pile capacity when refusal occurs during continuous driving.

1. INTRODUCTION

Pile driving is monitored using strain transducers and accelerometers attached near the pile top. The energy transmitted to the pile is obtained by integrating the product of the measured pile top force and velocity. The ratio of the transmitted energy to the rated hammer energy is defined as the system efficiency. The ram momentum is obtained by integrating the measured pile top force until the measured velocity equals zero. The ram impact velocity is obtained by dividing the ram momentum by the ram mass. The soil resistance to driving is determined from the measured force and velocity and a damping coefficient that is a function of soil type. The cushion stiffness and cushion coefficient of restitution are obtained by using force-time characteristics (rise time and peak-to-peak time) obtained in a pre-installation parametric study.

A signal matching program, such as the CAse Pile Wave Analysis Program (CAPWAP) developed by Rausche (1970), is used to estimate soil quake and damping parameters, and the distribution of the soil resistance to driving along the length and at the toe of the pile. The pile is divided into continuous segments and calculations are made using a traveling wave algorithm. Either the measured pile top force or velocity is used as a boundary condition, and the complementary quantity is computed and compared with the measured quantity. The set of soil parameters is

varied until a best match between measured and computed pile top force or velocity is obtained.

During continuous driving, the clay surrounding a pile is remolded and large excess pore water pressures are generated. Because the excess pore pressures decrease rapidly with radial distance from the pile, water will begin to flow laterally out of the disturbed zone and the clay will consolidate. As pore pressures dissipate, pile capacity increases. Field measurements (Bogard and Matlock, 1990) have shown that the time required for driven piles to regain full capacity can be relatively long. Redrive tests are valuable because a substantial increase in capacity occurs within a relatively short period of time after driving is terminated.

2. CASE HISTORY NO. 1

Our first case history is for a redrive test performed with a hammer that was large enough to mobilize the full soil resistance. Two 14-in.-square precast prestressed concrete piles having a length of 75 ft were driven with a Vulcan 010 hammer. Soil conditions consisted of fill to 8 ft, very soft to soft clay to 33 ft, medium-dense sand to 44 ft, underlain by firm to stiff clay. To aid the installation, a 9-in.-diameter pilot hole was drilled to a depth of 40 ft. The maximum resistance encountered during initial driving occurred in the sand stratum, even with pre-drilling. The piles were driven to a depth of 66 ft, with a final blow count of 10 blows per foot (bpf).

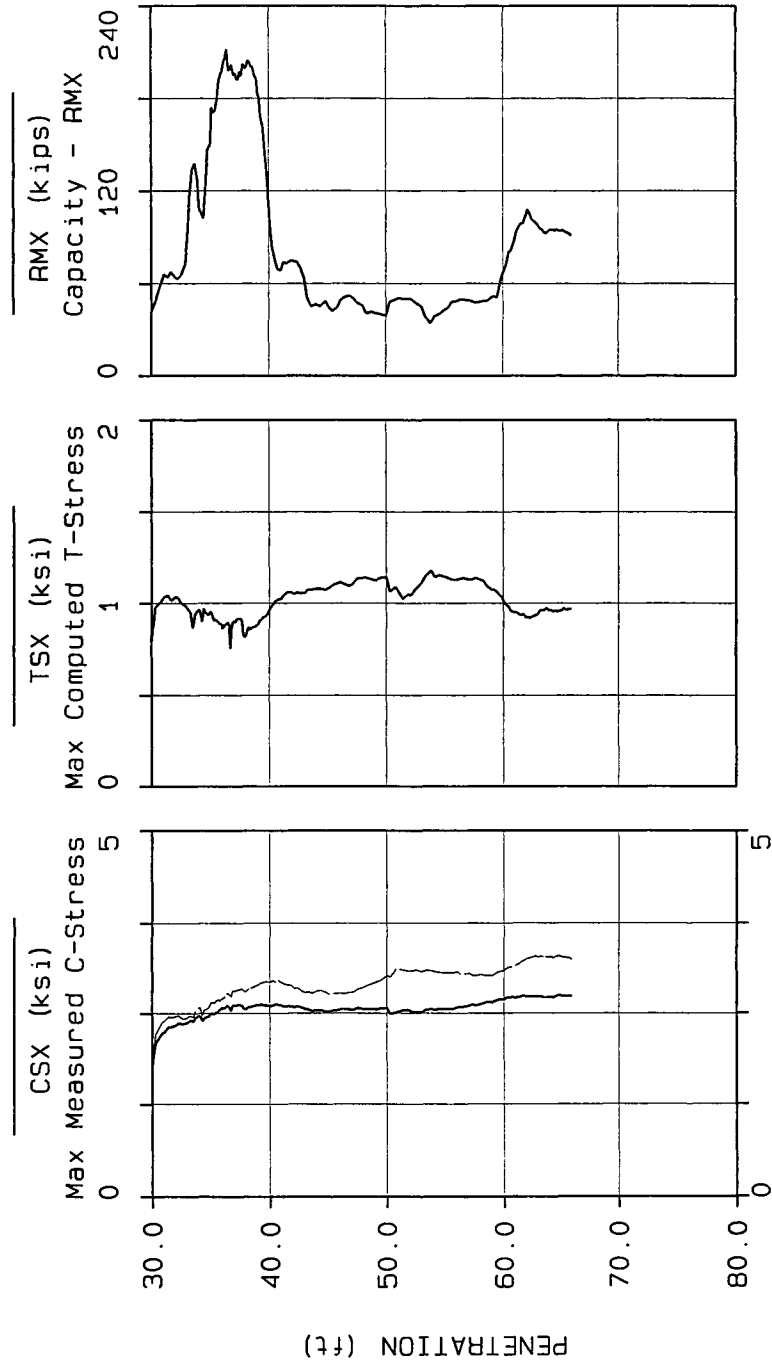


Figure 1. Stresses and Soil Resistance Measured for Continuous Driving of Pile 271

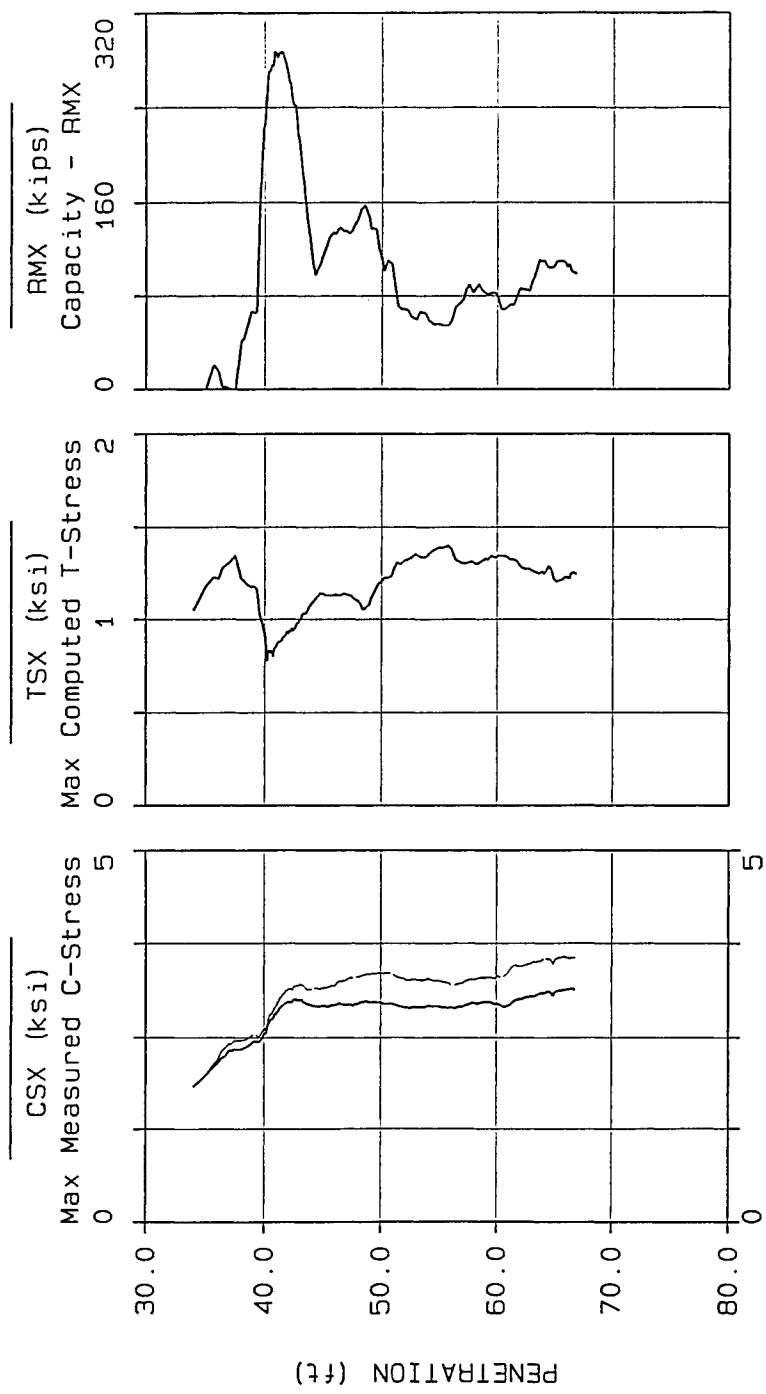


Figure 2. Stresses and Soil Resistance Measured for Continuous Driving of Pile 480

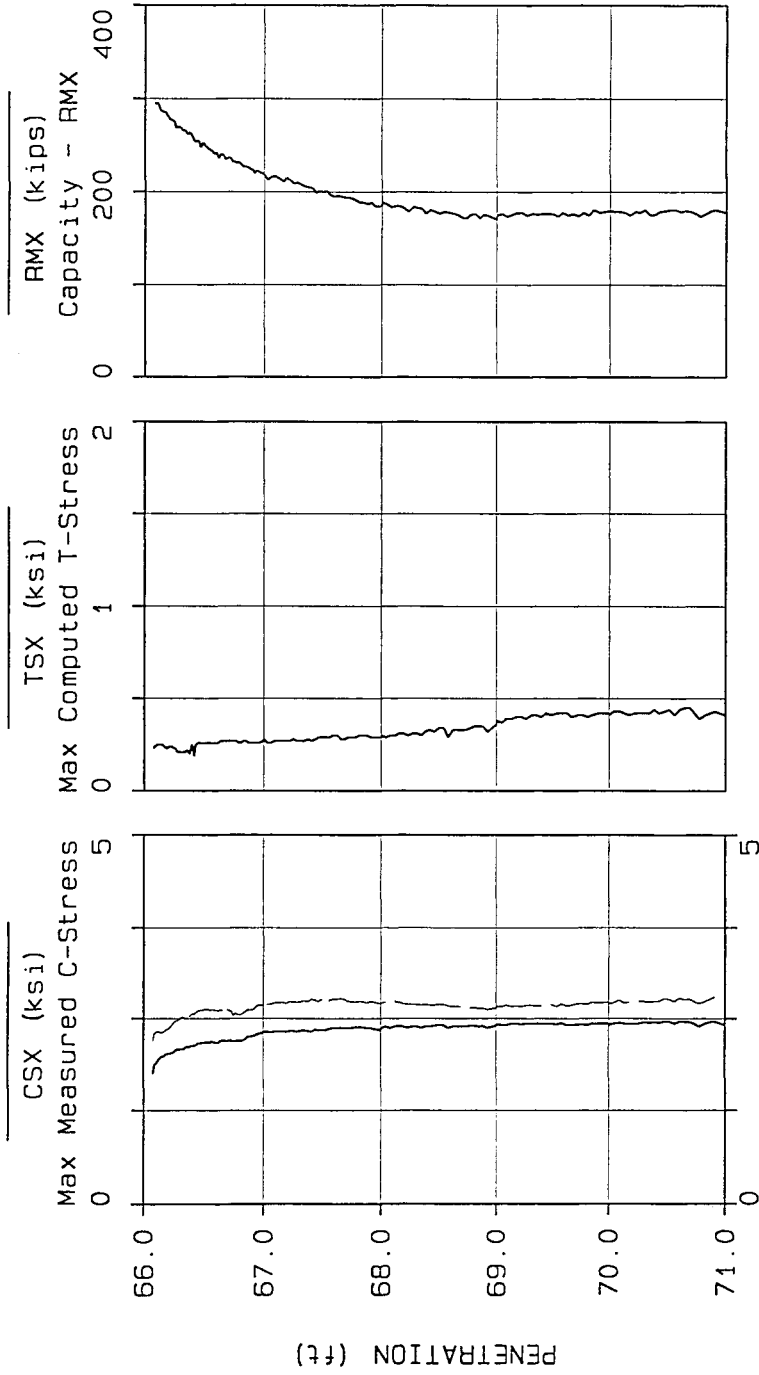


Figure 3. Stresses and Soil Resistance Measured for Redriving of Pile 271

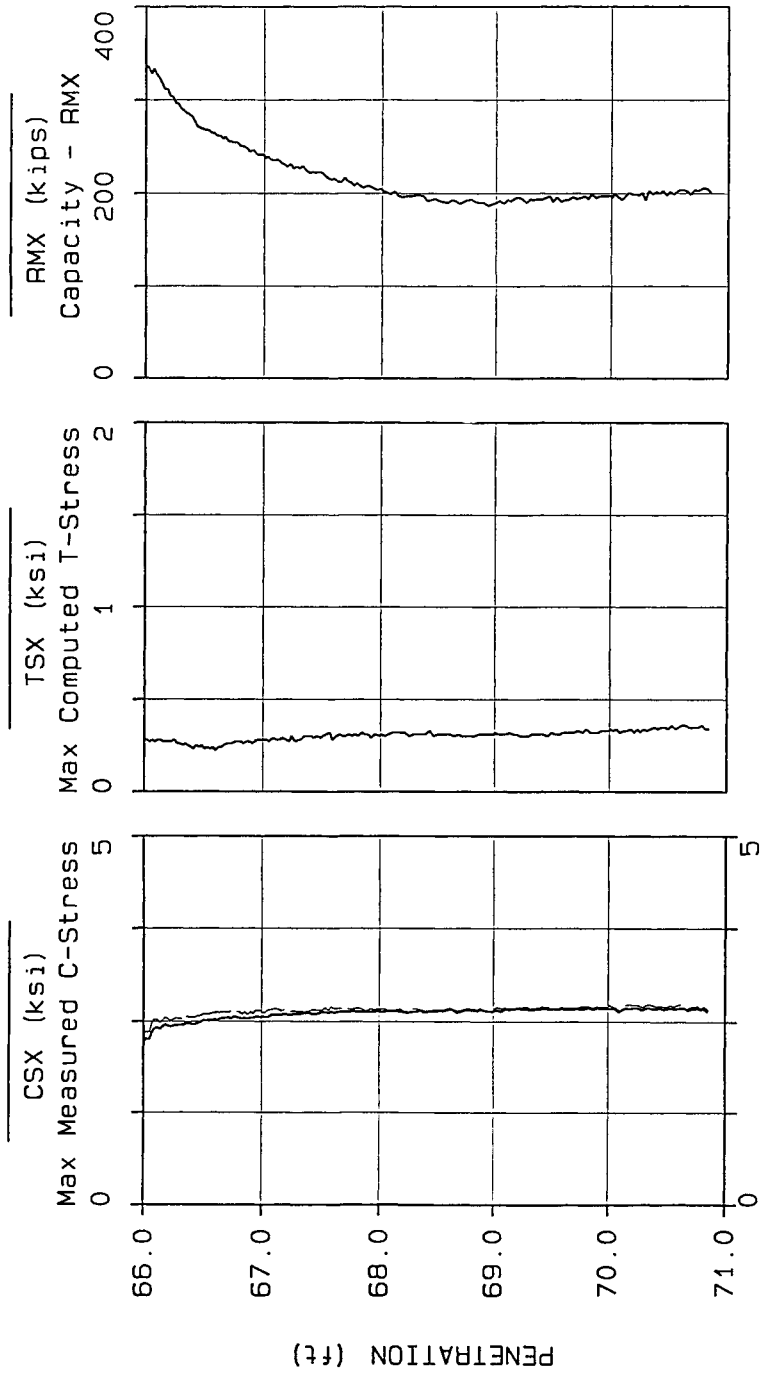


Figure 4. Stresses and Soil Resistance Measured for Redriving of Pile 480

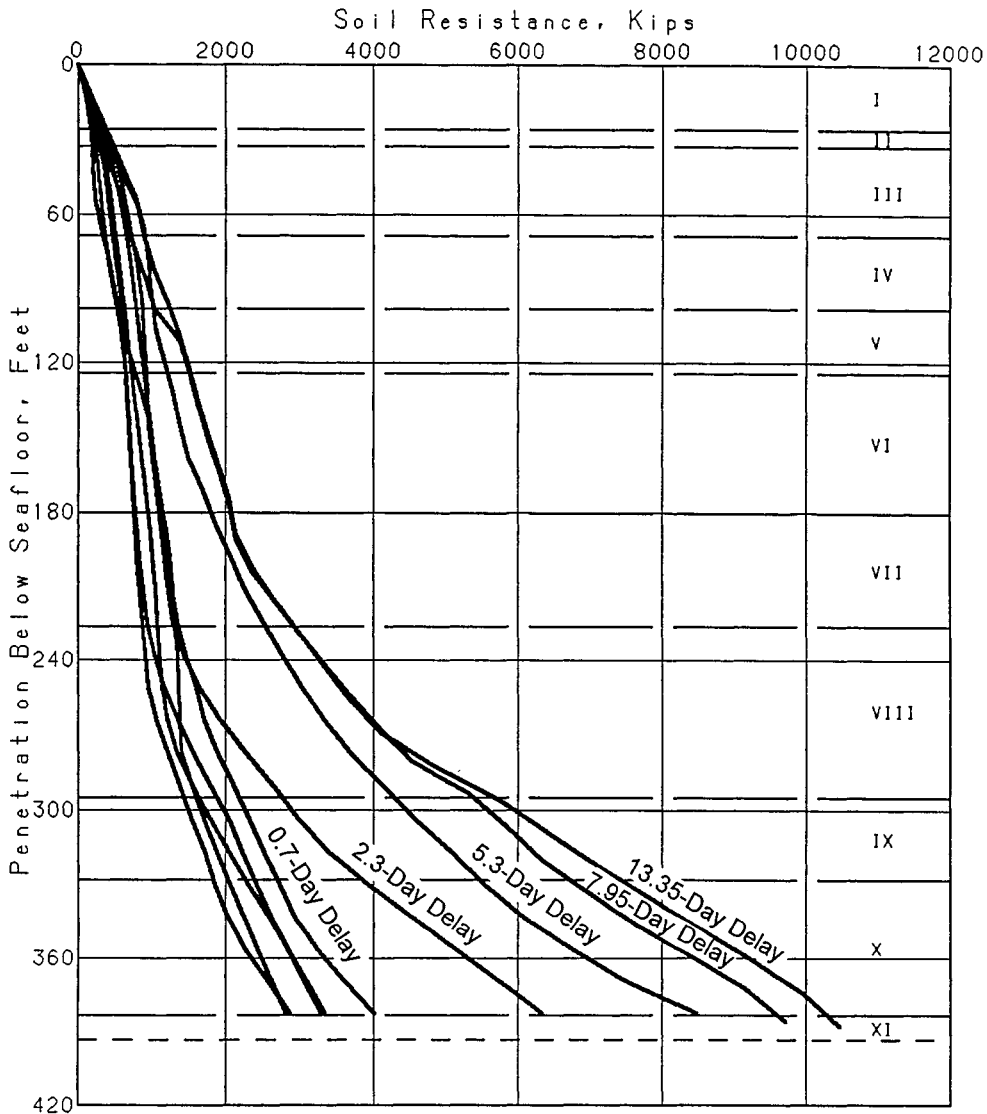


Figure 5. Soil Resistance Determined from CAPWAP Analyses

The soil resistance (RMX) at the end of continuous driving, as shown in Figs. 1 and 2, was about 91 kips (0.40 MN) for Pile 271, and 102 kips (0.45 MN) for Pile 480. Also shown are the maximum compressive (CSX) and tensile (TSX) driving stresses. The lower compressive stress plotted is the average of two strain transducers, and the higher compressive stress is the maximum value obtained from either transducer. The piles were redriven 5 ft (1.5 m) after a set-up period of 4.7 days. The restart blow counts were 52 bpf for Pile 271 and 41 bpf for Pile 480. The maximum

soil resistance, as shown in Figs. 3 and 4, was 295 kips (1.31 MN) for Pile 271 and 337 kips (1.50 MN) for Pile 480, resulting in a set-up factor of about 3.3 in less than 5 days. Also of interest is the shape of the soil resistance versus penetration curve during redriving. The soil resistance decreases about 40 percent as the pile is redriven 3 feet, but is about twice the soil resistance measured at the end of continuous driving.

<u>Pile</u>	<u>B5-2</u>	<u>A5-4</u>	<u>A5-2</u>	<u>A5-1</u>	<u>A1-4</u>
Blow Count, bpf	20	16	19	17	16
Penetration, ft	383	383	380	385	383
Hammer Efficiency, %	85	87	78	--	80
System Efficiency, %	51	57	51	--	50
Transmitted Energy, k-ft	439	496	443	--	430
Stress, ksi	18.8	22.0	20.7	--	21.0

<u>Pile</u>	<u>B5-2</u>	<u>A5-4</u>	<u>A5-2</u>	<u>A5-1</u>	<u>A1-4</u>
Blow Count	20/3"	26/3"	78/6"	50/3"	80/3"
Penetration, ft	383.25	383.25	380.5	385.25	383.25
Hammer Efficiency, %	80	81	72	82	--
System Efficiency, %	44	40	51	56	56
Transmitted Energy, k-ft	380	350	441	485	485
Stress, ksi	20.0	22.0	20.0	22.0	23.0
Delay, days	0.7	2.3	5.3	7.95	13.35

Figure 6. Summary of Driving System Performance Data

3. CASE HISTORY NO. 2

Our second case history is for a series of redrive tests performed with a hammer that was not quite large enough to mobilize the full soil resistance. Sixteen 72-in.-diameter open-ended pipe piles were driven to 383-ft (117-m) penetration with a Menck MRBS 8000 hammer. Soil conditions consisted of alternating strata of silty clayey sand or sandy clayey silt and stiff to very stiff sandy silty clay.

The distribution of the soil resistance was determined from CAPWAP analyses performed for a series of redrive tests. Results are presented for continuous driving at the end of driving for four different piles driven to final blow counts of only 16 to 20 bpf. Results are also presented for the beginning of redrive are for five different piles, each driven about 3 inches. The soil resistance along the length of the pile is presented in Fig. 5 for continuous driving and after set-up times ranging from 0.7 to 13.4 days. This plot shows that the full soil resistance was not mobilized for the redrive tests performed after the two longest delays, as indicated by a change in slope in the soil resistance along the bottom 15 ft (5 m) of the pile. A summary of the driving system performance data is presented in Fig. 6.

4. CASE HISTORY NO. 3

Our third case history is for a series of redrive tests performed with a hammer that is clearly not large

enough to mobilize the full soil resistance. The soil resistance mobilized during a series of redrive tests performed on a 1.6-m-diameter steel pipe pile driven to a penetration of 26 m in a very silty clay is presented in Fig. 7. The four lower bound soil resistance profiles are for continuous driving. The pile was redriven by applying only two consecutive hammer blows with a PMJ-400 hydraulic hammer after delays of 6 minutes, 15 minutes, 33 minutes, 2 hours, and 66 hours. The resistance generally increases with time, but the resistance after a 33-minute delay appears to be slightly smaller than the resistance mobilized after a 15-minute delay, and the resistance after a 66-hour delay is less than the resistance mobilized after a 2-hour delay. The maximum resistance overcome by the pile driving hammer is about 3300 kips (14.7 MN). The hammer is too small to mobilize the full soil resistance during the redrive tests. This is shown very clearly for the redrive test performed after the 66-hour delay. Almost no soil resistance was mobilized over the bottom quarter of the pile.

In our combined CAPWAP analyses, we have assumed that the soil resistance mobilized during continuous driving is a lower bound, i.e., the soil resistance mobilized on a particular pile segment is assumed to be the larger of the actual resistance mobilized or the resistance mobilized during continuous driving. The soil resistance mobilized after a 66-hour delay in the combined CAPWAP analysis is about 4400 kips (19.6 MN), as shown in Fig. 8. In the standard CAPWAP analysis, the resistance mobilized was only 3305 kips (14.7 MN).

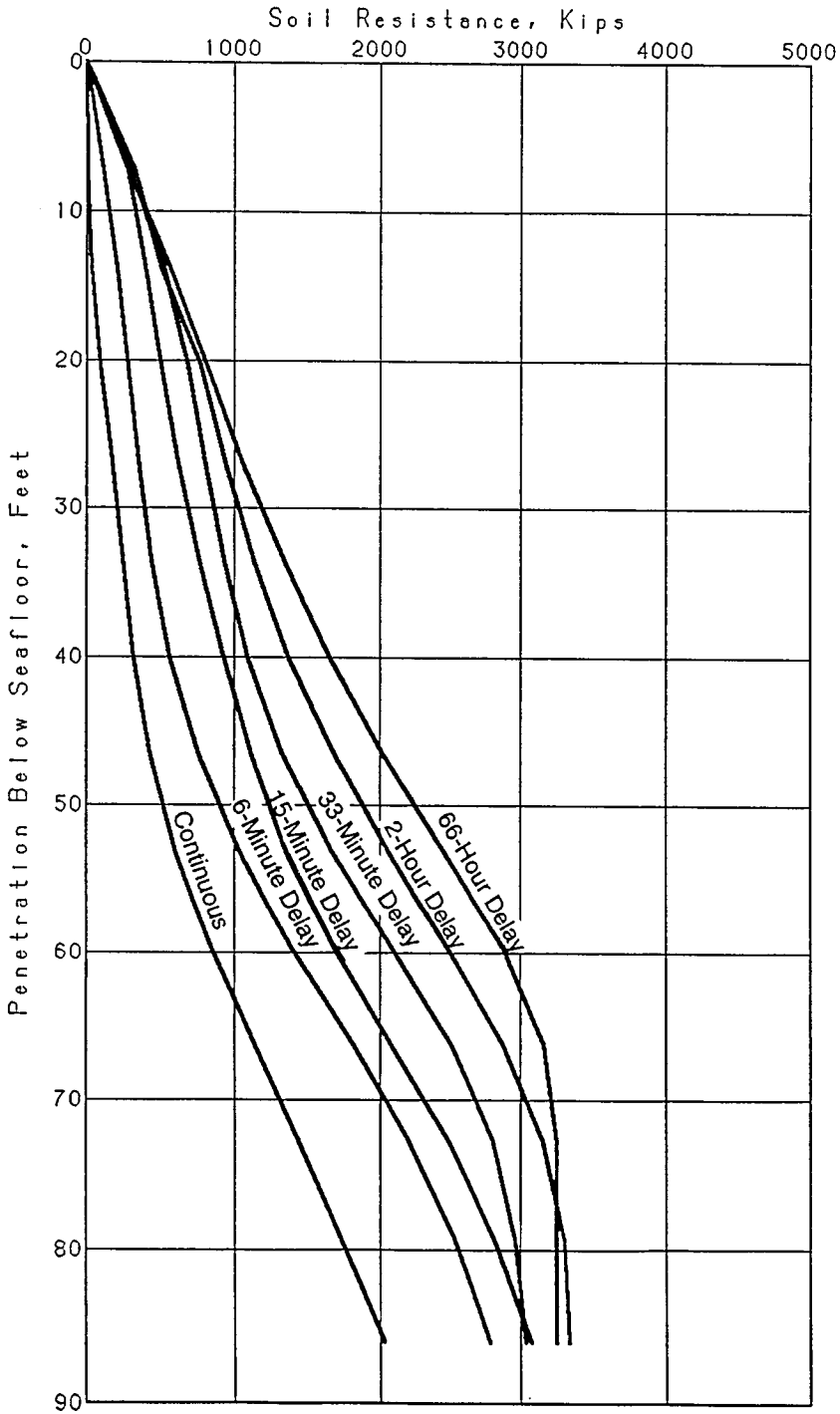


Figure 7. Soil Resistance Determined from CAPWAP Analyses

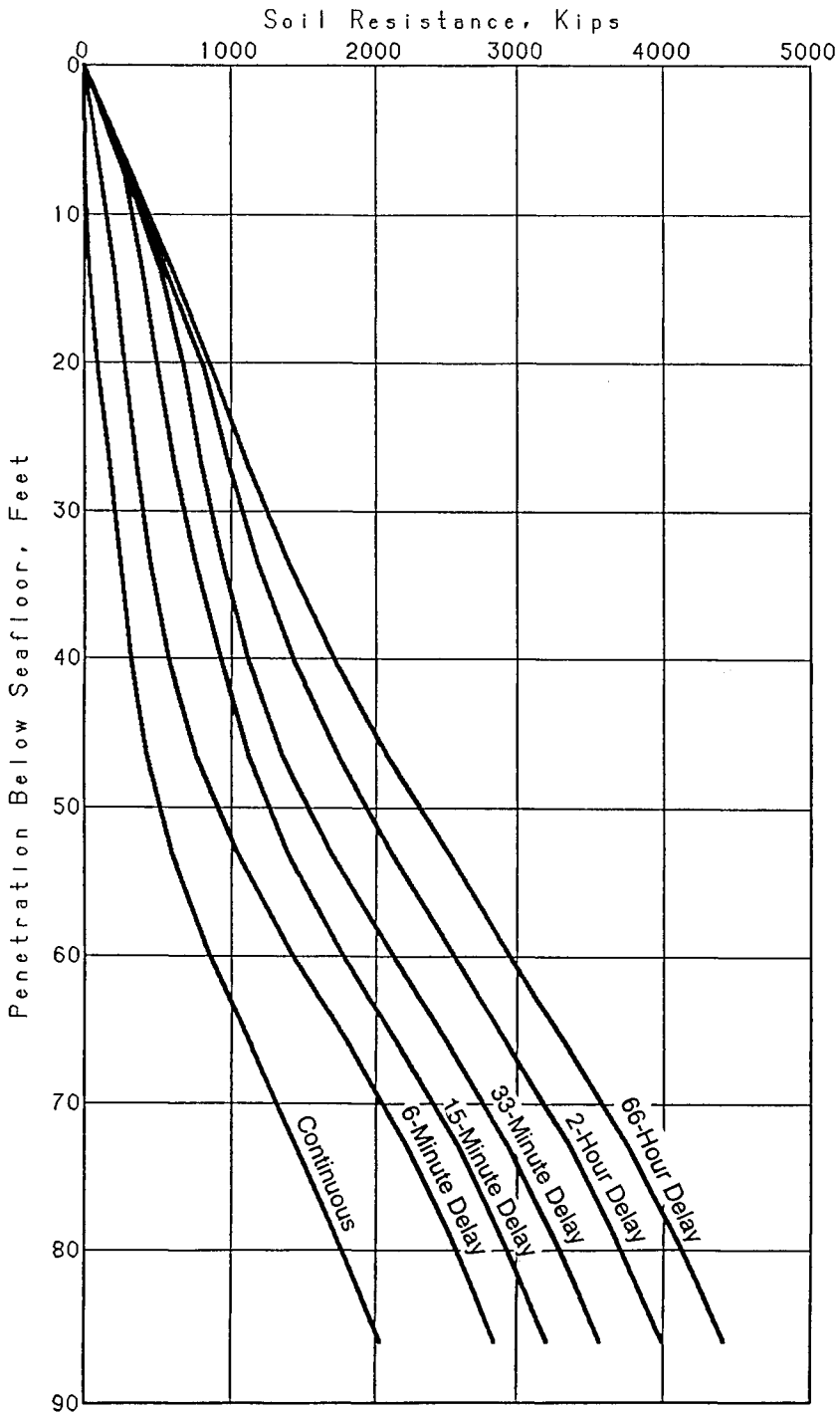


Figure 8. Soil Resistance Determined from Combined CAPWAP Analyses

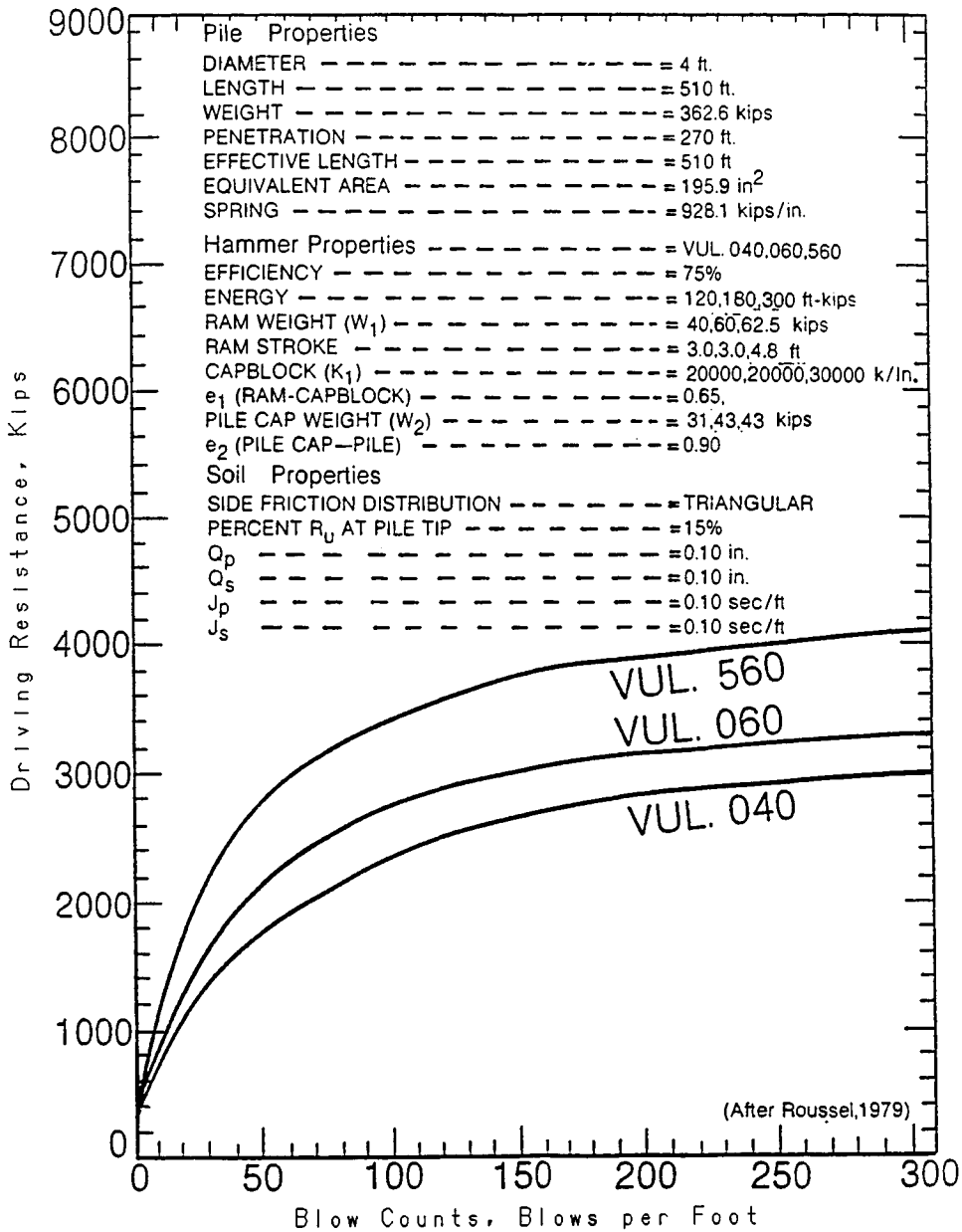


Figure 9. Driving Resistance-Blow Count Curves

To help put this in perspective, Fig. 9 shows that the resistance mobilized by a Vulcan 060 hammer is about 3300 kips (14.7 MN), and the resistance mobilized by a Vulcan 560 hammer is about 4100 kips (18.2 MN), assuming the same soil and pile parameters. Comparing the three hammers shown in Fig. 9, we see that by mobilizing a hammer having 50 percent more rated

energy results in only a 10 percent increase in the maximum soil resistance overcome, and mobilizing a hammer having 150 percent more rated energy results in a 37 percent increase in the maximum resistance overcome.

5. CONCLUSIONS

CAPWAP analyses were used to estimate the distribution of the soil resistance to driving along the length and at the toe of a pile during continuous driving and after a set-up period. Our final case history was for a series of redrive tests performed with a hammer that could overcome a maximum resistance of about 3300 kips (14.7 MN). The soil resistance mobilized after a 66-hour delay is shown to be about 4400 kips (19.6 MN) using combined CAPWAP analyses. In the combined CAPWAP analyses, the soil resistance mobilized on a particular pile segment is assumed to be the larger of the actual resistance mobilized, or the resistance mobilized during continuous driving.

REFERENCES

Bogard, J.D. and Matlock, H. (1990), "Application of Model Pile Tests to Axial Pile Design," Proceedings, Twenty-second Annual Offshore Technology Conference, Houston, Vol. 3, pp. 271-278.

Rausche, F. (1970), "Soil Response from Dynamic Analysis and Measurements on Piles," Ph.D. Dissertation, Division of Solid Mechanics, Structures, and Mechanical Design, Case Western Reserve University, Cleveland, Ohio, 320 p.

Roussel, H.J. (1979), Pile Driving Analysis of Large Diameter High Capacity Offshore Pipe Piles, Ph.D. Thesis, Department of Civil Engineering, Tulane University, New Orleans.



Taylor & Francis

Taylor & Francis Group

<http://taylorandfrancis.com>

Theoretical study on effect of pile shaft resistance on rebound during pile driving

Chen Ren-peng & Chen Yun-ming

Geotechnical Engineering Institute, Zhejiang University, Hangzhou, People's Republic of China

ABSTRACT: In this paper the effect of the shaft resistance on the rebound at pile-top during pile driving is studied. The soil around pile shaft is assumed to be rigid-plastic and that under pile-tip is assumed to be ideal elastoplastic. The driving force acted on pile-top is simplified to be a triangular impact. The kinematics equation of pile-tip is established. With the one-dimension wave equation, the movement of pile-tip and pile-top are obtained. The rebound at pile-top can be written in a very concisely form. It proves that the shaft resistance decreases the rebound at pile-top. When pile is long enough or the soil around pile is very stiff, the rebound decreases obviously. The neglect of the shaft resistance will bring on a large amount of errors.

1 INTRODUCTION

During pile driving, that rebound at pile-top gives more information about resistance than penetration has been recognized (Chen et al. 1996, Uto et al., 1992). The theoretical model of point resistance, obtained from PD- and PDA- measurements, has been developed in the recent years (Chen et al. 1996, van Weele et al., 1994). This makes it possible to estimate static point resistance during pile driving. In the method, shaft resistance is neglected for the reason that transverse vibration of pile greatly decreases the shaft resistance. Driving resistance is assumed to be mainly consisted of point resistance. Soil under pile-tip is supposed to be a ideal elastoplastic material, with the ultimate static resistance of R_s . In order to make the analysis more simple, impact force caused by hammer, is simplified as a triangular force. The driving model is shown in Figure 1(a). The kinematics equation of pile-tip can be easily established and solved. Then point resistance can be written as

$$R_s = C_s \frac{\text{Rebound}}{t_0} Z \quad (1)$$

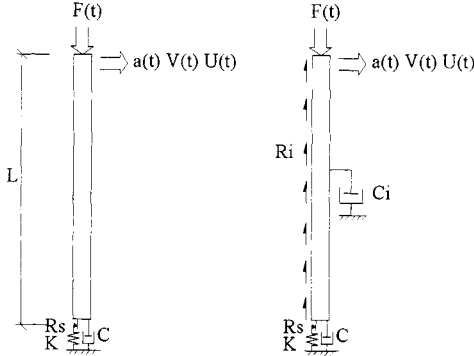
Where C_s is a dimensionless constant, almost equals to 1.3, t_0 is the duration of contact between hammer and pile, Z is the impedance of pile. By double integrating the recorded acceleration of the pile as a function of time, the pile-top settlement can be obtained. For it may take approx. 200ms before the pile-top is at rest after each blow and only then the permanent deflection is reached, it is imperfection in

the integration. Fortunately such problem has been solved by IFCO BV (van Weele, 1994).

In the equation (1), impedance of pile is known before pile driving, and t_0 for each blow can be obtained from the pile-top velocity. The rebound can be obtained from the pile-top settlement. Furthermore, the total settlement and the permanent settlement for each blow still can be presented. Figure 2 shows the typical diagram of the point resistance vs. depth, which clearly indicates the thickness of each soil-layer and agrees well with the results of CPT cone resistance. The new method requires only a single, small and robust sensor and the data collection and interpretation is done automatically by the field computer (van Weele et al. 1994). PDA- analyses in combination with the CASE- or CAPWAP-methods are different as they require more and also more complicated instrumentation. It also shows that the dropheight, cushion stiffness and soil damping have little effect on the point resistance compared with other method, such as CASE- and CAPWAP method. The method has been put into use (van Weele et al. 1994), and seems very helpful. The defect is that the shaft resistance is neglected. In practice, soil resistance includes shaft and point resistance during pile driving. If the pile penetrates through stiff soil or the pile is very long, the shaft resistance is always very great. The neglect of the shaft resistance certainly brings on great errors. In this paper, the shaft resistance is taken into account and the method is improved.

2 THEORETIC ANALYSIS

2.1 Theoretic model of pile driving



(a) pile driving model (b) analysis model presented in this paper. No shaft resistance is considered. Shaft resistance is considered.

Figure 1. Pile Driving Model

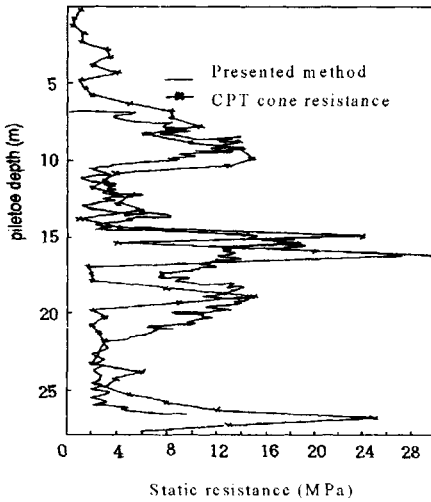


Figure 2. Point Resistance vs. Depth Estimated by the Method (Chen 1996)

As shown in Figure 1(b), soil at pile shaft is postulated to be rigid-plastic, and soil at pile-tip is postulated to be elastoplastic, and modeled by Smith soil model (Smith, E.A.L., 1960). The soil at pile shaft is homogenous, and the shaft resistance distributes evenly around the pile. The driving model is shown in Figure 1(b). The driving force is simplified to be a triangular impact force, as shown in Figure 3. In Figure 3, F_0 is the amplitude of the driving force. t_1 is the loading time. In Figure 1(b), R_i is the static shaft resistance and R_s is the static point resistance. C_i is the damping coefficient at pile

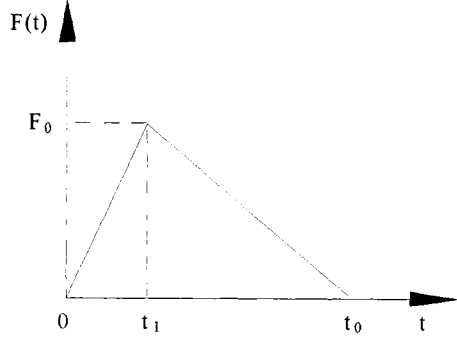


Figure 3. Driving Force Simplified as a triangular force

shaft. L is pile length and c is the stress wave velocity, which is described as $c = \sqrt{E / \rho}$, where E is the elastic modulus and ρ is the density of pile material. The reflection wave at pile-top is not considered. Up-going velocity is supposed to reach pile-top without attenuation.

2.2 Kinematics equation of pile-tip

The kinematics equation of pile-tip can be described as

$$CV(t) + K[U(t) - U_p(t)] = F_d(t) + F_u(t) \quad (2)$$

where $U(t)$ and $V(t)$ are the movement and the velocity of pile-tip respectively, $U_p(t)$ is the permanent movement of pile-tip. $F_d(t)$ is down-going force. Z is the impedance of pile. C is the damping coefficient of soil at pile-tip and K is the stiffness of soil at pile-tip. $F_u(t)$ is the up-going force, which can be described as

$$F_u(t) = F_d(t) - ZV(t) \quad (3)$$

Then Equation (2) is rewritten as

$$[C + Z]V(t) + K[U(t) - U_p(t)] = 2F_d(t) \quad (4)$$

or

$$[C + Z] \frac{dU(t)}{dt} + K[U(t) - U_p(t)] = 2F_d(t) \quad (5)$$

The movement of pile-tip $U(t)$ (or soil at pile-tip) can be divided into three stages: elastic movement, plastic movement and rebound. When the movement of pile-tip $U(t)$ is less than the maximum elastical movement of soil at pile-tip (denoted as Q_p), there is only elastic movement of soil. The static soil resistance increases linearly with the elastic movement of pile-tip until it reaches at the maximum static resistance R_s . Equation (5) is simplified as

$$[C + Z] \frac{dU(t)}{dt} + KU(t) = 2F_d(t) \quad (6)$$

When the movement of pile-tip $U(t)$ exceeds Q_p , plastic movement takes place. Then the maximum static soil resistance remains constantly. Equation (5) is written as

$$[C + Z] \frac{dU(t)}{dt} + R_s = 2F_d(t) \quad (7)$$

When the movement of pile-tip $U(t)$ reaches to its limit, then rebound takes place. The static soil resistance decrease when the movement of pile-tip $U(t)$ decreases. The movement of the pile-tip can be described with Equation (5).

Equation (5) can be solved step by step with the condition of the deformation compatibility at the end of each stage.

2.3 Velocity and movement at pile-tip

In the following, seven dimensionless parameters are introduced:

$$\eta = t_1/t_0, \quad n = R_s/F_0, \quad n_i = R_i/F_0, \quad m_1 = Z/(Kt_0),$$

$$m_2 = C/(Kt_0), \quad m_{21} = C_i/(Kt_0), \quad T = 2L/(ct_0).$$

With the assumption of the Smith damping law, there exist

$$m_1 = \frac{Q_p}{nV_{\max}^t t_0} \quad (8)$$

and

$$m_2 = \frac{J_p Q_p}{t_0} \quad (9)$$

where J_p is the Smith damping coefficient. V_{\max}^t is the maximum velocity of pile-top, where:

$$V_{\max}^t = F_0 / Z.$$

When pile hammer impacts on pile-top, the impact force propagates downward through pile. When the stress wave reaches point x , as shown in Figure 4, the shaft resistance is excited simultaneously. Then the tensile and compressive stress wave propagating in the opposite directions are generated. The tensile wave propagates downwards and the compressive wave propagates upwards. The amplitudes of the two kinds of stress wave equal to the half of the amplitude of the shaft resistance. When the driving force reaches to the pile-tip, the amplitude of the shaft resistance equals to the half of the total shaft resistance, i.e. $R_i/2$. The dynamic shaft resistance is

the multiplication of velocity caused by driving force and damping coefficient at pile shaft. Therefore at pile-tip down-going wave caused by soil resistance at pile shaft is

$$V_d^R(t) = \begin{cases} -\frac{F_0 C_i t}{2Z^2 t_1} - \frac{R_i}{2Z} & 0 \leq t < t_1 \\ -\frac{F_0 C_i (t - t_0)}{2Z^2 (t_1 - t_0)} - \frac{R_i}{2Z} & t_1 \leq t < t_0 \\ -\frac{R_i}{2Z} & t < t_0 \end{cases} \quad (10)$$

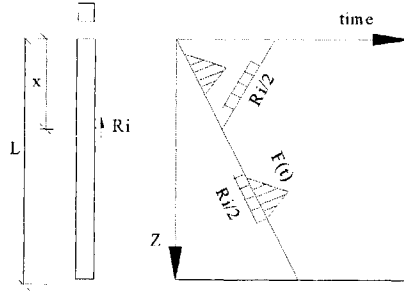


Figure 4. Stress wave propagating in pile

Down-going force $F_d(t)$ can be described as

$$F_d(t) = F(t) + ZV_d^R(t) \quad (11)$$

Furthermore, up-going wave reaching pile-top is expressed as

$$V_u^R(t) = \begin{cases} -\frac{F_0 C_i t}{2Z^2 t_1} - \frac{R_i t}{2ZT} & 0 \leq t < t_1 \\ -\frac{F_0 C_i (t - t_0)}{2Z^2 (t_1 - t_0)} - \frac{R_i t}{2ZT} & t_1 \leq t < t_0 \\ -\frac{R_i}{2Z} & t < t_0 \end{cases} \quad (12)$$

Substituting Equation (12) into Equation (11), Equation (6), Equation (7) and Equation (5) step by step, dimensionless form of the movement and the velocity at pile-tip are derived by

$$\frac{K}{F_0} U(\tau) = \begin{cases} \frac{2}{\eta} \tau - n_i - \frac{2m}{\eta} - \frac{m_{2i}}{m_1 \eta} (\tau - m) + (n_i + \frac{2m}{\eta} - \frac{mm_{2i}}{m_1 \eta}) e^{-\frac{\tau}{m}} & 0 \leq \tau < \eta \\ \frac{2}{(\eta-1)} (\tau-1) - n_i - \frac{2m}{(\eta-1)} - \frac{m_{2i}}{m_1(\eta-1)} (\tau-m-1) + \left[(n_i + \frac{2m}{\eta} - \frac{mm_{2i}}{m_1 \eta}) e^{-\frac{\eta}{m}} + \frac{m}{\eta(\eta-1)} (2 - \frac{m_{2i}}{m_1}) \right] e^{-\frac{\tau-\eta}{m}} & \eta \leq \tau < \tau_n \\ \frac{(\tau-1)^2}{m(\eta-1)} - \frac{(n+n_i)}{m} \tau - \frac{m_{2i}(\tau-1)^2}{2mm_1(\eta-1)} + w_1 & \tau_n \leq \tau < \tau_e \\ \frac{2(\tau-1)}{(\eta-1)} - n_i + \frac{K_{set}}{F_0} - \frac{2m}{(\eta-1)} - \frac{m_{2i}}{m_1(\eta-1)} (\tau-m-1) + w_2 e^{-\frac{\tau}{m}} & \tau_e \leq \tau \leq 1 \end{cases} \quad (13)$$

and

$$\frac{Kt_0}{F_0} V(\tau) = \begin{cases} \frac{2}{\eta} - \frac{m_{2i}}{m_1 \eta} - (\frac{n_i}{m} + \frac{2}{\eta} - \frac{m_{2i}}{m_1 \eta}) e^{-\frac{\tau}{m}} & 0 \leq \tau < \eta \\ \frac{2}{(\eta-1)} - \frac{m_{2i}}{m_1(\eta-1)} - \left[(\frac{n_i}{m} + \frac{2}{\eta} - \frac{m_{2i}}{m_1 \eta}) e^{-\frac{\eta}{m}} + \frac{(2m_1 - m_{2i})}{m_1 \eta (\eta-1)} \right] e^{-\frac{\tau-\eta}{m}} & \eta \leq \tau < \tau_n \\ \frac{2(\tau-1)}{m(\eta-1)} - \frac{(n+n_i)}{m} - \frac{m_{2i}(\tau-1)}{mm_1(\eta-1)} & \tau_n \leq \tau < \tau_e \\ \frac{2}{(\eta-1)} - \frac{m_{2i}}{m_1(\eta-1)} - \frac{w_2}{m} e^{-\frac{\tau}{m}} & \tau_e \leq \tau \leq 1 \end{cases} \quad (14)$$

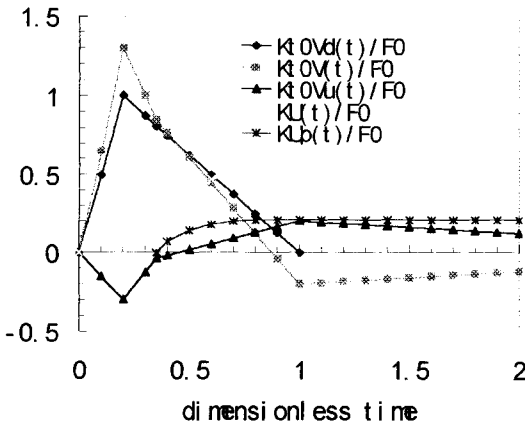


Figure 5. Typical solution of Equation (2) and pile-tip

where $\tau = t/t_0$, τ_n and τ_e are the dimensionless time when plastic movement and rebound take place respectively, w_1 and w_2 are integration constants, set is residual movement when rebound takes place. From Equation (13) and Equation (14) τ_n and τ_e can be written as

$$\tau_n = \frac{nm_1 m^2}{m_1 n_i \eta + 2mm_1 - mm_1 n_i - mm_{2i}} \quad (15)$$

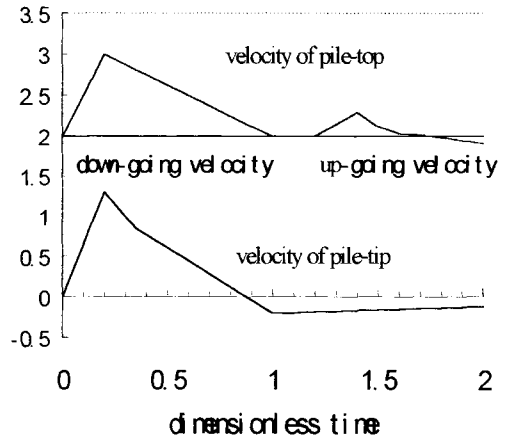


Figure 6. Velocity and movement of pile-top

and

$$\tau_e = \frac{(n+n_i)(\eta-1)}{2-m_{2i}} + 1 \quad (16)$$

where: $m^{-1} = m_1 + m_2$. From down-going velocity and velocity at pile-top, up-going velocity can be derived by

$$V_u(t) = V(t) - V_d(t) \quad (17)$$

With the previous assumption, up-going velocity will reach pile-top without attenuation. Figure 5 shows typical solution of Equation (2).

2.4 Rebound at pile-top

Assuming there is no residual compression in pile, the final residual movement of pile-tip is equals to that of pile-top. The rebound of pile-top can be expressed as

$$Rebound = U_{max}^t - U_{max}^b + Q_p \quad (18)$$

where: U_{max}^t and U_{max}^b are the maximum movement of pile-top and pile-tip respectively. U_{max}^t and U_{max}^b can be derived by integrating velocity at pile-tip and pile-top as shown in Figure 6. Because velocity caused by up-going soil resistance, $V_u^R(t)$, is little compared with $V^t(t)$ and $V_u(t)$, it can be assumed that the movement of pile-top reaches its maximum when up-going velocity, $V_u(t)$ reaches zero.

β is denoted as the dimensionless time when up-going velocity reaches zero. As shown in Figure 5 there exists

$$\begin{aligned} \frac{K}{F_0} [U_{max}^t - U_{max}^b] &= \int_0^1 V^t(\tau) d\tau + \int_0^\beta V_u(\tau) d\tau \\ &\quad - \int_0^{\tau+\beta} V_u^R(\tau) d\tau - \int_0^\tau V(\tau) d\tau \\ &= \frac{(1-\beta)(n+n_i)}{2(2-m_{2i})} - \left[\frac{(T^2-\beta^2)}{4T} + \frac{\beta}{2} + \frac{m_{2i}(1-\beta^2)}{2m_1n_i(1-\eta)} \right] \frac{n_i}{m_1} \\ &= \alpha_1 \frac{n}{m_1} - \alpha_2 \frac{n_i}{m_1} \end{aligned} \quad (19)$$

where

$$\alpha_1 = \frac{(1-\beta)}{2(2-m_{2i})} \quad (20)$$

and

$$\alpha_2 = -\alpha_1 + \frac{(T^2-\beta^2)}{4T} + \frac{\beta}{2} + \frac{m_{2i}(1-\beta^2)}{2m_1n_i(1-\eta)} \quad (21)$$

Equation (19) can be written as

$$U_{max}^t - U_{max}^b = \alpha_1 \frac{R_s t_0}{Z} - \alpha_2 \frac{R_i t_0}{Z} \quad (22)$$

Substituting Equation (22) into Equation (18), the static resistance at pile-tip can be obtained

$$R_s = C_s \frac{Rebound}{t_0} Z + C_d R_i \quad (23)$$

where

$$C_s = (\alpha_1 + m_1)^{-1} \quad (24)$$

and

$$C_d = \frac{\alpha_2}{(\alpha_1 + m_1)} \quad (25)$$

Assuming $\lambda = R_i / R_s$, Equation (23) can be written as

$$R_s = \frac{C_s}{(1-\lambda C_d)} \frac{Rebound}{t_0} Z \quad (26)$$

or

$$Rebound = \frac{R_s t_0}{Z} \frac{1-\lambda C_d}{C_s} \quad (27)$$

3 POINT RESISTANCE

If $\lambda = 0$, Equation (23) can be rewritten as

$$R_s = C_s \frac{Rebound}{t_0} Z \quad (1)$$

which is the same as that obtained by Chen et al. (1996). Commonly, during pile driving there exist $t_0=(10\sim 15)$ ms, $Q_p=(5\sim 10)$ mm, $J_p=(0.5\sim 1.5)$ s/m, $V_{max}^t=(2.5\sim 4.0)$ m/s. Therefore the ranges of the dimensionless parameters can be known: $n=(0.1\sim 0.5)$, $n_i=(0.03\sim 0.02)$, $\eta=(0.1\sim 0.5)$, $m_i=(0.08\sim 0.25)/n$, $m_2=(0.15\sim 1.5)$, $m_{2i}=(0.05\sim 0.5)$, $T=(1.0\sim 2.0)$. Substituting the dimensionless parameters into Equation (25) the range of C_d can be known: $C_d=(0.5\sim 0.9) \cong 0.7$. C_s can be estimated by Equation (24). In-situ measurement also shows that C_s varies little, and equals to 1.3 (Chen et al. 1996). In Equation (26), the rebound of pile-top, duration time of driving force t_0 can be obtained from the acceleration signal.

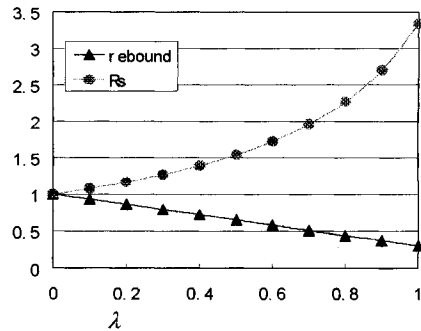


Figure 7. Effect of shaft resistance on rebound and estimated point resistance

The curve of the point resistance versus depth is very similar to that of cone resistance of CPT. With the curve, it is convenient to decide the depth of the bearing stratum and pile capacity.

4 EFFECT OF SHAFT RESISTANCE ON REBOUND

The effect of λ on R_s is shown in Figure 7. When $\lambda = 0$, it means that the shaft resistance is neglected. When $\lambda = 1$, it means the shaft resistance is the same as point resistance. It can be seen from Figure 7, the shaft resistance has a very obvious effect on rebound. If the error of the neglect of the shaft resistance is supposed to be less than ten percent, λ must be less than 0.16, which means shaft resistance is less than thirteen percent of point resistance. Soil resistance at pile-tip obtained with the consideration of soil resistance at pile shaft is stronger than that obtained without the consideration of soil resistance at pile shaft.

Equation (23) shows the influence of shaft resistance on rebound. The shaft resistance distinctly decreases the pile-top rebound. The greater the shaft resistance is, the greater the decrease is. When $\lambda = 0.7$, the rebound is only half of that neglecting the shaft resistance. It was also proved in-situ measurement that when the driving of the pile is stopped for some reasons, the rebound will decrease greatly during redriving. It is due to the increase of the shaft resistance during the break.

5 CONCLUSION

In this paper the effect of the shaft resistance on the pile-top rebound during pile driving is studied. The soil around pile shaft is assumed to be viscous-rigid and that under pile-tip is assumed to be viscous-elastic. The driving force acted on pile-top is simplified to be triangular impact. The kinematics equation of pile-tip is established. With the one-dimension wave equation, the movement of pile-tip and pile-top are obtained. The rebound at pile-top can be written in a very concisely form. It proves that the shaft resistance decreases the rebound at pile-top. When pile is long enough or the soil around pile is very stiff, the rebound decreases obviously. The neglect of the shaft resistance will bring on a large amount of errors.

REFERENCES

- Chen, Y.M. et al. 1996. Determining soil resistance from pile driving by using an accelerometer. *Proc. 5th Int. Conf. on Application of Stress-wave Theory to Piles* : USA.
- Smith, E.A.L. 1960. Pile driving analysis by the wave equation. *J. Soil Mech. & Found. Eng. Div. ASCE*, 1960 86(4).
- Uto, K., Fuyuki, M. & Omori, H. 1992. New development of pile driving management system. *Proc. 4th Int. Conf. on Application of Stress-wave Theory to Piles* 1992: 351-356, the Hague.
- Weele, A.F. & Schellingerhout, A.F.G. 1994. Efficient driving of precast concrete piles. *Proc. Conf. Development in Geotech. Eng.* 1994. Bangkok.

Time effect in determining pile capacity by dynamic methods

M.R.Svinkin

VibraConsult, Cleveland, Ohio, USA

ABSTRACT: Knowledge of pile capacity as a function of time is important for proper performance of pile foundations. This paper shows the advantages of the dynamic methods in determining pile capacity and points out the necessity of considering the time effect for correct assessment of the accuracy of dynamic methods. The prediction of pile capacity in pre-driving wave equation analysis can be made by the use of variable damping as a function of time. Pile capacity obtained from a static loading test cannot be accepted as a unique standard because the static loading test yields the pile capacity at the time of test only, due to the consolidation phenomenon. Dynamic capacity testing has this same limitation. Any comparison of static and dynamic tests has to be made for tests performed within a short duration.

1 INTRODUCTION

Pile capacity changes after pile installation. Accurate and reliable determination of pile capacity is very important for design, construction and reliability of pile foundations.

Static analysis and the static loading test are traditionally used for calculation and verification of pile capacity. Contemporary dynamic methods have advances in evaluation of the hammer-pile-soil system and in data acquisition during pile driving and restrikes. Therefore during the two last decades, dynamic methods have become an integral part of pile capacity prediction and measurement for numerous projects.

Dynamic methods have certain advantages and some uncertainties in their application. Wave equation analysis of driven piles is a prevalent method of pile driving stress calculations. Besides driveability analysis, the wave equation method is used for prediction and determination of pile capacity during both the design stage and for construction control during pile installation. Unfortunately in most cases, computed pile capacity differs substantially from results of both static and dynamic load tests.

Dynamic measurements of force and velocity at the pile head during pile driving, followed by a signal matching procedure, is the most common method for dynamic determination of pile capacity.

This method is a convenient tool in the pile driving industry. However, though dynamic methods have been used in practice for years, actual reliability of dynamic methods is vague because their comparison with static loading tests is made incorrectly in most cases.

This paper considers the time effect on prediction and determination of pile capacity by dynamic methods after pile installation.

2 PILE CAPACITY VARIATIONS WITH TIME

Pile capacity determined at the end of initial driving (EOID) in various soils changes with time. During pile installation, the soil around the pile experiences plastic deformations, remolding, and pore pressure changes. Excess pore water pressure developed during driving reduces the effective soil shear strength and ultimate pile capacity. After the completion of pile driving, soil reconsolidation, manifested by the dissipation of excess pore pressure at the soil-pile interface zone, is usually accompanied by an increase in pile capacity (soil setup). The amount of increase in pile capacity depends on soil properties and pile characteristics. In saturated sandy soils, ultimate pile capacity may decrease (soil relaxation) after initial driving due to dissipation of negative pore pressure. Changes of strength in soil after driving and the time required

for return of equilibrium conditions are highly variable and depend on soil type, and pile size and type.

Piles have to withstand design loads for a long period of time. Therefore, the consequences of soil modification around the pile are essential with respect to changes of pile capacity. The phenomenon of time-dependent strength gain and loss in soils related to pile driving has been studied and published, for example Axelsson (1998), Chow et al. (1998), Fellenius et al. (1989), Long et al. (1999), Randolph et al. (1979), Seed & Reese (1955), Skov & Denver (1988), Svinkin (1996a), Thompson & Thompson (1985), Thorburn & Rigden (1980), Tomlinson (1971), Wardle et al. (1992), York et al. (1994) and others.

Pile capacity as a function of time is displayed, for example, in Figure 1. Static loading test (SLT) as well as dynamic testing (DT) yields the pile capacity at the time of testing, Svinkin (1997, 1998b). By way of illustration, results of DT and SLT are shown in Figure 1 for two identical cylindrical, 1372 mm x 127 mm, prestressed concrete piles, TP1 and TP2. The depth of penetration of each pile was approximately 24.4 m. The soil consisted of about 25.6 m of mainly gray clays followed by a bearing layer of silty sand. The water table was at the ground surface. A Delmag D 46-13 hammer was employed for initial driving and restrikes. Each of the piles TP1 and TP2 was tested 2, 9 and 22 days after the end of initial driving. The difference was that three restrikes were made for TP1 and three SLTs were made for TP2. Pile capacity from three SLTs was a function of time as was the pile capacity obtained from DT.

3 DYNAMIC FORMULAS

The well-known dynamic formulas have been criticized in many publications. Tested data in Figure 1 help to explain the causes of unsatisfactory prediction in pile capacity by dynamic formulas. Dynamic formulas using maximum energy, pile set and maximum displacement from DT do not take into account the time between SLT and DT. In the case of a few SLTs made on one pile, like three SLTs performed on pile TP2, what would be the reliability of pile capacity prediction by the energy approach methods? Which SLT should be taken for comparison? Currently, there are no answers to these questions. In principle, dynamic formulas cannot predict time-dependent pile capacity (Svinkin 1998b).

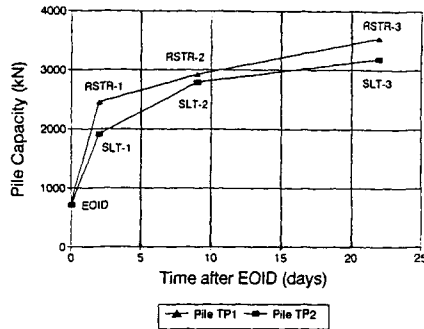


Figure 1. Pile capacity versus time for prestressed concrete piles in clayey soil, after Svinkin & Woods (1998a)

4 WAVE EQUATION ANALYSIS

The main goal in using the wave equation method is to provide a better prediction of the pile capacity, as a function of pile penetration resistance, than can be obtained from classical dynamic formulas.

The wave equation method was originally suggested by Smith (1960) to compute the pile capacity at the end of driving. This method is also used for prediction of pile capacity at restrike (RSTR) performed at any time after EOID. By adjusting wave equation analysis input with results of dynamic measurements, some researchers, for example, Hunt and Baker (1988), York et al. (1994) have obtained good correlation between computed and observed pile capacities. However, in most other cases, computed pile capacity differs substantially from results of static or dynamic tests.

Existing dynamic models of the pile-soil system mainly use a velocity-dependent approach for calculation of the dynamic resistance as a damping component of the total resistance during pile driving. There are various linear and nonlinear relationships between the damping component and the velocity.

For certain pile capacity, the dynamic resistance depends only on pile velocity and the damping coefficient.

Statistical analysis indicates no correlation between the pile penetration resistance and velocity values. The pile-soil system changes with time after the completion of driving, but the pile velocity is only a pile property and remains in the same range for EOID and RSTRs. The largest values of pile velocity measured at the upper end of the pile and calculated along a pile shaft depend only on pile parameters and energy transferred to the pile and cannot reflect regain in soil strength and pile-soil

adhesion after EOID. This is the first cause of unsatisfactory prediction of pile capacity with time after EOID.

The basic disadvantage of many models is the attempt to select the model parameters directly from actual soil properties. This can yield acceptable results for some cases, but in general this approach is not successful in finding good correlation between predicted and actual pile capacity after EOID. The use of the constant damping coefficients for calculation of the dynamic resistance is the second cause of unsatisfactory prediction of pile capacity with time after EOID.

Neither the pile velocity nor the damping constant can reflect time-dependent variation of the pile-soil system after EOID, Svinkin (1996c). The existing approach of computing the dynamic resistance does not take into account soil consolidation around the pile after EOID and therefore cannot provide determination of pile capacity as a function of time after pile installation.

For the idealized Smith wave equation model, it is important to find an appropriate combination of parameter values, mainly paying attention to soil variables, in order to achieve the accurate prediction of pile capacity. Probably, there is only one direction to enhance prediction accuracy of the dynamic resistance with the velocity dependent approach. Variation of the pile-soil system after the completion of driving can be taken into account by a *variable damping coefficient* which should be considered as a function of time and other parameters characterizing soil consolidation around the pile. For example, the soil shear modulus or the frequency of the fundamental mode of the pile-soil system could be considered, Svinkin (1996b). It is assumed that the variable damping coefficient is independent of pile velocity. Inclusion of variable damping is thought to be the next step in the development of Smith's model with the velocity dependent approach for representation of the dynamic resistance.

The damping coefficient as a function of time can be found on the basis of back calculations using the wave equation model of the pile-soil system with known capacity. The five soil damping options, available in GRLWEAP program (GRL Manual 1997), were investigated: Standard Smith Damping, Viscous Smith Damping, Case Damping, Coyle-Gibson Damping, and Coyle-Gibson/GRL Damping. A trend of the damping coefficient increase with time after EOID was found for all the considered dynamic soil models and this trend is independent of the damping resistances (Svinkin 1996b). Standard

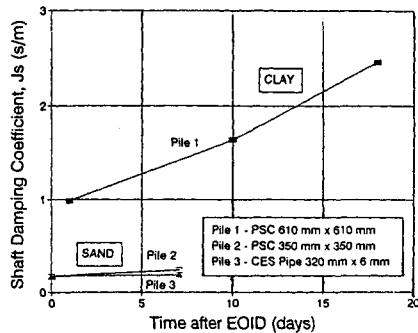


Figure 2. Variable Smith damping in clay and unsaturated sand, after Svinkin (1995a)

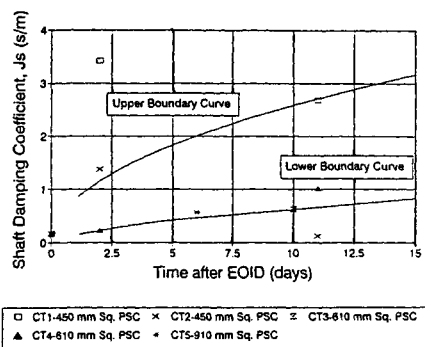


Figure 3. Variable Smith damping in saturated sand, after Svinkin (1995b)

Smith damping as a function of time for various soil types is shown in Figures 2 and 3. It can be seen that the shaft damping coefficient in clay is much higher than in unsaturated sand, but upper values of this coefficient in saturated sandy soil (sand with high damping) are close to ones in clay, Svinkin (1995a, 1995b).

The idea of variable damping has been confirmed by results of statistical analysis performed by Liang and Zhou (1997) who have found that the damping coefficient is affected by the time.

Soil damping is the key parameter for adjustment of wave equation solutions with time-dependable soil properties in pre-driving analysis. The use of the variable damping coefficient gives an opportunity to compute the time-dependent pile capacity by the wave equation method.

5 DYNAMIC TESTING AND ANALYSIS

Dynamic testing followed by a signal matching procedure has obvious advantage in determining pile capacity at any time after pile installation. Since dynamic testing is often used to replace the static loading tests, it is important to ascertain the adequacy of both SLT and DT. Design methods predict pile capacity as the long term capacity after soil consolidation around the pile is complete. Independently of the time elapsed between the driving of the test pile and the static loading test, the ratio of the predicted ultimate load to the measured ultimate load from static loading test is used for approximate evaluation of the reliability of design methods, Briaud and Tucker (1988). According to the traditional approach, the main criterion for assessment of the pile capacity prediction based on dynamic measurements is the ratio of capacities obtained by dynamic and static tests or vice versa (Figure 4).

It is necessary to point out that a ratio of DT/SLT or vice versa, taken for arbitrary time between compared tests, is not a verification of dynamic testing results. It is well-known that dynamic testing methods yield the real static capacity of piles *at the time of testing*, Rausche et al. (1985). This is not a predicted value. Moreover, the static capacity from SLT is considered as a unique standard for assessment of dynamic testing results. Unfortunately, that is a major error. As a matter of fact, *pile capacity from Static Loading Tests is a function of time* and the so-called actual static capacity from SLT is not a constant value. As it was shown in Figure 1, SLT, as well as DT, yields a different pile capacity depending on the time of testing, as measured after pile installation.

For a few separate piles, it is possible to find published information regarding the time between static and dynamic tests. However, for the general case of assessment of reliability of the DT, the ratio of restrikes to SLT results has been considered for various pile types, soil conditions and times of testing lumped together as shown in Figure 4. What is the real meaning of such mixture? Nobody knows. It is not a verification of dynamic testing at restrikes and it is not assessment of real setup factor because everything is lumped together without taking into account the time between different tests. Such a comparison of the pile capacities from SLT and DT is invalid for piles driven in soils with time-dependent properties because the soil properties at the time of DT do not correspond to the soil properties at the time of SLT i.e. soil consolidation

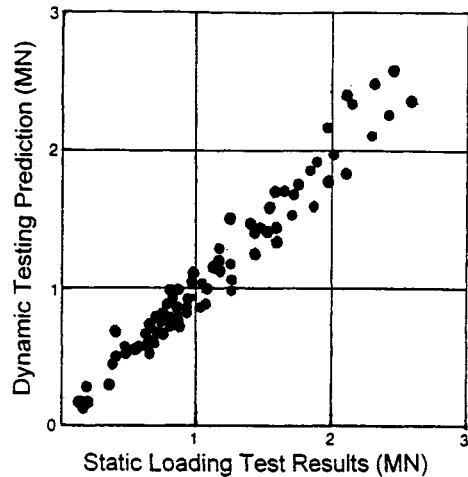


Figure 4. Typical dynamic and static tests capacity correlation

is taken into account for restrikes using the DT but is not in the SLT.

Static Loading Tests and Dynamic Testing present different ways of determining pile capacity at various times after pile installation, but for valid correlations two principal conditions have to be the same for both kinds of tests. 1) *static and dynamic capacities must be compared at the same time after pile installation in both SLT and DT methods*, and 2) the ultimate pile capacity is obtained in the SLT only if it provides the fully mobilized pile capacity (long term capacity), similar to the DT, Svinkin (1997).

The adequacy of SLT and DT have to be confirmed by proper correlation of time. Due to the consolidation phenomenon in soils, comparison of SLT and DT can only be made for tests performed immediately one after another. In practice, it is sometimes difficult to make two immediately successive tests, but nonetheless the time difference between both comparable tests should not exceed 1-2 days during which soil setup changes only slightly. Closely time correlated comparisons of SLT and DT have to be made in order to clarify the reliability of pile capacity by dynamic testing in soils with time-dependent properties.

6 CONCLUSIONS

Contemporary dynamic methods are appropriate tools to determine the time-dependent pile capacity:

The prediction of pile capacity in pre-driving wave

equation analysis can be performed by the use of variable damping as a function of time. Variable damping is the key parameter to enhance accuracy of wave equation solutions because this damping takes into consideration soil consolidation after pile installation.

The main criterion for accurate assessment of pile capacity prediction based on dynamic measurements of force and velocity at the pile head during driving is the ratio of capacities obtained by dynamic and static tests. Such a ratio, taken for arbitrary time between compared tests, is not a verification of dynamic testing results.

Dynamic testing and analysis yield the real, not predicted, static capacity of piles at the time of testing. The static capacity from a static loading test is not a unique standard for assessment of dynamic testing results. Both static loading test and dynamic testing yields the pile capacity at the time of testing.

In soils with time-dependent properties, comparison of static loading test and dynamic testing must be made only for tests performed immediately, in short succession.

Dynamic testing and analysis is a great tool to determine the time-dependent pile capacity after pile installation.

REFERENCES

- Axelsson, G. 1998. Long-term increase in shaft capacity of driven piles in sand. *Proc. Fourth Inter. Conf. on Case Histories in Geotechnical Engineering, St. Louis, 8-15 March*, Paper 1.25.
- Briaud, J.L. and L.M. Tucker 1988. Measured and predicted axial response of 98 piles. *Journal of Geotechnical Engineering*, ASCE, 114(9): 984-1001.
- Chow, F.C., R.J. Jardine, F. Brucy & J.F. Nauroy 1988. Effects of time on capacity of pipe piles in dense marine sand. *Journal of Geotechnical and Geoenvironmental Engineering*, ASCE, 124(3): 254-264.
- Fellenius, B.H., R.E. Riker, A.J. O'Brien & G.R. Tracy 1989. Dynamic and static testing in soil exhibiting set-up. *Journal of Geotechnical Engineering*, ASCE, 115(7): 984-1001.
- GRL and Associates, Inc. 1997. *GRLWEAP - Wave Equation Analysis of Pile Driving, Manual*, Cleveland, Ohio.
- Hunt, S.W. & C.N. Baker 1988. Use of stress-wave measurements to evaluate piles in high set-up conditions. In B. Fellenius (ed.), *Proc. Third Inter. Conf. on the Application of Stress-Wave Theory to Piles, Ottawa, 25-27 May*: 689-705, Vancouver: BiTech Publisher.
- Long, J.H., J. Kerrigan & M.H. Wysockey 1999. Measured time effects for axial capacity of driven piling. *Proc. 1999 Transportation Research Board, 13 January*, Washington, D.C.
- Randolph, M.F., J.P. Carter & C.P. Wroth 1979. Driven piles in clay - the effect of installation and subsequent consolidation. *Geotechnique*, 29(4): 361-393.
- Rausche, F., G.G. Goble & G. Likins 1985. Dynamic determination of pile capacity. *Journal of Geotechnical Engineering*, ASCE, 111(3): 367-383.
- Scov, R. & H. Denver 1988. Time-dependence of bearing capacity of piles. In B. Fellenius (ed), *Proc. Third Inter. Conf. on the Application of Stress-Wave Theory to Piles, Ottawa, 25-27 May*: 879-888, Vancouver: BiTech Publisher.
- Seed, H.B. & L.C. Reese 1955. The action of soft clay along friction piles. *Transactions*, ASCE, 122: 731-754.
- Smith E.A.L. 1960. Pile driving analyses by the wave equation. *Journal of the Soil Mechanics and Foundation Division*, ASCE, 1960, 86: 35-61.
- Svinkin, M.R., C.M. Morgano & M. Morvant 1994. Pile capacity as a function of time in clayey and sandy soils. *Proc. Fifth Inter. Conf. and Exhibition on Piling and Deep Foundations, Bruges, 13-15 June*: 1.11.1-1.11.8, Rotterdam: Balkema.
- Svinkin, M.R. 1995a. Pile-soil dynamic system with variable damping. *Proc. 13th International Modal Analysis Conference, IMAC-XIII, Beyond the Modal Analysis, Nashville, 13-16 February*, 1: 240-247, Bethel, Connecticut: SEM.
- Svinkin, M.R. 1995b. Soil damping in saturated sandy soils for determining capacity of piles by wave equation analysis. *Proc. DFI Annual Member's Conference, Charleston, South Carolina, 16-18 October*: 199-216, Englewood Cliffs: DFI.
- Svinkin, M.R. 1996a. Discussion of 'Setup and relaxation in glacial sand' by York et al., *Journal of Geotechnical Engineering*, ASCE, 122(4): 319-321.
- Svinkin, M.R. 1996b. Soil damping in wave equation analysis of pile capacity. In F. Townsend, M. Hussein & M. McVay (eds.), *Proc. Fifth Inter. Conf. on the Application of Stress-Wave Theory to Piles, Orlando, 11-13 September*: 128-143, Gainesville: University of Florida.
- Svinkin, M.R. 1996c. Velocity-impedance-energy

- relationships for driven piles. In F. Townsend, M. Hussein & M. McVay (eds.), *Proc. Fifth Inter. Conf. on the Application of Stress-Wave Theory to Piles, Orlando, 11-13 September*: 870-890, Gainesville: University of Florida.
- Svinkin, M.R. 1997. Time-Dependent Capacity of Piles in Clayey Soils by Dynamic Methods. *Proc. XIVth Inter. Conf. on Soil Mechanics and Foundation Engineering, Hamburg, 6-12 September*, 2: 1045-1048, Rotterdam: Balkema.
- Svinkin, M.R. & R.D. Woods 1998a. Accuracy of determining pile capacity by dynamic methods. *Proc. Seventh Inter. Conf. and Exhibition on Piling and Deep Foundations, Vienna, 15-17 June*: 1.2.1-1.2.8, Rickmansworth: Westrade Group Ltd.
- Svinkin, M.R. 1998b. Discussion of 'Probability method applied to dynamic pile-driving control' by Liang & Zhou, *Journal of Geotechnical and Geoenvironmental Engineering*, ASCE, 122(4): 319-321.
- Thompson, C.D. & D.E. Thompson 1985. Real and apparent relaxation of driven piles. *Journal of Geotechnical Engineering*, ASCE, 1985, 111(2): 225-237.
- Thorburn, S. & W.J. Rigden 1980. A practical study of pile behavior. *Proc. 12th Annual Offshore Technology Conf.*, Houston.
- Tomlinson, M.J. 1971. Some effects of pile driving on skin friction behavior of piles. *Proc. Institution of Civil Engineers*: 107-114, London.
- Wardle, I.F., G. Price & T.J. Freeman 1992. Effect of time and maintained load on the ultimate capacity of piles in stiff clay. *Piling: European practice and worldwide trends*, *Proc. Institution of Civil Engineers*: 92-99, London: Telford.
- York, D.L., W.G. Brusey, F.M. Clemente & S.K. Law 1994. Setup and relaxation in glacial sand. *Journal of Geotechnical Engineering*, ASCE, 1994, 120(9): 1498-1513.

Set-up considerations in wave equation analysis of pile driving

C.W.Cho

Visiting researcher: University of Western Australia, Perth, W.A., Australia

M.W.Lee

Piletech, Consulting Engineers, Seoul, Korea

M.F.Randolph

University of Western Australia, Perth, W.A., Australia

ABSTRACT: Set-up effects should be accounted for to obtain reliable estimates of driving resistance using WEAP analysis because both the bearing capacity of driven piles, and other dynamic parameters, show a tendency to change with time. Unfortunately, there are no reliable methods that take set-up effects into consideration in wave equation analysis, even though much research has been conducted in this area. Therefore it is desirable to propose new soil input parameters to account for time dependent characteristics. For this purpose, statistical analyses of dynamic measurements for both 'end of driving' and 'restrike' conditions have been undertaken. The paper recommends new parameters that take account of set-up effects for wave equation analysis, and quantifies the reliability of the recommended values by means of statistical analyses on independent pile tests. It is shown that the recommended quake and damping parameters are more reliable than existing suggestions for wave equation analysis of driven piles.

1 INTRODUCTION

WEAP (wave equation analysis of pile driving: GRL (1996)) is based on the ideas developed originally by Smith (1960) to predict drivability and bearing capacity at the time of driving. WEAP, however, has also been used to predict the bearing capacity after driving. In dynamic pile loading tests, the former is referred to as an EOID (end of initial driving) test, while the latter is referred to as a restrike test. Even though the pile-soil system changes due to time dependent effects such as consolidation, single values of soil parameters are input in WEAP. This means that the pile capacity calculated by WEAP can be different from the actual value.

The prediction of driving resistance using WEAP has been found to be reasonably reliable at EOID using parameters suggested in the literature. However, due to the changes in the ground condition around piles after driving, the bearing characteristics also change with time and there is much greater uncertainty regarding the bearing capacity, and other dynamic parameters, at restrike conditions. In spite of this, there are many cases reported where the capacity calculated by WEAP, without considering the time effect, was compared directly with that measured from a static pile load test carried out some time after the initial driving.

In WEAP, soil properties are represented as unit values of shaft or base resistance, and quake and damping coefficients; quake is a parameter that con-

trols the static stiffness, while the damping coefficient is a parameter for representing dynamic enhancement of the soil resistance.

Hunt et al (1988), York et al (1994) have reported good correlations between computed and measured pile capacities by using dynamic measurements. However, those methods have some limitations in practical applications because it is possible to use them only after carrying out dynamic tests. Meanwhile, Thendean et al (1996) did not clarify the time lag between the restrike tests and static tests, and used the same damping and quake properties for WEAP analysis at EOID and restrike. In their study, the change of set value was modelled only by changing the unit values of soil resistance at EOID and restrike in WEAP. At worst, it is often reported that the bearing capacity deduced at EOID is considered as the long term static capacity in practice.

Svinkin and Woods (1998) have suggested a variation of damping coefficient with time through back calculation by WEAP to account for time dependent characteristics of the soil parameters (see Fig. 1). In their study, the damping coefficient was considered, but the quake was disregarded, essentially implying that only the dynamic soil properties, and not the static parameters, are affected by time. However, according to experience in the field, the quake actually varies significantly with time.

To use Svinkin and Wood's method in practice, the function of damping with time has to be determined in advance, since different curves of the type

shown in Fig. 1 were obtained for different pile and soil conditions. Thus dynamic measurements are needed for the particular site, but, WEAP is mostly used in preliminary design where dynamic data are unavailable. Consequently it is desirable to suggest new soil input parameters to account for time dependent characteristics. To do so, it is first necessary to analyze and appraise the soil parameters measured for the same piles at both EOID and at any time after driving.

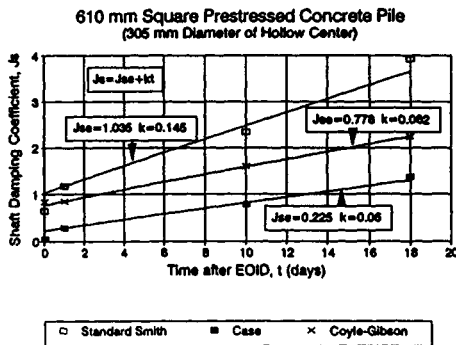


Figure 1. Change in damping coefficients with time (after Svinkin and Woods, 1998)

Statistical analyses of dynamic measurements (quake, damping coefficients, set-up factor) are presented in this paper, which recommends new parameters to consider time effects in wave equation analysis and confirms the reliability of the values recommended. Although time effects may be divided into two types, set-up and relaxation, only the former will be dealt with in this paper.

2 DATA AND ANALYSIS METHOD

Dynamic pile loading tests for the same pile at different times after driving were carried out at 28 sites. To avoid bias in the statistical analysis, a maximum of only 2 data points were used from any one site. For the determination of the set-up factor, the ratio of bearing capacity at restrike to bearing capacity at EOID, 54 piles from 28 sites were investigated and analyzed, while to estimate time effects on quake and damping parameters, 46 piles were analyzed due to the lack of some data. The piles comprised 18 steel pipe piles, 23 concrete piles and 5 H-piles. The diameters of piles ranged from 300 mm to 600 mm. Time lags between EOID and restrike ranged from 1 day to 30 days (averaging about 8 days). Further details of the data are given by Cho (1998).

Data for statistical analysis were drawn from CAPWAP (Case Pile Wave Analysis Program,

GRL, 1996) analyses of dynamic measurements at EOID and restrike. Only the datum at the final restrike was used in cases where multiple restrike tests were undertaken. Since many of the restrike tests were not able to fully mobilize the pile capacity due to limitations of either hammer capacity or material strength of the piles, the set-up factors were determined from the larger of: (i) the ratio of failure load (interpreted from the static response computed using CAPWAP, and using Davisson's criterion for failure) at restrike to that at EOID; or (ii) the ratio of the value (toe resistance at EOID + shaft resistance at restrike) to the bearing capacity at EOID.

Because of the lack of data, it was not possible to account for each different pile type, apart from the toe condition (closed or open-ended). Soils for the pile base response were divided into 4 types: cohesionless soil (S), cohesive soil (C), silty sand (SM), and sandy gravel (SG); while soil for the shaft parameters were divided into 3 types: cohesionless soil (S), cohesive soil (C), and silty sand (SM). The silty sands for the pile shaft responses were mostly weathered residual soils, which are commonly used as the bearing stratum. The soil type for the shaft response was based on the soil layer that provide the majority of shaft resistance for the pile.

CAPWAP is a trial and error method of signal matching, which is known to lead to subjective, non-unique, sets of parameters. As such, it is possible to fail to discover any distinct trends in the parameters, since each parameter determined from CAPWAP is influenced by the other parameters. In order to minimize operator-dependent trends in the statistical analyses, only data with high matching quality (MQ in CAPWAP) were analyzed.

In order to confirm the validity of the parameters deduced from the CAPWAP analyses, they were used in WEAP analyses for real sites (with new pile data independent of the original set of data). Wave equation analyses were performed for a total of 24 pile tests at 6 sites (4 tests per site).

In wave equation analysis, adjustments of the maxima of force (FMX) and the transferred energy (EMX) on the basis of the value analyzed by CAPWAP were made in order to increase the accuracy of the compared data. The adjustment was considered sufficient when the calculated and measured EMX values agreed to within 10 %, following the guidelines in FHWA (1996). Other input parameters (except the soil parameters) were based on the CAPWAP data and test conditions in the field. New soil parameters were then used as the input data for WEAP to match the measured drivability.

For the reliability analysis of the results of wave equation analysis, using the new parameters drawn from the statistical data, a log-normal probability function was used. The log-normal function was chosen to allow consideration of the non-symmetrical characteristics and distribution of the

ratios. The calculated capacities by WEAP were divided by the measured capacity, and then the ratios were evaluated by the log-normal function. From the log-normal function, mean standard deviation, and coefficient of variance were evaluated. The coefficient of variance is defined as the standard deviation divided by the mean.

3 RESULTS AND DISCUSSION

The set-up factors for shaft resistance, determined from the statistical analysis, are shown in Fig. 2 for the 3 soil types. In Fig. 2, m, SD, and N stand for mean, standard deviation and number of data, respectively. The set-up factor increases as the soil particle size decreases, and their mean values are 1.5 in cohesionless soils and silty soils, 2.5 in cohesive soils. Although these values are larger than those in WEAP (GRL, 1996) or FHWA (1996) as shown in Table 1, they are still likely to be conservative, because most restrrike tests failed to mobilize the full (ultimate) bearing capacity of the piles.

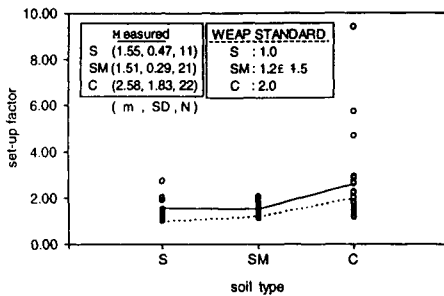


Figure 2. Deduced set-up factors for shaft resistance

Table 1. Shaft set-up factors (WEAP, FHWA)

Predominant soil type in the shaft	Set-up factors (conservative)
Clay	2.0
Silt - Clay	1.0
Silt, Sand - Clay	1.5
Sand - Silt, Fine Sand	1.2
Sand, Sand - Gravel	1.0

Table 2. Ratio of velocity at EOID and at restrrike

	VMX ratio	EMX ratio	Toe Velocity ratio	Toe Energy Ratio
Mean	0.94	0.89	1.69	3.26
SD	0.19	0.19	0.87	4.8
N	43	43	43	43
Remarks	VMX	EMX	Vtoe	Etoe

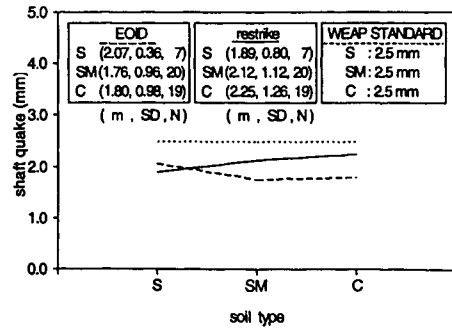


Figure 3. Shaft quake at EOID and restrrike

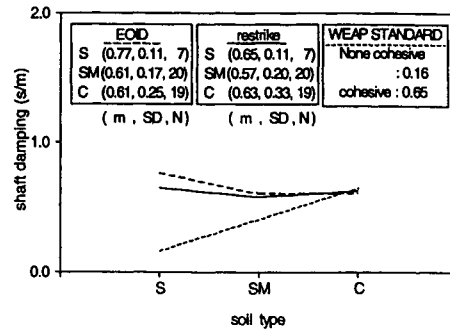


Figure 4. Shaft damping coefficient at EOID and restrrike

The drilling logs for the data with high set-up factors in Fig. 2 were analyzed. It was found that the sites comprised mostly alluvial deposits. As a result, it is suggested that set-up effects are influenced by not only the particle size but also the formation history. Cho (1998) reported that mineral formation and relative density highly influence set-up effects in alluvial deposit soils even if they are sandy soils.

Fig. 3 shows the change of shaft quake with time and soil type, and also the values suggested in WEAP. There is no distinct trend in the change of shaft quake, which lies in the range 2.0 ± 0.2 mm. This is marginally lower than the value of 2.5 mm suggested in WEAP.

Fig. 4 shows the change of shaft damping coefficients (Smith damping coefficient) with time and soil type, and also the values suggested in WEAP. It may be seen that again there is no distinct trend in the change of shaft damping coefficient. The range of shaft damping coefficient represents about 0.65 ± 0.1 s/m regardless of time since driving, and is higher than the values suggested in WEAP. This may be because the soil type in the field is not as simple as in the WEAP classification (and generally includes some clay fraction). A possible reason for the lack of time effects on the damping coefficient is that the appropriate value is closely linked to the pile maximum velocity (VMX), which for the shaft is

dictated by the maximum energy (EMX). These vary little between EOID and restrrike (Table 2). As such, it is inferred that the damping coefficient for the shaft, unlike that for the pile toe, is not highly influenced by set-up effects.

Fig. 5 shows that the toe quake at restrrike is smaller than that at EOID, implying that the quake decreases with time. This trend is particularly apparent in cohesive soils, because set-up effects are more significant in fine-grained soils (see Fig 2). From those results, it seems that Svinkin and Wood's method has some limitations in accounting for set-up effects. According to Fig. 5, there is no distinct trend in the relationship between soil type and quake. As shown by Davisson (1973), the quake is also related to diameter of pile and shape of toe, etc, and cannot be expressed in terms of soil type only.

Therefore, the change of the quake with pile diameter, D, was explored through regression analysis, as indicated in Table 3. Table 3 shows that although the correlation factor (r^2) is low, the general trend is apparent, and that the quake (D/52 at EOID, D/94 at restrrike) is much higher than the value suggested in WEAP (D/120). In particular, there is a large difference in the value at EOID. From the analysis, it is concluded that the quake decreases with time and its change is large in clay soils. The toe quake for closed-ended piles is also smaller than that for opened pile, which is presumably related to the compressibility of the soil plug.

Fig. 6 shows that the toe damping coefficient increases with time. This is assumed to be linked to the reduction in particle velocity and transmitted energy at the pile toe, as indicated in Table 2. Thus, the non-linear nature of real damping means that a higher (linear) coefficient is needed for low velocities than for high velocities. Fig. 6 also shows that the increase in the toe damping coefficient is small in fine-grained soils, perhaps due to limited consolidation in the time between EOID and restrrike. Fig.6 shows that the toe damping coefficients at EOID lie in the range about 0.25 ± 0.02 s/m, and the values are smaller than that suggested in WEAP.

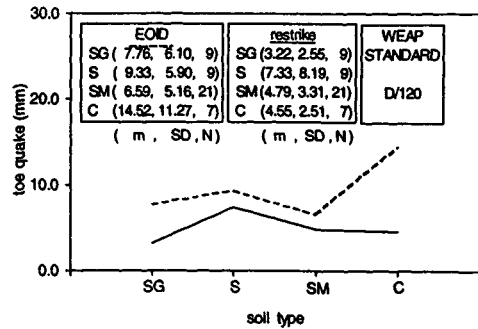


Figure 5. Toe quake with time and soil types

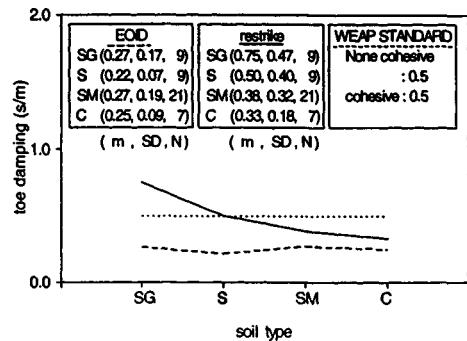


Figure 6. Toe damping coefficient with time and soil types

4 RECOMMENDED NEW PARAMETERS AND THEIR RELIABILITY

As shown in the previous section, there are significant differences between the analysis results and the values suggested in WEAP. Therefore, new parameters for both EOID and restrrike, have been recommended in the light of the statistical analyses, as detailed in Table 4.

Table 3. Relation of diameter of pile and the quake

		EOID			Restrike			No of data
		Equation	r^2	SD	Equation	r^2	SD	
Soil type	C	D/25	0.53	10.31	D/80	0.64	2.07	7
	S	D/51	0.52	7.06	D/72	0.45	9.53	9
	SM	D/62	0.21	5.40	D/87	0.34	3.59	21
	SG	D/71	0.54	7.36	D/177	0.61	3.17	9
All data		D/52	0.28	7.64	D/94	0.39	5.10	46
Toe shape	Open	D/58	0.10	3.83	D/102	0.54	4.07	23
	Closed	D/47	0.34	10.14	D/88	0.32	6.03	23

The dynamic parameters used in WEAP are not inherent properties of the soil but changeable ones with time or test conditions. Consequently, it is inevitable that suggested values will not represent accurately a given set of conditions in the field. Previous suggestions for the dynamic parameters in WEAP have been given by Reese et al (1964) and Coyle et al (1970). From this viewpoint, the recommended values in Table 4, which are based on reliable data from various sites, should prove reasonable for application in WEAP. However, it should be emphasized that the recommended values are at best average values for the sites in question and are strictly applicable only over the relatively limited range of pile diameters (76 % between 400 mm and 500 mm).

The set-up factors in Table 4 are the averages of the data excluding data beyond 1 standard deviation from the mean in the statistical analyses. Considering that bearing capacities at restrike were mostly determined from dynamic tests where the full pile capacity was not mobilised, the set-up factors are regarded as conservative values.

It is interesting that the suggested values in WEAP are more similar to those recommended at restrike in this study rather than ones at EOID, although WEAP was originally developed for drivability analysis at EOID. The recommended values in Table 4 can be appropriately adjusted with site conditions, and are particularly useful for the determination of bearing resistance at restrike.

To analyze the reliability of the recommended parameters, a comparison was performed between key predictions (such as pile capacity) calculated by WEAP with the parameters recommended in this study and those calculated by WEAP using parameters suggested in the WEAP manual.

The ratio of the values calculated by WEAP to the measured ones using CAPWAP were then obtained. Finally the ratios were used for the reliability analysis using a log-normal probability function.

The results of the reliability analysis using a log-normal probability function are shown in Fig. 7 to Fig. 10. In those figures, each initial stands for as follows:

- M : mean,
- SD : standard deviation,
- CV : coefficient of variance (=SD/M),
- ES : WEAP calculation with the parameters suggested in WEAP at EOID,
- RS : WEAP calculation with the parameters suggested in WEAP at restrike,
- ER : WEAP calculation with the parameters recommended in this study at EOID,
- RR : WEAP calculation with the parameters recommended in this study at restrike.

Function value : probability density distribution

Fig. 7 and Fig. 8 show that the capacity ratios based on the recommended parameters in this study are closely grouped around unity, while those based on parameters suggested in WEAP show a much broader range. This suggests that the bearing capacities predicted using the recommended parameters are more reliable than those using the suggested ones in WEAP.

From Fig. 9 and Fig 10, it is found that there are some differences in the predicted and measured maximum force, FMX, using the suggested parameters in WEAP, while the new parameters proposed here give improved accuracy. Either set of parameters lead to good prediction of maximum energy, EMX.

Table 4. Recommended parameters for WEAP

	EOID				Restrike				Set-up Factor
	Shaft		Toe		Shaft		Toe		
	Quake	Damping	Quake	Damping	Quake	Damping	Quake	Damping	
	(mm)	(s/m)	(mm)	(s/m)	(mm)	(s/m)	(mm)	(s/m)	
Clayey soil	2.0 (2.54)*	0.65 (0.65)*	D/25 (D/120)*	0.25 (0.5)*	2.0	0.65	D/80	0.5	2.0 (2.0)*
	2.0 (2.54)*	0.65 (0.16)*	D/50 (D/120)*	0.25 (0.5)*	2.0	0.65	D/70	0.5	1.3 (1.0)*
Soil with Gravel	2.0	0.65	D/70	0.25	2.0	0.65	D/180	0.5	-
Weathered Soil	2.0	0.65	D/60	0.25	2.0	0.65	D/90	0.5	1.5
Remarks			1.2 times smaller in open pile				1.2 times smaller in open pile		

* means the values suggested in WEAP

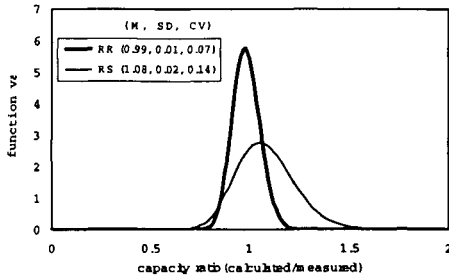


Figure 7. Log normal distribution of capacity ratio at restrike

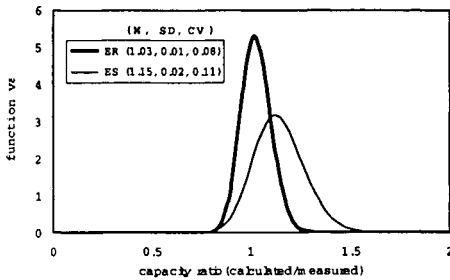


Figure 8. Log normal distribution of capacity ratio at restrike

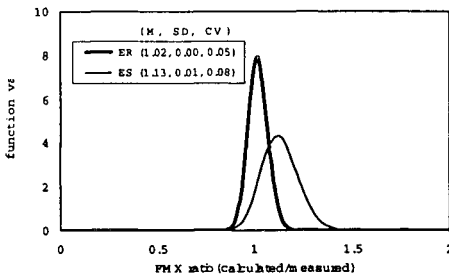


Figure 9. Log normal distribution of FMX ratio at EOID

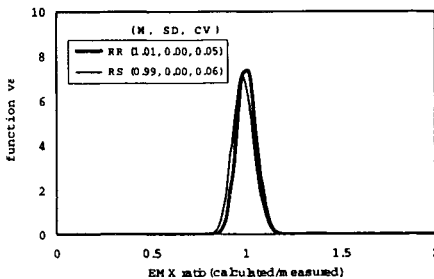


Figure 10. Log normal distribution of EMX ratio at EOID

5 CONCLUSIONS

The bearing capacity of piles after driving changes with time. Set-up effects need therefore to be considered in order to deduce the bearing capacity from restrike data using WEAP. A statistical analysis of data from 46 piles tested at initial driving (EOID) and restrike indicates that there are significant differences between the parameters deduced from this study and those suggested in the WEAP manual. Accordingly, new soil parameters (damping, quake) for wave equation analysis at EOID and restrike are recommended in this paper.

WEAP analyses were carried out using both the recommended parameters and those previously suggested and their results were compared with the measured values through reliability analysis. It was found that the new parameters recommended in this paper showed higher reliability compared with those suggested in the WEAP manual.

REFERENCES

- Cho, C. W. 1998. A study on the time dependent capacity gain of driven piles. Ph. D Thesis: Hanyang University. Seoul. Korea.
- Coyle, H.M. & Gibson, G.C. 1970. Empirical damping constants for sand clay. *Journal of the Soil Mechanics and Foundation Division, ASCE*, Vol. 96. SM3 : 949-965.
- FHWA. 1996. US FHWA Dpt. of Transportation. Design and construction of driven pile foundation. Workshop Manual : 16.1 - 17.70.
- GRL Associates, Inc. 1996. GRLWEAP/CAPWAP User Manual
- Hunnigan, P. 1984. Large quake development during driving of low displacement piles. *Proc. of the 2nd Int. Conf. on the Application of Stress-Wave Theory to Piles* : 126-133.
- Hunt, S.W. & Baker, C.N. 1988. Use of stress-wave measurements to evaluate piles in high set-up conditions. *Proc. of the 3rd Int. Conf. on the Application of Stress-Wave Theory to Piles*. BiTech Publisher. Ottawa : 689-705.
- Parmar, H. & Brown, D. 1996. Comparison of dynamic and static of evaluating static pile capacity. 6th Int. Conf. and Exhibition on Piling and Deep Foundations. Bombay : 4.6.1 - 4.6.6.
- Smith, E.A.L. 1960. Pile driving analyses by the wave equation. *Jour. of the Soil Mechanics and Foundation Division, ASCE*. Vol.86 : 35-61.
- Thendean, G., Rausche, F., Svinkin, M. & Likins, G. 1996. Wave equation correlation studies, *Proc. of the 4th Int. Conf. on the Application of Stress-Wave Theory to Piles* : 144-162.
- Reese, J.L. & Forehawd, P.W. 1964. Prediction of pile capacity by the wave equation. *Journal of the Soil Mechanics and Foundation Division, ASCE*. Vol. 90. SM2 : 1-25.
- Svinkin, M. R & Woods, R. D. 1998. Accuracy of determining pile capacity by dynamic methods. 7th Int. conf. and Exhibition on Piling and Deep Foundations : 1.2.1-1.2.8.
- York, D.L., Brusey, W. G., Clemente, F.M. & Law, S.K. 1994. Setup and relaxation in glacial sand. *Journal of Geotechnical Engineering, ASCE*. 120(9) : 1498-1513.

Drivability and performance of model piles driven into cemented calcareous sand

D. Bruno, M.F. Randolph, C.W. Cho & H.A. Joer

Centre for Offshore Foundation Systems, University of Western Australia, Perth, W.A., Australia

ABSTRACT: This paper reports the results of a centrifuge model study of pile drivability in cemented calcareous sand. The tests were carried out at a scaling ratio of 1:150, on piles of equivalent prototype diameter 1.42 m, driven to depths of 20 to 24 m into cemented sand with cone resistances ranging from 14 to 60 MPa. Two samples were prepared, one with three layers of gradually increasing cone resistance, and one with a high strength intermediate layer approximately 2 pile diameters thick. Different pile toe configurations were examined ranging from open-ended (with no change of pile section near the toe) to closed-ended with a conical tip and either flush with the outer pile shaft, or slightly oversized. The effect of the different toe configurations on the drivability was examined. It was found that pile refusal occurred in the deepest (most highly cemented) layer, and that drivability became marginal for the closed-ended piles in the intermediate strong layer (in both cases, cone resistance was around 40 MPa). The hard driving was consistent with high measured static capacities of the piles, and the observed drivability was found to be consistent with results from a numerical drivability study, leading to recommended soil parameters for cemented calcareous sediments.

1 INTRODUCTION

The low shaft capacity of driven open-ended piles in calcareous soils has led to alternative construction techniques such as drilled and grouted, or grouted driven, piles. An alternative approach, which may also be useful for grouted driven pile construction, is to drive closed-ended piles (de Mello et al, 1989). Closed-ended piles have rarely been driven offshore, because of concerns of refusal. In calcareous soils, the main concern is the presence of intermediate cemented layers (prior to the founding stratum) that could cause premature refusal for a closed-ended pile.

Grouted driven piles, where post-installation grouting is carried out on driven piles (Barthelemy et al, 1987), are an economically attractive alternative to drilled and grouted piles because of the much shorter construction period. While the original technology for grouted driven piles was based on open-ended piles, with grouting conduits pre-installed inside each pile (Rickman and Barthelemy, 1988), a closed-ended configuration would allow greater reliability and potential for remedial actions.

The potential advantages of driven closed-ended piles, either grouted or ungrouted, must be weighed against the higher risk of premature refusal, compared with open-ended piles of a similar diameter. The work reported in this paper was aimed at assessing, through physical model tests, the drivability

of open and closed-ended piles in cemented calcareous sands. Two different stratigraphies were investigated, one with three layers of gradually increasing strength, and one with an intermediate strong layer. Three different pile toe configurations were tested, open and closed-ended, and with either a flush or oversized toe closure.

2 EQUIPMENT AND PILE DETAILS

The model tests were carried out on the geotechnical centrifuge at UWA, an Acutronic Model 661 with a 40 g-tonne capacity and platform radius of 1.8 m (Randolph et al, 1991).

The model pile tests were conducted at an acceleration of 150 g using a combined pile-driving and static loading actuator (de Nicola and Randolph, 1994). Figure 1 shows a photograph of the pile-driving actuator mounted on the centrifuge strong-box, prior to a pile test. The mechanical driving apparatus is in the form of a detachable carriage that houses the driving ram and moves down with the pile during driving. A small potentiometer measures the gap between the ram (in its retracted position) and the pile cap, and a feedback loop is used to control the position of the carriage in order to maintain a specified drop-height. Table 1 summarises the key mechanical properties of the system.

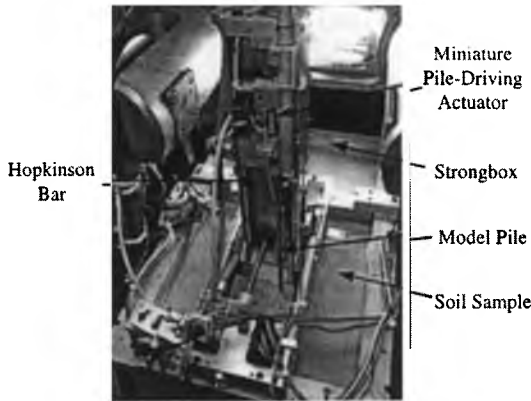


Figure 1 Model pile-driving hammer on strong-box

Table 1. Key properties of model pile-driving system

Mechanical property	Range
Vertical displacement	240 mm
Horizontal displacement	150 mm
Hammer driving frequency	1 - 20 Hz
Ram drop height	0 - 20 mm
Ram mass	37 or 54 g
Static pile test driving speed	0 - 3 mm/s
Maximum vertical driving load	6 kN

The model pile was fabricated from a thin-walled cylindrical stainless steel section with the outer surface roughened by sandblasting. The main section of the pile, 200 mm long has internal and external diameters of 8.5 and 9.5 mm respectively. An additional instrumented section, 60 mm long, has an increased external diameter of 10.5 mm. All tests were conducted at a nominal acceleration level of 150 g, so that the 9.5 mm diameter of the model pile represents a prototype pile diameter of $150 \times 9.5 = 1425$ mm (or 1.425 m). The pile was instrumented with a single pair of half-bridge strain gauges located 230 mm from the tip of the pile, which ensured they remained above the sample surface even at the deepest pile penetrations. These gauges provided the measurement of total bearing load in the pile during static testing as well as the transient stress-wave force during dynamic testing.

The pipe pile could be fitted with two different conical driving shoes, rendering the piles closed-ended. The driving shoes, shown in Figure 2, are made from stainless steel and were sandblasted to the same degree as the model pile. The 9.5 mm diameter shoe is flush with the model pile - these piles are referred to as CE (closed-ended), whilst the piles fitted with the 10.5 mm shoe are referred to as CEO (closed-ended oversize). The open ended piles (no shoe attached) are referred to as OE.

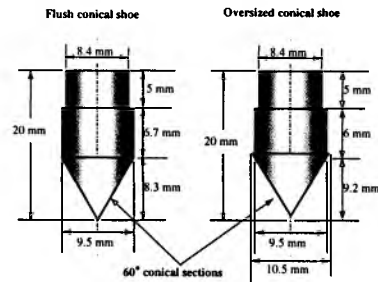


Figure 2 Conical tips for closed-ended piles

A Hopkinson Bar, in the form of a strain-gauged PVC strip attached at the pile head, was used to measure the transient stress-wave velocity during the dynamic tests, (Bruno and Randolph, 1998). This arrangement obviates the need for miniaturizing an accelerometer, as would be used in the field. The Hopkinson Bar can be seen attached to the pile in Figure 1. Essentially, the strip acts as a transmission line whereby the strain in the strip, induced by the movement of the pile head, is converted to a velocity. This conversion is only valid for uni-directional waves. Hence the strip is made from PVC, which has a low wave-speed, and is made sufficiently long so that it is able to transmit several return waves from the pile toe before receiving reflected waves from the end of the strip.

3 SOIL CONDITIONS

The model tests were carried out in calcareous silt dredged from the sea bed on the North-West Shelf of Australia. The material was dried in an industrial kiln and sieved to give an effective particle size range of 0.1 to 0.4 mm, with a mean particle size of just under 0.2 mm.

The dry soil was mixed with 4 to 10 % (by weight) of Portland cement, and then with water to give a water content of 30 %. The slurry was mixed for a further 30 minutes before being transferred to the strongbox and placed under a consolidation press. A 100 kPa surcharge was applied to the soil surface for around 1 hour. This process was repeated for each layer of cementation, with new layers being poured on top of the pre-consolidated bottom layers. The sample was then sealed and left for at least 7 days in order for the cement to cure.

Cement contents of 4, 6 and 10 % were used, to give nominal unconfined compressive strengths of 250, 500 and 1000 kPa, and corresponding cone resistances, q_c , of 15, 27 and 50 MPa. In practice, some variation from the above values of q_c was found, with the second of the two samples have somewhat higher strengths than the first.

The nominal layers depths (at equivalent prototype scale) were 0 - 11 m (4 %), 11 - 22 m (6 %)

and 22 – 36 m (10 %) for Sample 1, and 0 – 11 m (4 %), 11 – 14 m (10 %), 14 – 24 m (6 %) and 24 – 36 m (10 %) for Sample 2. Four cone penetration tests were carried out ‘in-flight’ in each sample, using a 7 mm diameter cone. These showed excellent repeatability, and gave the average cone profiles shown in Figure 3. As may be seen, the ranges of cone resistances for the different cement contents are 13 to 18 MPa, 21 to 30 MPa and 35 to 60 MPa respectively (although it appears that there may have been some shortcomings in preparing the base layer for Sample 1).

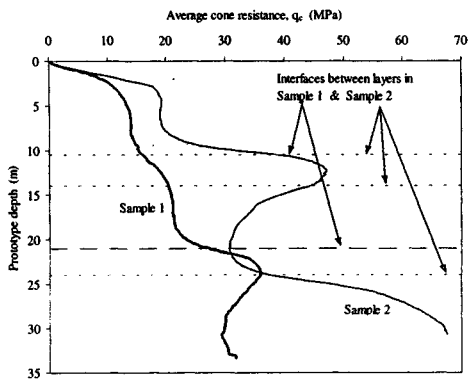


Figure 3 Average profiles of cone resistance

4 TESTING PROCEDURES

The standard ‘strongbox’ (or soil container) used on the UWA centrifuge is an aluminium segmented box, with internal dimensions 390 mm wide by 650 mm long and 325 mm high. The total soil depth in each sample was between 240 and 250 mm, and six driven pile tests were carried out in each sample, (two of each type) down the centre-line of the box. The minimum pile spacing between tests was 7 diameters, and a minimum of 14 pile diameters was maintained from the end-walls of the box.

For Sample 1, it was intended to perform dynamic and static tests in each of the three different cementation layers, but this was only achieved in the first two layers owing to premature refusal before entering the deepest layer. For Sample 2, the intention was to test the piles at a penetration of 1 pile diameter, d , past the top 10 % cement layer, as well as at an ultimate penetration into the deepest layer. Again, however, premature refusal of some of the piles frustrated this plan, as described later.

All piles were driven into the soil samples using the model pile driving actuator, with a blow frequency of 10 Hz and drop heights ranging from 10 mm initially, to 17 or 18 mm at deeper penetrations. Dynamic tests were performed prior to static loading, usually at a drop height of 17 mm.

The model piles were driven continuously between one test penetration and another. The blow count for each pile was recorded by monitoring the number of times the hammer was fired between each sampling point. Two ram masses were used in the centrifuge tests. In Sample 1, the first two open-ended piles were installed with a 37 g mass; this was later replaced with a 54 g mass, which was used throughout the remainder of the testing programme.

In the centrifuge model, the scaling law for mass is given by:

$$(\text{Mass})_{\text{prototype}} = (\text{Mass})_{\text{model}} \times N^3 \quad (1)$$

where N is the g level in the centrifuge tests. Although an acceleration of 150 g was applied to the soil samples, the g level is affected by the distance from the axis of the centrifuge. The hammer was initially positioned around 325 mm above the sample surface, moving down with the pile to a final height of around 175 mm. Since the acceleration field varies linearly with the radius of rotation, the g level is considerably less at the position of the actuator. Hence, the actual g levels at the initial and final actuator positions are approximately 104 g and 122 g respectively. This corresponds to an average prototype ram mass of 94 tonne (for the 34 g mass) and 137 tonne (for the 54 g mass), and average rated hammer energies in the range 980 kJ to 3000 kJ. Thus the model hammer is equivalent to a Menck 8000 or 12500 offshore hammer.

After installation of the piles, static load tests were conducted either in tension (T) first or compression (C), up to vertical displacements of approximately 40 % of the pile diameter (0.4 d). The tests were all performed at a (model) rate of 0.05 mm/sec, which ensured a drained condition around the pile. The static pile capacity, Q_s , was taken as the load measured at a pile head displacement of 0.1 d , although this was usually close to a distinct yield point and dramatic reduction in loading stiffness.

The transient stress-wave force, F and velocity, v , were measured throughout pile driving as well as during dynamic tests carried out prior to static loading, (Bruno & Randolph, 1998¹). The Case analysis was used to estimate pile capacity (or mobilised soil resistance), R_s , during installation, as given by the following expression:

$$R_s = \frac{1-j_c}{2} \frac{2Z_2}{Z_1+Z_2} (F+Z_1v)_t + \frac{1+j_c}{2} \frac{Z_1+Z_2}{2Z_1} (F-Z_1v)_t \frac{2L}{c} \quad (2)$$

where Z_1 and Z_2 are the impedances of the upper (instrumented) and lower (embedded) pile sections and the other notations are standard terminology. This modified form of the Case formula has been found to give accurate estimates of soil resistance (Bruno and Randolph, 1999), although rigorously an additional correction should be made to the returning

stress-wave, $(F - Z_1 v)_{t+2L/c}$, to allow for downward travelling waves reflected from the interface between the upper and lower pile sections.

The deduced mobilised soil resistance, R_s is sensitive to the value adopted for the damping parameter, j_c . However, here it was possible to calibrate this parameter from the static tests, and a value of $j_c = 0.1$ provided the best estimate to the measured static capacities.

5 RESULTS

5.1 Driving Characteristics

Typical driving records are shown in Figures 4 to 7 for an open-ended and (flush) closed-ended pile in Samples 1 and 2. In addition, the driving record for one of the over-sized closed-ended piles in Sample 2 is shown in Figure 8, as it reveals an interesting phenomenon associated with the strong layer.

In Sample 1, the open-ended pile was driven with the smaller ram mass, and thus lower energies and showed much easier than for the closed-ended pile

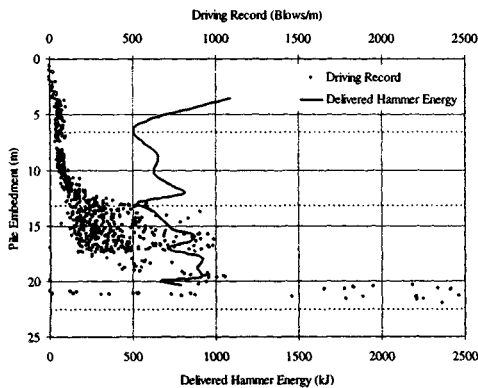


Figure 4 Driving record for open-ended pile, Sample 1

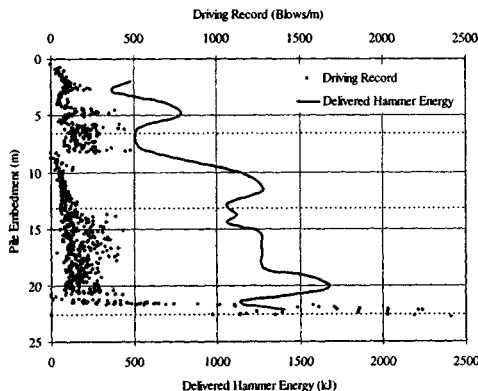


Figure 5 Driving record for closed-ended pile, Sample 1

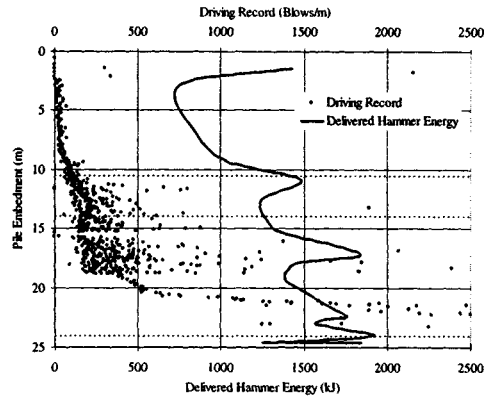


Figure 6 Driving record for open-ended pile, Sample 2

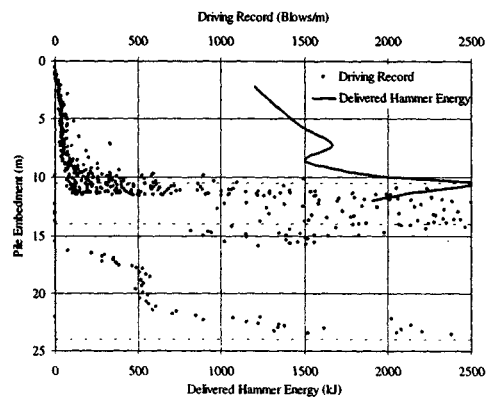


Figure 7 Driving record for closed-ended pile, Sample 2

(comparing Figures 4 and 5). The easier driving of the open-ended piles is more apparent for Sample 2, where both open and closed-ended piles were driven with the same ram mass. Figures 6 and 7 show that the closed-ended pile essentially reached refusal at the high strength layer between 11 and 14 m. Eventually, the pile was forced through the layer, but only after a very large number of blows, at a rate of advance that would be impractical in the field. (Note that the velocity monitoring instrumentation failed in the latter stages of penetration of the closed-ended pile in Sample 2, hence the lack of information on delivered energy.)

Comparison of the soil plug monitoring for the open-ended piles showed that the plug advance was very similar for each pile, with an incremental filling ratio of about 0.8 over most of the driving record. This accounts for the easier driving of the open-ended piles.

The breakthrough of the closed-ended pile in Sample 2, which occurred only after the tip was fully through the strong layer, was also seen for one of the over-sized closed-ended piles, but this time while the tip was still within the strong layer (see Figure 8).

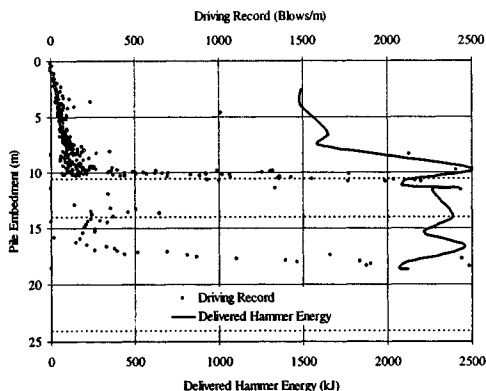


Figure 8 Driving record for over-sized closed-ended pile, Sample 2

Interestingly, however, the pile refused mid-way through the subsequent (6 % cement) layer. The implication is that the breakthrough halfway through the strong layer must have carried a large fragment of that strong layer down into the weaker zone below, eventually leading to refusal of the pile.

5.2 Mobilised Soil Resistance and Pile Capacity

Profiles of mobilised soil resistance for the different pile types are compared with pile capacities deduced from static load tests in Figures 9 and 10, for Samples 1 and 2 respectively. The mobilised soil resistance has been obtained from Case analyses of the stress-wave data, using a damping parameter of $j_c = 0.1$.

Agreement between the dynamic and static estimates of pile capacity is reasonably good at low capacities, but the dynamic analyses underestimate the measured values at high capacities. This may be attributed to the very small movements with each dynamic blow once the pile capacity exceeds 25 to 30 MN. It should be noted that, in general, the delivered hammer energy was higher for Sample 2 than for Sample 1, as the pile-driving hammer was serviced in the intervening period.

6 PILE DRIVABILITY

Drivability studies have been undertaken using WEAP (GRLWEAP, 1997) in order to ascertain appropriate soil parameters to use for cemented calcareous soils. The hammer has been modelled as a Menck 12500 hammer delivering energies consistent with average values shown earlier in Figures 4 to 8.

Since WEAP cannot model the soil resistance within open-ended piles explicitly, the open-ended pile has been modelled by increasing the specific weight of the pile over the plugged length of the pile, as suggested in the WEAP manual.

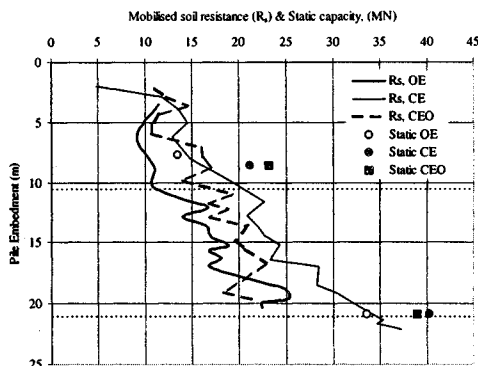


Figure 9 Profiles of dynamic and static resistance, Sample 1

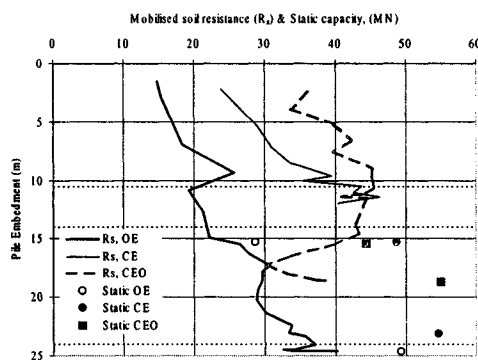


Figure 10 Profiles of dynamic and static resistance, Sample 2

Shaft friction was taken as 0.43 % (open) and 0.73 % (closed) of the cone resistance, while quake and damping values of 2.0 mm and 0.65 s/m have been assumed along the shaft. At the pile base, the resistance has been taken 40 % (open – assumed to act over the complete base) and 60 % (closed) of the cone resistance, q_c , while quake and damping have been taken as $d/50 = 30$ mm and 0.25 s/m respectively (consistent with Cho et al, 2000).

The resulting profiles of pile capacity are shown in Figure 11, and are reasonably consistent with the measured capacities shown in Figure 10. Results from the drivability analyses are shown for an open-ended and closed-ended pile for the Sample 2 stratigraphy in Figures 12 and 13.

For both piles, good agreement is observed with results shown earlier in Figure 6, with only slight increase in blow-count as the open-ended pile passes through the intermediate high strength layer, but the closed-ended pile effectively refusing in the layer. The predicted reduction in blow-count just below this layer is less dramatic than measured, partly due to the coarse depth spacing of the drivability data, but possibly also reflecting overprediction of the shaft friction in the strong layer.

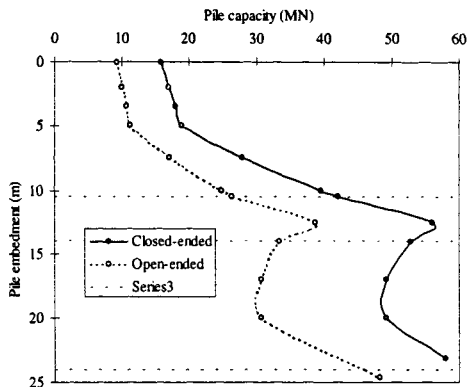


Figure 11 Pile capacity profiles for drivability study: Sample 2

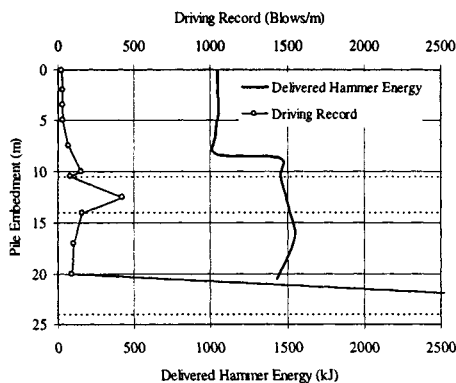


Figure 12 Drivability study for open-ended pile in Sample 2

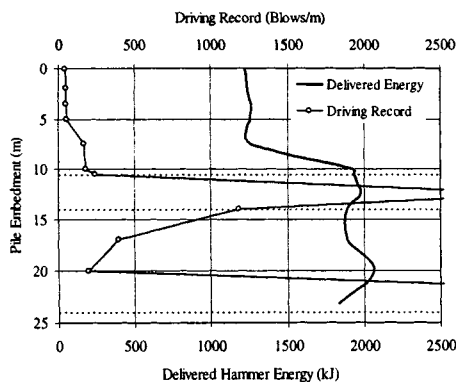


Figure 13 Drivability study for closed-ended pile in Sample 2

7 CONCLUSIONS

This paper has described a study of the drivability of open and closed-ended piles into cemented calcareous soils. The study was undertaken with a view to assessing the feasibility of driving closed-ended piles in such soils, with or without post-installation

grouting, in view of the low shaft resistance of driven open-ended piles in calcareous sediments.

As expected, closed-ended piles were found to be much more difficult to drive than open-ended piles, although both pile types met refusal in thick layers of cemented material with cone resistance in excess of 35 to 40 MPa. It was found that open-ended piles could be driven relatively easily through a layer of strong material only 2 pile diameters thick. Closed-ended piles essentially refused in such a layer, breaking through only after more than 8000 blows.

Drivability studies showed that the measured driving characteristics could be simulated using conventional values of quake and damping parameters, unit shaft friction of 0.4 (open) to 0.7% (closed) of the cone resistance, q_c , and toe bearing resistance of $0.4q_c$ (open) to $0.6q_c$ (closed). These values are reasonably consistent with field experience reported by de Mello et al (1987), and give confidence in the validity of the centrifuge model study.

ACKNOWLEDGEMENTS

This work was undertaken for Heerema Marine Contractors as part of research into grouted driven piles, and is presented with their kind permission. It forms part of the activities of the Centre for Offshore Foundation Systems, established and supported under the Australian Research Council's Research Centres Program.

REFERENCES

- Barthelemy, H., Martin, R., Le Tirant, P., Nauroy, J.F. & Cipriano de Meideros, J. 1987. Grouted driven piles: An economic and safe alternate for pile foundations. *Proc. 19th annual Off. Tech. Conf. (OTC)*, Houston, Texas, 427-436.
- Bruno, D. & Randolph, M.F. 1998. Dynamic testing of driven piles in dense sand. *Proc. International Conference CENTRIFUGE 98 (ISSMFE Centrifuge 98)*, Tokyo, 519-524.
- Bruno, D. & Randolph, M.F. 1999. Dynamic and static load testing of model piles driven into dense sand. *J. Geot. Eng. Div. ASCE*, 125(11), 988-998.
- Cho C.W., Lee, M.W. and Randolph, M.F. 2000. Set-up considerations in wave equation analysis of pile driving. *Proc. 6th Int. Conf. On Application of Stress-Wave Theory to Piles*, Sao Paulo.
- De Mello, J.R.C., Amarai, C.D.S., Maia de Costa, A., Rosas, M.M., Decnop Coelho, P.S. & Porto, E.C. 1987. Closed-ended pipe piles: Testing and piling in calcareous sand. *Proc. Annual Offshore Technology Conf.*, Houston, Paper OTC 6000.
- De Nicola, A. & Randolph, M.F. 1994. Development of a miniature pile driving actuator. *Proc. Int. Conf. Centrifuge '94*, Singapore, 473-478.
- Randolph, M.F., Jewell, R.J., Stone, K.J.L. & Brown, T.A. 1991. Establishing a new centrifuge facility. *Proc. Int. Conf. Centrifuge 91*, Boulder, Colorado, 3-9.
- Rickman, J.P. & Barthelemy H.C. 1988. Offshore construction of grouted driven pile foundations. *Proc. Int. Conf. on Calcareous Sediments*, Perth, 1, 313-319.

Automatic signal matching with CAPWAP

F. Rausche & B. Robinson

Goble Rausche Likins and Associates Incorporated, Cleveland, Ohio, USA

L. Liang

Pile Dynamics Incorporated, Cleveland, Ohio, USA

ABSTRACT: CAPWAP® Provides the most reliable means of analyzing dynamic pile top force and velocity records from the Pile Analyzer® (PDA). This is a signal matching approach which requires that certain soil parameters are adjusted until measured and calculated pile top variables reach a reasonable match. The number of unknown soil parameters depends on the depth of pile penetration and therefore the computational effort can be appreciable if the pile is long. The process can be either done in an interactive manner or automatically with great time savings. Current practice requires that the automatic results are checked by interactive analysis.

In an attempt to make the automatic solution reliable, several additional matching parameters have been included in the CAPWAP model. Among these variables, the most important is the final set (inverse of blow count) of the hammer blow analyzed. Unfortunately, since restrike data is usually analyzed by CAPWAP for long term static capacity predictions, final set is not always accurately known. For this reason a study was undertaken to evaluate the accuracy of the automated CAPWAP results including blow count matching compared to the traditional approach. More than 30 cases where static load tests and restrike tests had been performed were analyzed using the automatic procedure provided by the Windows based CAPWAP Version 1999-1. This program also calculates the total dynamic resistance (the sum of damping and static resistance) allowing for an assessment of the ratio of total dynamic resistance to static resistance and its relationship with soil type.

1 INTRODUCTION

Dynamic pile testing has two distinctly different goals: (a) monitoring the installation of impact driven piles to avoid pile damage and assure sufficient pile penetration for bearing capacity at the time of installation and (b) dynamic load testing for an assessment of the long term bearing capacity of either a driven pile or a drilled shaft. The following paper deals with the analysis of dynamic load test records, i.e., force and velocity as a function of time.

Dynamic load testing requires measurement of pile top force and velocity and therefore the pile top displacement is also known. Because of stress wave effects caused by the rapid loading of the pile, a plot of measured force vs. measured displacement does not resemble the static load-set curve. For the calculation of the static load-set curve it is therefore necessary to reduce the dynamic force to a static one by removing dynamic effects of both pile and soil. This calculation is usually done by signal matching (Rausche et al., 1972) a process that has been continuously improved (Mure et al, 1983, Hannigan et al., 1987, Hussein et al., 1991). Today, CAPWAP

(Goble Rausche Likins and Associates, Inc., 1999) is the most widely accepted computer program for the calculation of the static load set curve from dynamic test records. The latest version, a Windows program, includes a blow count matching option. This paper briefly describes the fundamental features of CAPWAP and presents a correlation study, which investigates the potential benefits of the expanded, automated search. The correlation utilizes information of GRL's data base which has been described by Thendean et al. (1996) in a paper that discussed the performance of an earlier CAPWAP version. The present paper also briefly investigates the relationship between total capacity and static capacity.

2 THE CAPWAP PROCEDURE

With two measurements at the pile top available, both input to and response of the pile top are known, however, one part of the system, the soil, which produces the response is unknown. In order to calculate the soil properties, a so-called inverse

analysis has to be performed which identifies the unknown parameters of a soil model (Figure 1). This inverse analysis is commonly called a Signal Matching Analysis (Balthaus, 1986, Reiding et al., 1988), or a System Identification (Klingmüller, 1984). The solution has to be achieved iteratively: an assumption of the unknown soil parameters is made and tested by performing an analysis with one of the measured quantities as a top boundary condition. If there is disagreement between the other measurement and its calculated counterpart the calculation is repeated with a corrected set of soil model parameters. Obviously, the more realistic the soil model, the better its capability to match the measured quantities. On the other hand, a very sophisticated soil model may have too many unknowns and may not be uniquely defined by the matching process. For that reason, the relatively simple Smith soil model (Smith, 1960) has been most successfully employed for pile dynamic signal matching.

The traditional iterative matching procedure can be summarized as follows:

1. Data Input: select a record with appropriate energy and data quality
2. Data Check and adjustment (normally automatic)
3. Build pile model (normally automatic)
4. Check and change resistance distribution
5. Recheck data adjustment
6. Check damping parameters
7. Check quakes and unloading parameters
8. Find absolutely best match quality
9. Produce output

An important part of the matching procedure is the evaluation of the match quality, i.e. quantifying the difference between measured and computed quantity. In CAPWAP the match quality is the normalized, weighted sum of the absolute values of the differences between computed and measured values of all analyzed time steps. Normalization is achieved with respect to both maximum pile top force and the number of data points. The match over a 3 ms time period, following the first return of the stress wave from the pile toe, is given a double weight because of its importance for total capacity determination.

CAPWAP can either be used in an interactive mode or automatically. The automatic procedure searches for a best match using a step by step procedure that is also recommended to the analyst for interactive signal matching. In other words, the automatic CAPWAP is not a standard minimization software which would search in a more or less random manner for a set of soil parameters that produces a minimum difference between computed and measured pile top variable. Experience has shown that such a relatively mindless procedure may lead to unsatisfactory results. On the other hand, the

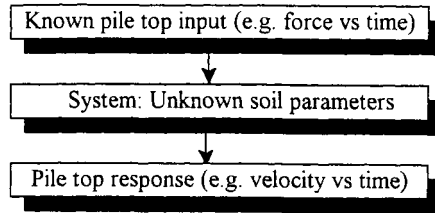


Figure 1. Inverse analysis problem

automated CAPWAP procedure produces capacity results that are very similar to those obtained by experienced engineers working interactively on a computer. On occasion, however, the automatic method calculates an unsatisfactory resistance distribution near the pile toe. An experienced analyst must therefore always check the solution by means of additional trial analyses. For the simplification of the interactive matching task the CAPWAP program does provide difference minimization routines for individual soil resistance parameters.

3 MATHEMATICAL MODEL

The pile is modeled as a series of uniform, elastic segments, typically 1 m long, of equal stress wave travel time. Calculations involve tracking the upward and downward traveling waves and their reflections where segment properties change or soil resistance effects exist. The simplicity and strictly elastic nature of this model is, unfortunately, a disadvantage when modeling non-linear or non-elastic situations such as cracks in concrete piles or certain types of mechanical pile splices.

The effect of the soil, resisting the pile motion, is modeled as a series of N lumped forces at intervals not greater than 2 m which depend on pile velocities and displacements. The parameters of this Smith soil model are the unknown quantities that CAPWAP must determine. In the standard analysis situation, the displacement dependent (static) resistance forces are represented by both a stiffness and a capacity value. The velocity dependent (dynamic) resistance forces are calculated using a damping factor. For the resistance forces acting on the shaft, soil stiffness and damping parameters are chosen proportional to the static capacity values and in this way, the number of shaft unknowns is kept to a manageable $N + 2$ values. For the toe an additional 3 unknowns have to be determined. To produce a good signal match over a long record time period several additional parameters had to be defined. The most important ones allow for a modification of the static soil stiffness and plastic limit (upward directed capacity) for the rebound phase of the pile and therefore have little or no effect on the calculated total static pile capacity.

Under certain conditions, particularly when the pile set under a hammer blow is very small, the assumption that soil resistance only depends on pile motion becomes inaccurate because the soil motion then has a magnitude comparable to that of the pile. The CAPWAP radiation model helps improve the calculated soil model for such cases by representing the soil surrounding the pile by a mass and a dashpot (Likins et al, 1996).

4 DATA CHECK (RECORD LENGTH AND SET MATCH)

In earlier versions of CAPWAP, the analyzed record length was generally set to 25 ms after the first return of the impact wave from the pile toe. This relatively short record length saved computer time but did not always allow for an accurate calculation of the final set. Today modern personal computers and more sophisticated operating systems provide the analyst with high computational speeds and huge memory space at a low cost. It has therefore become possible to economically analyze dynamic pile records over longer time periods and to perform many more trial analyses for more reliable results. The longer analysis time period assures that the calculation can be carried out until the pile stops moving, i.e. until the pile velocity becomes zero and the displacement has reached the final set. To be sure, the recommendation for Pile Driving Analyzer® users is a record length of 200 ms for normal land piles. Figure 2 is the example of a pile top force, velocity and displacement record which includes major vibrations after 100 ms. The record also indicates a final displacement value that matches the pile set or the inverse of blow count.

Ideally, the pile top set per blow is verified by independent observation so that the double integration of the acceleration can be checked and, if necessary, corrected. This two point data check and adjustment process is automatically performed in CAPWAP by slightly shifting the zero line of the acceleration. This zero line shift starts at impact, has a somewhat higher magnitude for a few milliseconds and a lower magnitude over the remainder of the record. The magnitude of this zero line shift is only a small fraction of the maximum measured pile top acceleration.

5 NEW DEVELOPMENTS

With a record that correctly double integrates to final set and with computational speeds allowing for an analysis to final zero velocity at the end of the record, the final pile set or its inverse, the blow count, can be calculated for all segments of the pile. As long as the final set is the same for several

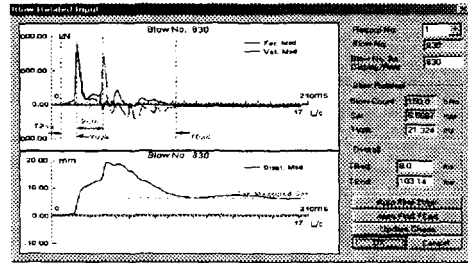


Figure 2. Typical force-velocity curves and displacement matching.

consecutive blows, this condition requires that all points along the pile achieve the same final set equal to that at the pile top. It is reasonable to require that the CAPWAP signal matching process also produces a match of calculated with observed pile top set; in other words, the average of all the sets of all segments equal the observed set. For lack of computing power this requirement had not been imposed on previous analyses. (It should be added that the most accurate method of calculating the final set of the pile is a residual stress analysis (RSA), which repeats the analysis several times thereby calculating the stresses locked into pile and soil. This analysis method is available as an option in CAPWAP. Regrettably, RSA is infrequently used because of its complexity.)

6 PROGRAM PERFORMANCE

The enhanced analysis procedure is available in the Windows based CAPWAP. To check whether or not the blow count matching (BCM) procedure would help improve the program performance, most of the data presented by Likins et al. (1996) was reanalyzed. The reanalysis involved adjustment of the acceleration values for both a zero final velocity and a final displacement matching the observed blow count at a later record time. The soil model parameters were then re-initialized to reset all soil parameters to the CAPWAP start up conditions. Any modifications to the pile profile were removed, the analysis count was reset to 1 and the initialized data file was saved. These steps assured the same results would be obtained as if the analysis had been started from the very beginning. With the reinitialized data file the automatic procedure was then run first with blow count matching and then again without blow count matching. The analyst did not interfere with the automatic analysis process in any way. Capacity, computed final set and match quality results were then subjected to a variety of correlation studies. As in the 1996 study, correlations were done using the ratio of CAPWAP divided by static load test capacity. Also, the time

Table 1. Calculated CAPWAP capacity divided by static load capacity at different time ratios

Time Ratio	BCM			No BCM		
	<.33	.33 - 1.25	>1.25	<.33	.33 - 1.25	>1.25
Min	0.57	0.62	0.50	0.41	0.56	0.51
Max	1.92	1.40	1.14	2.11	1.43	1.31
Mean	0.93	0.97	0.94	0.99	0.95	0.97
St Dev	0.28	0.17	0.19	0.40	0.19	0.24
COV	0.30	0.18	0.20	0.41	0.20	0.24
No. of Piles	26	37	11	26	37	11

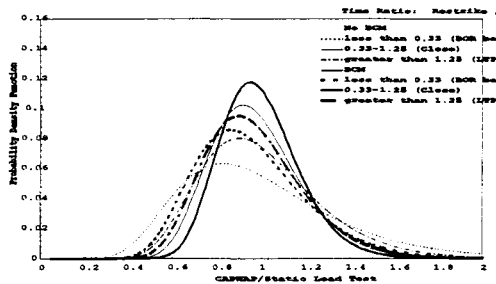


Figure 3. Log-normal probability density function for CAPWAP capacity

factor was introduced, i.e. time between restrrike test and pile installation divided by time between load test and installation. Thus, a time factor less than one indicates that the dynamic load test was performed prior to the static test. For a meaningful correlation, the time factor should be close to unity. Indeed, Figure 3 and Table 1 show that the data marked "close" with time factors between 0.33 and 1.25 yielded the best correlations. For "No BCM" the mean was .95 and the coefficient of variation .20. Blow count matching (BCM) significantly improved the correlation to a mean of .97 with a COV of .18. Even the other time factor categories showed a clear gain in accuracy and precision.

7 QUALITY OF BLOW COUNT MATCH

Computed blow counts are presented in the form of histograms of calculated divided by observed final set (inverse of blow count) in Figure 4, both for "No BCM" and "BCM." Clearly, the calculated sets improved although, in quite a few cases they did not change appreciably compared to those cases where blow count match was not attempted. It is concluded that either the observed blow count was not accurate - and since these are all restrrike tests it would be expected that observed blow counts are generally inaccurate - or the dynamic data, the pile model or soil model did not accurately enough represent the test conditions.

8 MATCH QUALITY

Obviously, a number of automatic CAPWAP predictions are not satisfactory. In the data set under consideration, one prediction was nearly twice the static capacity and one was one half the static load test result. Ideally, the match quality number would reflect the reliability of prediction. In fact, Hannigan, et al. (1987) presented good correlations with one exception whose match was not satisfactory. It was therefore concluded that match quality is an indicator of the reliability of prediction. To further study the relationship between match quality and capacity prediction, Figure 5 was plotted which is normalized capacity vs. match quality. The cases presented were done with BCM; match qualities were therefore slightly higher than those achieved without BCM (BCM adds the final set error to the quality of the signal match.) Obviously, there is no correlation whatsoever between match quality and capacity prediction. However, it would be wrong to assume that match quality for a particular data set does not matter because for each case the program determined the best possible match or lowest MQ value. The match quality number for a particular case is therefore specific and may be used to judge the reliability of only that one data set. It is not possible to make a general requirement on match quality: in one case even an MQ = 24 yielded an acceptable result. However, it was probably more a matter of luck that a good correlation was achieved. In general, results with MQ > 5 should be considered with suspicion. In all cases the CAPWAP analyst must check the results calculated by the automated routine and determine whether or not additional MQ improvements are warranted and possible.

9 PREDICTED SOIL MODEL PARAMETERS

Table 2 presents damping and quake values calculated by either BCM or No BCM. The mean values of the calculated shaft damping differed little (.74 vs .72 s/m), however, the blow count matching procedure produced less scatter (COV .49 vs .63).

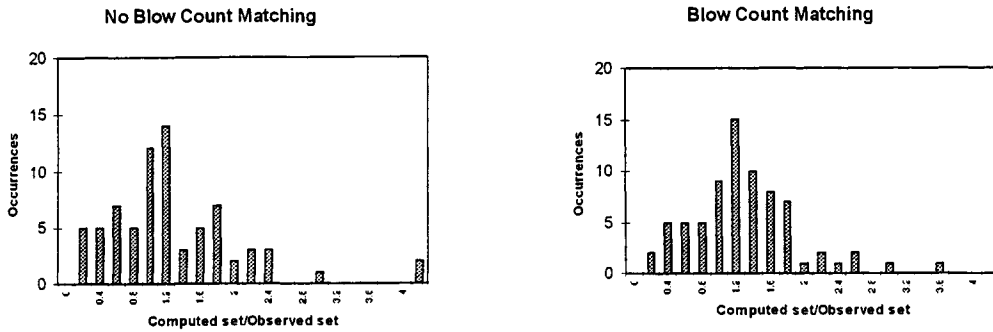


Figure 4. Computed to observed set comparison with and without blow count matching

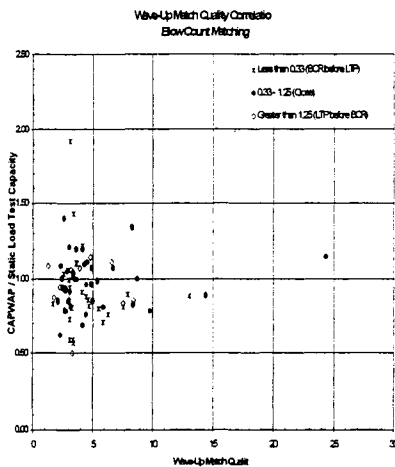


Figure 5. Match quality comparison with capacity prediction, blow count

This is not significant since the data represented a variety of soil types. Toe damping is generally assumed to be independent of soil type. Its magnitude is, however, highly dependent of the magnitude of end bearing since viscous damping is divided by toe resistance to produce the Smith damping value. The new CAPWAP routine produced much more reasonable results than the previous code with mean values of .84 vs 3.79 s/m and COV's of .99 vs 2.95.

Calculated quake values were non-dimensionalized by their GRLWEAP recommended values. Thus, a calculated skin quake of 2.5 mm would be presented as 1.0 as would be a toe quake value equal to D/120 (where D is the diameter or width of a displacement pile). The non-dimensional calculated shaft quakes were 1.00 and 1.17 for No BCM and BCM with a slightly greater scatter for the new calculation method, probably because variation of quake values often help to improve the blow count match. Toe quakes were very similar for the two calculation methods with mean non-dimensional

values of approximately 2.0 (1.93 for BCM and 2.06 for No BCM) with significant scatter. This result matches the D/60 recommendation currently in GRLWEAP for certain types of soils.

Table 2. Dynamic soil parameter comparison

	Damping (s/m)		Quake	
	Shaft	Toe	Shaft/(D/120)	Toe/(D/120)
No blow count matching				
Max	1.94	67.92	2.83	6.73
Min	0.13	0.00	0.39	0.28
Mean	0.72	3.79	0.99	2.06
St. Dev	0.46	11.19	0.45	1.33
COV	0.63	2.95	0.45	0.65
Blow count matching				
Max	1.85	4.56	2.97	6.72
Min	0.14	0.02	0.41	0.36
Mean	0.74	0.84	1.17	1.93
St Dev	0.36	0.83	0.56	1.32
COV	0.49	0.99	0.48	0.68

10 TOTAL, STATIC AND DYNAMIC RESISTANCE

CAPWAP calculates soil resistance as the sum of a static plus a damping resistance. The maximum static resistance component is equated to the static bearing capacity according to Smith (1950). Another approach would be the calculation of peak total resistance, i.e. the sum of maximum static plus peak dynamic resistance, multiplied by a reduction

factor to account for dynamic resistance losses. A justification for this approach is the difficulty of separating static from dynamic components by signal matching when the pile displacements are small. The static, displacement dependent components then differ little from the damping, velocity dependent components which easily introduces errors in the calculation. Worse yet, in a hard or very dense soil or in a rock, the static toe resistance components sometimes appear to be velocity dependent and could therefore be misinterpreted as damping resistance by the traditional CAPWAP approach, leading to an underprediction of static capacity. To check for possible improvements in capacity prediction, various methods of interpretation of the total shaft and/or toe resistance values were explored. Table 3 shows the most promising method which adds the calculated static shaft resistance to the total, factored toe resistance. Sorting the results by dominant soil type, a marked improvement of the traditional approach was achieved for sands, where the mean of the ratio of predicted capacity to load test capacity would be 1.02 with a COV of 0.24. Further exploration of this method is warranted. However, at this time too little experience is available (only 14 cases for the sands) and the time factors should also be considered in future studies.

Table 3: CAPWAP static shaft resistance and total toe resistance divided by static load test capacity for different soil types

Soil Type	No. of Piles	Mean	St. Dev	COV
Clay	6	1.30	0.50	0.38
SandyClay	4	1.23	0.22	0.18
SiltyClay	8	1.08	0.20	0.18
Rock	6	1.15	0.18	0.15
Sand	14	1.02	0.25	0.24
ClayeySand	8	1.03	0.24	0.24
SiltySand	8	1.12	0.24	0.21
ClayeySilt/Silt	4	1.93	1.51	0.78
SandySilt	5	1.07	0.15	0.14

11 CONCLUSIONS

The correlation between CAPWAP predicted pile bearing capacity and static load test capacity can be improved if not only the difference between computed and calculated pile top quantity but also the difference between calculated and observed blow count is included in the match quality evaluation. The improvement over the traditional method, which ignored the calculated blow count, is significant and since, with modern computers, the additional computational effort is minor, blow count matching should always be done. Great care should be taken

in the measurement of restrike blow count. It is believed that lack of accurate blow count measurement limited the improvement over the traditional CAPWAP approach. On the other hand, the signal matching process itself already incorporates blow count matching to a certain degree, since the measured velocity and therefore the top displacement are imposed as top boundary conditions. The improvement achieved with the new CAPWAP program should therefore be primarily attributed to a more accurate analysis over a longer time period.

As in earlier correlation studies, the time factor (time between load testing and installation divided by time between restriking and installation) proved to have the greatest effect on the accuracy of the CAPWAP prediction. Obviously waiting times comparable to those of the static test assures the best possible prediction of long term bearing capacity by CAPWAP.

REFERENCES

- Balthaus, H., 1986. Zur bestimmung der tragfaehigkeit von pfaehlen mit dynamischen pfaehlpruefmethoden, Dissertation, TU Braunschweig, Germany.
- Goble Rausche Likins and Associates, Inc., 1999, CAPWAP background report, Cleveland, OH.
- Hannigan, P., and Webster, S. W., 1987. Comparison of static load test and dynamic pile testing results, Second Int. Symposium, Deep Foundations Institute, May.
- Hussein, M., and Rausche, F., 1991. Bearing capacity of deep foundations from dynamic measurements and static tests - ten correlation cases, Piletalk International '91, Malaysia.
- Klingmüller, O., 1984. Dynamische pfaehlpruefung also nichtlineare systemidentifikation, dynamische probleme - modellierung und wirklichkeit, tagungsband, Curt-Risch-Institut, TU Hannover, Oktober.
- Likins, G., Rausche, F., Thendean, G., and Svinikin, M., 1996. CAPWAP correlation studies, Proceedings of the 5th Int. Conf. on the application of stress wave theory to piles, F. Townsend ed., Orlando, Florida.
- Mure, J.N., Kightley, M.L., Grävare, C.J., and Hermansson, I., 1983. CAPWAP - an economic and comprehensive alternative to traditional methods of load testing of piles, Paper 16, Piling and ground treatment for foundations, Thomas Telford, pp 167-174.
- Rausche, F., Goble, G.G., and Moses, F., 1972, Soil resistance predictions from pile dynamics, *Journal of the Soil Mechanics and Foundation Division, ASCE*.
- Reiding, F.J., Middendorp, P., Schoenmaker, R.P., Middeldorp, F.M., and Bielefeld, M.W., 1988. FPDS-2, A new generation of foundation pile diagnostic equipment, Proceedings, Third Int. Conf. on the appl. of stress wave theory to piles, Bengt Fellenius, ed., Ottawa, Canada.
- Smith, E.A.L., 1960. Pile driving analysis by the wave equation, *Journal of Soil Mechanics and Foundations, ASCE*, 86, August 1960, 35-61.

Combining static pile design and dynamic installation analysis in GRLWEAP

F.Rausche & B.Robinson

Goble Rausche Likins and Associates Incorporated, Cleveland, Ohio, USA

J.Seidel

Monash University, Melbourne, Vic., Australia

ABSTRACT: Wave equation simulations of pile installations by impact driving have become an important part of the pile design process in many countries. In its traditional form, the wave equation approach replaces a dynamic formula, i.e. it leads to a bearing graph which is a relationship between pile bearing capacity and blow count. In addition, the simulation calculates realistic dynamic pile stresses. GRLWEAP, probably the most widely used wave equation program, also enables the user to calculate blow count stresses vs depth in a so-called driveability analysis. This procedure requires soil resistance vs depth input which thus far had to be precalculated in a separate analysis either manually or using another computer program. The program has now been expanded to include this pre-analysis. This paper presents the method itself, its correlation with static tests and another similar method. It also briefly discusses limitations and special considerations that make this method somewhat different from other static pile analysis formulas..

1 INTRODUCTION

As originally proposed by Smith (1960) the wave equation method generates a so-called bearing graph which is a relationship between pile bearing capacity and blow count. In addition, maximum tension and compression pile stresses are usually plotted. These results are well suited for the selection of hammers, hammer performance parameters and cushions for a given pile type and soil condition.

The GRLWEAP program (Goble et al. 1999) not only calculates bearing graphs but also offers a convenient method for predicting the blow count as a function of pile penetration. However, for meaningful results, this so-called driveability analysis requires a much more detailed soil parameter input than the original approach. The required static and dynamic soil resistance input parameters should reflect the various layers that the pile penetrates. For realistically calculated blow counts vs depth, it is necessary that these soil parameters are determined with as much accuracy as possible based on quality geotechnical information. From such improved analysis, it is possible to obtain the best estimate of both the total number of blows required to install the pile, and the total installation time. In addition, the GRLWEAP program allows

for consideration of different pile lengths during installation and hammer and pile cushion parameters, which may be adjusted as driving resistance varies to most closely model the pile installation process.

For user-friendliness the GRLWEAP program has now been expanded to accept soil strength and soil-type data input. Based on this information, an automated static formula approach has been devised which estimates the static soil resistance parameters and calculates a load-movement curve at the design depth. The program automatically selects the dynamic soil resistance parameters including resistance loss factors, which relate static resistance to driving to static long term capacity values. The complete GRLWEAP driveability approach is described in this paper and its benefits and shortcomings are discussed.

It has to be emphasized, however, that there is no universal approach which is fully reliable, and that the pile driveability analysis requires the local knowledge of an experienced geotechnical engineer to be most accurate. It is also evident that the quality of the prediction is a function of the quality of the soil information which is available. The method presented here should not replace the design calculation that the geotechnical normally performs

for pile type selection.. Instead, GRLWEAP's analysis is an additional effort in the preparation of the driveability analysis.

2 GENERAL CONSIDERATIONS

Driven pile analysis is generally performed in two steps (Hannigan et al. 1996): an initial static analysis which is followed by a dynamic or wave equation analysis. Static analysis can be based on one of the many proposed approaches, which calculate shaft resistance and end bearing for a particular pile penetration depth. Depending on the quality of the available soil strength data, the variability of the soil properties over the site, and the realism of the calculation procedure, the reliability of the results obtained from such analyses varies significantly. Statically calculated capacities are indirect estimates based on site soil parameters estimated from the foundation investigation, not based on the additional information provided by the installation process. Because of this inherent shortcoming, engineers often prefer the use of a dynamic formula and/or wave equation analysis which provide a more direct method of capacity evaluation for each individual pile. In these approaches, blow counts from pile installation observations, plus a calculated relationship between blow count and bearing capacity (the bearing graph) is used to make a pile capacity prediction. The driveability approach can also be used prior to pile installation to predict rather than confirm the installation process. In this case, field observations of the installation process are not available to improve the reliability of the analysis procedure.

In traditional methods of static pile analysis, the requirement that the analysis provide a safe design is paramount. Efficiency of design is something for which all engineers should strive, however, it is of less importance than providing a safe structure. Conservatism in the design is provided in several ways:

1. In conservative interpretations by the engineer of the site soil strength parameters;
2. In upper limits on strength values imposed by the design method;
3. In a conservative appraisal of the data on which the design method is premised;
4. In the application of safety factors or strength reduction factors.

The last of these factors affects only the maximum structural load which can be allowed on the foundation element during its service life. However, the first three of these factors ensure that most design methods applied in practice will underestimate ultimate pile capacity.

Driveability analyses are conducted as part of the design process for a number of reasons:

1. To evaluate the ability of a given pile driving hammer to drive the pile to the nominated capacity and/or penetration;
2. To estimate the final blow count;
3. To evaluate the stresses which will be induced in the pile during the installation process.

In such an analysis, a conservative choice of soil strength parameters has an ambiguous meaning. For instance, when assessing tension stresses or the required penetration, an underestimate of soil resistances would usually produce a conservative analysis, whereas in assessing, compression stresses, an overestimate of soil resistances would generally be conservative. Assessment of the bearing capacity which can be achieved by a given hammer may not be significantly affected by the assumed distribution of resistance. Because of this ambiguity, and because the consequences of an incorrect assessment of soil resistance distribution does not have the same implications as traditional static design with regard to the safety of the structure, it is most appropriate to undertake driveability analysis using the most realistic assessment of soil strength parameters.

In the GRLWEAP static calculation method, it was therefore attempted to avoid a static resistance bias as much as possible. Again, the assessment of the pile's bearing capacity should always be done with prudent limits or reductions as dictated by experience.

Having calculated the static soil resistance based on in-situ soil strength parameters, an estimate has to be made of the static soil resistance that is actually present during pile driving. For example, pore water pressure changes in the ground during pile installation tend to change the effective stress regime and therefore the resistance acting on the pile. Unfortunately, no matter how accurately the soil exploration and static analysis was conducted, estimating the Soil Resistance to Driving (SRD) based on its static capacity may generate significant errors and although experience values are available, the selection of so-called gain-loss or capacity reduction factors is one that should always be carefully reviewed. These uncertainties are greater for sensitive soils such as marine clays and it is common practice to estimate both a lower and an upper bound SRD and calculate lower and upper bound blow counts by the wave equation.

When performing a dynamic analysis using GRLWEAP, it is not only necessary to calculate the static resistance and its distribution, additional dynamic soil resistance parameters, damping and quake, both at shaft and toe have to be estimated. Actually, GRLWEAP recommendations (Goble et al. 1999) are rather simple for standard analyses where little is known about the soil. Based on these commonly accepted rules, unless dynamic test results indicate otherwise, only the shaft damping factor is a function of soil type. Toe damping is

probably independent of soil type because the dynamic resistance component at the pile toe is more a function of inertia forces caused by the soil being displaced around the pile toe than with forces of viscous flow. Similarly, shaft shakes are assumed independent of soil type with no evidence that this assumption affects the accuracy of wave equation predictions. For the toe quake, experience indicates that pile size has to be considered and, in the case of rock, the hardness of that material. With soil type and pile size known, it is therefore a simple task to assign the necessary additional parameters automatically.

3 THE GRLWEAP STATIC ANALYSIS

To estimate the ultimate static capacity of a pile, two quantities must be calculated: the shaft resistance and the toe resistance. Many methods of static capacity estimation exist for cohesionless and cohesive soils. These range from empirical methods based on SPT and CPT values (e.g. Meyerhof, 1976 and Nottingham and Schmertmann, 1975) to semi-empirical effective stress and total stress methods (e.g. Fellenius, 1991 and Tomlinson, 1980). All of these methods require that soil type and some soil strength parameter (SPT-N value, CPT cone pressure, friction angle, unconfined compressive strength, etc.) is known. Unfortunately, the methods often give no clearly defined solutions for certain ranges of soil strength parameters, because their experience base is limited.

While it is certainly desirable, and theoretically more accurate, to know as much about the geotechnical properties of a site as possible, funds allocated for soil exploration studies typically are kept to a minimum, usually in a false sense of economy. Particularly for small projects, only a few soil borings with depth, soil type and SPT N-value are available to the deep foundation designer. In such instances, a sophisticated analysis method will not add much to the quality of the prediction. In fact, there is often a wide gap between what should be known about the soil to satisfy a method's input requirements and the available data. For example, specific weight, friction angle and pile adhesion often must be known, however, the soil exploration yielded only soil type and SPT N-value. The designer therefore has to choose an empirical approach to convert soil type and SPT N-value to the required parameter, before the calculation method can be employed. This two-step approach has been automated in GRLWEAP.

GRLWEAP estimates shaft resistance based on an effective stress approach. The unit shaft resistance at a point along the pile is therefore calculated from

$$f_s = k \sigma_{v, \text{mid}} \tan \delta \quad (1)$$

In Equation 1, k is the lateral earth pressure coefficient, $\sigma_{v, \text{mid}}$ is the mid-layer vertical effective stress and δ is the friction angle at the soil-pile interface. The effective stress requires that the

Type Number
Gravel 100
Sand 200
Silt 300
Silt 300
Sandy Silt 310
Silt 311
Elastic 312
Organic 313
Calcareous 314
Carbonate 315
Cemented 316
Weathered 317
Hard 318
Soft 319
Clayey Silt 320
Silt 321
Elastic 322
Organic 323
Calcareous 324
Carbonate 325
Cemented 326
Weathered 327
Hard 328
Soft 329
Clayey Sandy Silt 330
Clay 400
Clay 400
Sandy Clay/Gravelly Clay/Sandy Gravelly Clay 410
Silty Clay 420
Lean 421
Organic 423
Calcareous 424
Carbonate 425
Cemented 426
Weathered 427
Hard 428
Soft 429
Sandy Silty Clay 430
Rock 500

Figure 1. Partial list of soil types in GRLWEAP

buoyant weight of the soil is calculated and that requires knowledge of water table and specific weight. The depth of the water table is therefore an additional input into GRLWEAP. The specific weight (as well as the friction angle) is based on SPT -value and soil type. Thus, an extensive soil type table was developed which also serves to estimate dynamic soil resistance parameters such as quake and damping. A portion of that "click-on" table is shown in Figure 1. The table contains much more detail than necessary for a simple SPT based soil and